UM-HSRI-PF-74-6

BASELINE TESTS OF THE LONGITUDINAL TRACTION PROPERTIES OF TRUCK TIRES

R.D. Ervin

C.C. MacAdam

A REPORT ON RESEARCH IN TRUCK TIRE MECHANICS

SUPPORTED BY

The Motor Vehicle Manufacturers Association

April 1974

ACKNOWLEDGMENTS

A large number of individuals and corporate organizations have contributed to the construction and application of the test device which is described herein. In addition to the basic research support which derived from the MVMA member truck-producing companies, conspicuous contributions of hardware and/or engineering support were received from the following companies:

Kelsey Hayes Company (especially Mr. Kurt Rinker, Principal Engineer, Disc Brakes)

Bendix Corporation (especially, Mr. John Einhorn, Project Engineer, Bendix Automotive Development Center)

Fruehauf Corporation (especially Mr. John E. Getz, Manager, Consulting Engineering)

North American Rockwell (especially Mr. Robert Svenson, Assistant Chief Engineer, Brake Engineering)

Uniroyal, Inc. (especially Mr. Wallace Marshall, Research Scientist, Advanced Tire Products Department)

Firestone Tire and Rubber Company (especially Mr. William Straub, Manager, Tire Test Laboratory)

In addition, HSRI personnel who contributed major efforts in this program were Mr. J. Boissonneault who supervised the construction of the mobile dynamometer and Mr. R. Wild who conducted the truck tire test program.

TABLE OF CONTENTS

BASELINE TESTS OF THE LONGITUDINAL TRACTION PROPERTIES OF TRUCK TIRES

INTRODUCTION

This document presents experimental measurements of the longitudinal shear force behavior of a sample of eight truck tires. The tires were tested using a mobile dynamometer which has been constructed by the Highway Safety Research Institute under support by the Motor Vehicle Manufacturer's Association.

The selected set of test tires was a duplicate of a sample which was tested on the HSRI flat bed tire tester and reported previously in Reference [1]. The mobile tests, reported herein, were conducted at the facilities of the Bendix Automotive Development Center, New Carlisle, Indiana, in October and November 1973.

Each tire in the sample was subjected to a break-in procedure and subsequently tested under a matrix of pavement, velocity and load conditions.

Tire preparation practice is described in Section 1, together with a description of the test matrix and the data processing methodology. A tabular summary of the data itself is presented in Section 2, while a graphic display of the μ-slip histories is presented in Appendix 1. The truck tire test device is described in Appendix 2.

Certain caution is suggested in interpreting the presented data beyond the constraints imposed by accuracy tolerances which are specified in the text. Due to problems associated with mechanical fastening of the main force transducer of the test machine, the absolute values of measured forces are qualified by a rather large level of uncertainty—relative findings concerning "peak-to-slide" relationships, velocity sensitivity, etc., are not so uncertain and indeed are seen to suggest certain marked

peculiarities in truck tire performance. These data are presented, despite their indicated shortcomings, in response to the great interest which exists in the truck engineering community. Preliminary findings such as are supported by the presented data will be challenged in the near future as improvements in our experimental apparatus are effected.

1.0 METHODS EMPLOYED IN CONDUCTING EXPERIMENTS AND PROCESSING DATA

1.1 TIRE PREPARATION

Truck tires were prepared for testing through the maintenance of certain practices intended to assure consistency of test conditions as well as representativeness of measured traction performance. All tires were mounted on their respective Tire and Rim Association recommended Rims (disc wheels).

The inflation pressure of each tire was first set to the rated "cold" inflation level, with the tire at an equilibrium temperature equal to the ambient temperature of the site. The tire was then operated in a freely rolling condition at 60 mph, and at rated load for a distance of 10 miles. Following this period of running, the inflation pressure was checked and the prevailing "hot" value was maintained as the reference setting throughout the tire testing sequence.

Each tire was "broken-in," on the test machine, for a distance of 50 miles, and at a velocity of 60 mph. The tire was operated at its rated load and at the reference value of inflation pressure described above.

1.2 TIRE TEST PROCEDURE

Tires were tested at each of the following conditions:

DRY ASPHALT PAVEMENT

(Skid Number ~ 78)

Velocity:
- 40 mph
- 60 mph

Vertical Load:
- 50% rated load
- 100% rated load
- 150% rated load

WET COATED ASPHALT PAVEMENT

(Skid Number ~ 20)

(Tests conducted using on-board water delivery—with nominal film thickness of 0.025 inches)

Velocity: 20 mph

Vertical Load:

50% rated load
100% rated load
150% rated load

At each condition, the tire was subjected to ten lockup cycles, as described in Appendix 2. The duration of the locked-wheel condition (100% slip) was minimized using an automatic lock-up-detection/brake-release system. The gathering of a very brief sample of locked-wheel data was mandated by discovery of serious profile deterioration of test tires following somewhat extended lockup periods. As an example, Figure 1 illustrates a time history of vertical load; (a) immediately preceding brake application with a new tire, and (b) following a single, one-second-duration lockup. The serious pollution of the vertical load condition was deemed to be an unacceptable price to pay for extended locked-wheel data. Accordingly, the 100% slip condition was allowed to persist in each of the baseline experiments for a period of only 100 to 200 milliseconds.

1.3 DATA PROCESSING AND ERROR TOLERANCES DISCUSSION

The recording of raw tire force and wheel velocity data was accomplished using an FM analog tape recorder, with backup oscillographic recordings for visual checking. The tape recordings were processed by a two-stage computerized data reduction method. The first stage, utlizing a hybrid computing

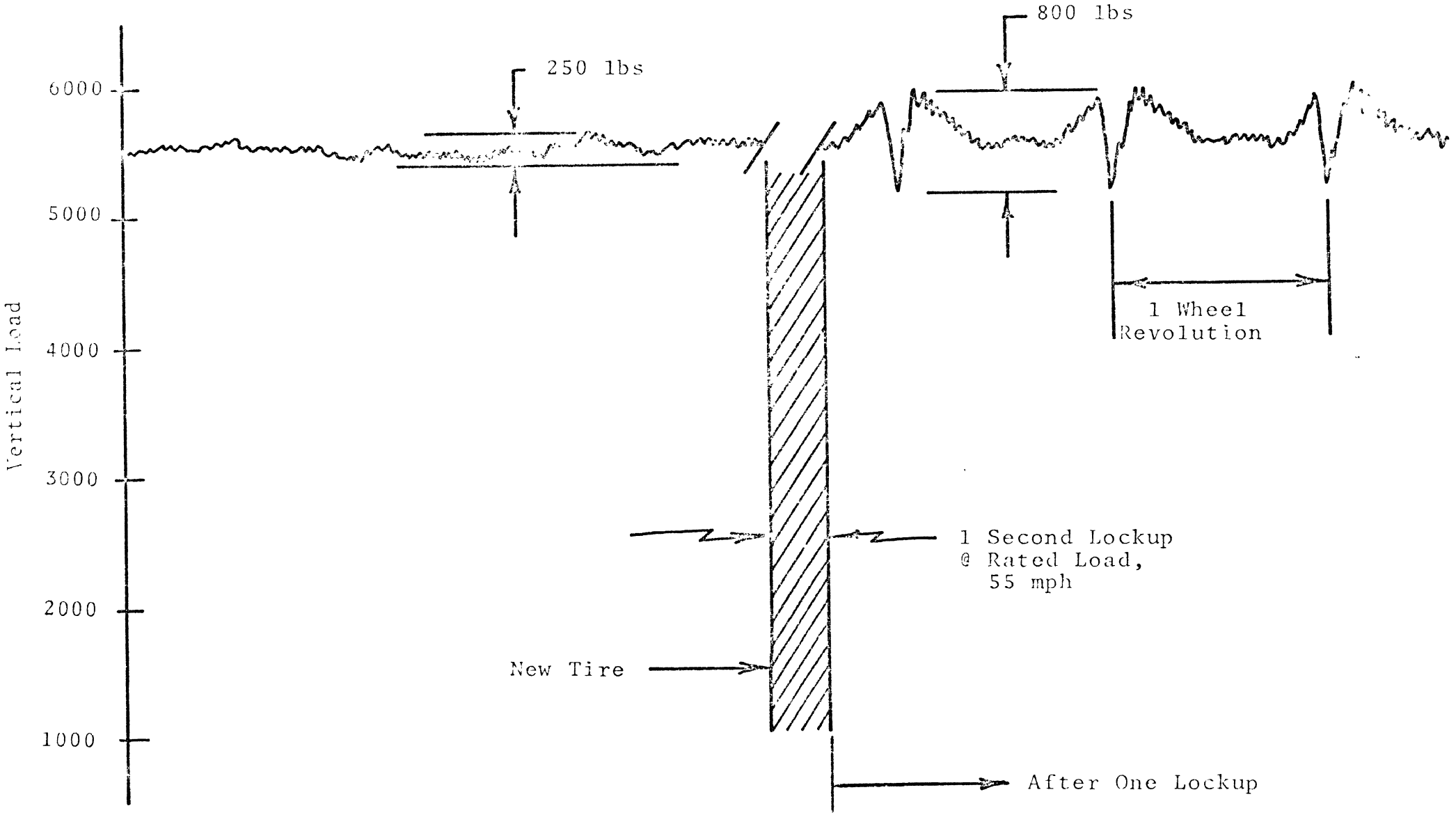

Figure 1. Vertical load oscillations following a single, one-second lockup at rated load.

facility, involved the transfer of data from analog to digital tape format. In the following stage, the digitized data was manipulated to produce longitudinal force and brake torque tables as functions of longitudinal slip.

The digital manipulations included:

1. A numerical smoothing routine.
2. Data scaling using recorded calibration signals.
3. Sampling of wheel velocity and longitudinal force signals to determine the freely-rolling and locked-wheel conditions.
4. Computation of a special scale factor adjustment for F_x (as discussed later in this section).
5. Sampling and subsequent averaging of force, torque, and slip histories for each of the repeat lockup cycles within a given file, or test condition.
6. Tabulation of the averaged variable histories at values of longitudinal slip which were spaced as follows:

   every 2% for $0 < \text{slip} < 20\%$
   every 5% for $20 < \text{slip} < 100\%$

7. Final output printing, in both tabular and print-plot format.

Due to a problem related to the "seating" of the load cell on its fastenings during the tire test program, it was necessary to determine the F_x scaling as an after-the-fact operation during data processing. This was accomplished in three steps, utilizing the raw data signals for F_z, T_b, and F_x, where F_x = longitudinal tire shear force; F_z = vertical load; T_b = brake torque.

For a given file of data (defined by a unique combination of test conditions), samples were made of the F_z signal—while the tire was in a freely-rolling state, but loaded to the equilibrium test condition loading. Using this value of load, a computation was made to determine the static loaded radius of the sample tire. This computation was performed using a set of radial loading data which had been gathered using the HSRI flat bed machine [1]. As shown below, individual relationships were utilized to derive the prevailing static loaded radius for each tire in the test sample.

Static Loaded Radius (inches)	Tire Size
$R_s = 18.5 - \frac{F_z}{3700}$	8.25 x 20/E
$R_s = 19.4 - \frac{F_z}{3850}$	9.00 x 20/E
$R_s = 20.3 - \frac{F_z}{4700}$	10.00 x 20/F
$R_s = 20.1 - \frac{F_z}{5200}$	11.00 x 22.5/F
$R_s = 21.9 - \frac{F_z}{5400}$	11.00 x 22/F
$R_s = 21.6 - \frac{F_z}{5000}$	12.00 x 20/G
$R_s = 20.7 - \frac{F_z}{5200}$	12.00 x 22.5/F
$R_s = 20.8 - \frac{F_z}{5300}$	15.00 x 22.5/H

The calculated value for static radius (R_s) was used as representing the effective radius (R_{eff}) at which the F_x-induced component of brake torque is applied. Then, samples were made of both the F_x and brake torque signals during lockup (at which time

the inertial component of torque is equal to zero), and a scale factor for F_x was determined, assuming

$$F_x = T_b/R_{eff} = T_b/R_s$$

The associated scale factor was then used in reducing the F_x data signal to obtain measures of absolute force level, in pounds. This scale factor is known to be somewhat larger, in terms of lbs/volt, say, than is actually appropriate due to the fact that the compliant tire structure suffers a rearward deflection of its vertical load vector during the generation of "braking" shear forces. As shown in Figure 2, the deflection, Δx, gives rise to an $(F_z \Delta x)$ component of torque which is additive to the $(F_x R_{eff})$ component.

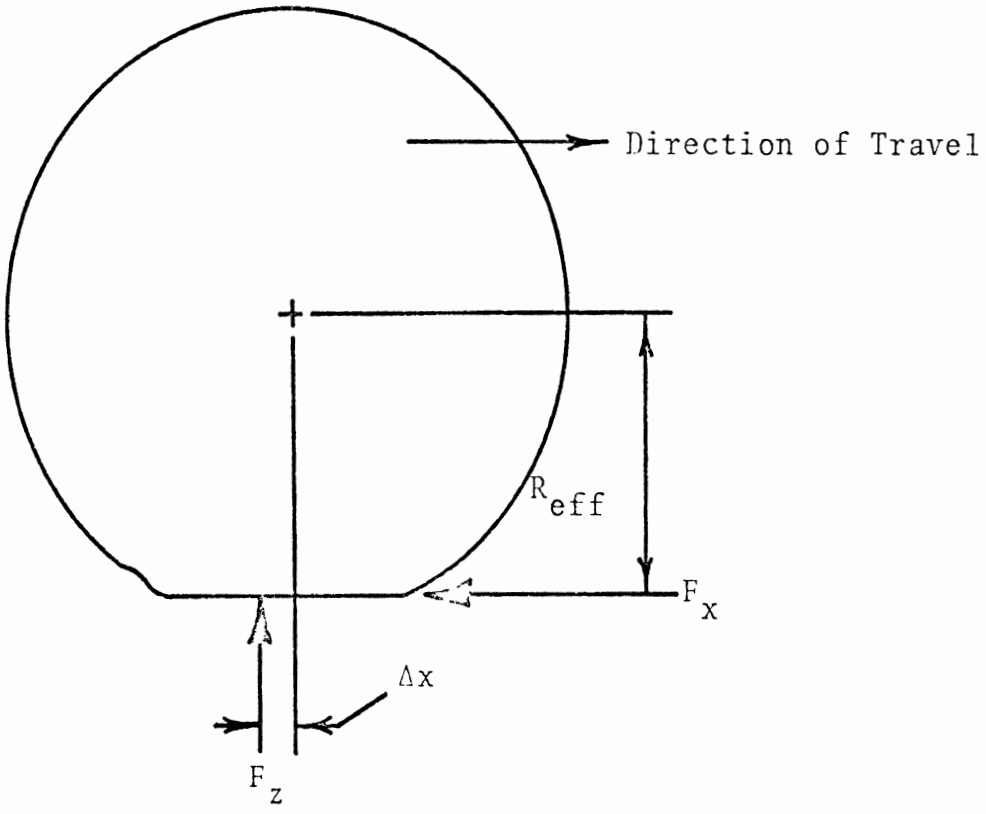

Figure 2

Measurements have been made [2] of the errors in force measurement which might derive from the presence of this torque component—and its accompanying influence on torque-to-force scaling such as we conducted. These experiments, performed for passenger car tires, show the measured longitudinal force to be 2 to 9% higher than the actual force level, with radial ply tire constructions accounting for the upper end of this range. While no data had been reported in the literature relating these numbers to truck tires, there is reason to believe that errors in longitudinal force such as apply to truck tire data reported herein will be somewhat smaller than the 9% upper range of error as applies to passenger car tires. This conclusion is based upon two observations, namely that:

(a) the ratio of the tangential spring rates of cross-bias truck versus car tires is about equal to the ratio of their respective rated loads [3, 4], that is,

$$\frac{K_x(\text{Truck tire})}{K_x(\text{Car tire})} \approx \frac{F_z \text{ rated (Truck tire)}}{F_z \text{ rated (Car tire)}}$$

(b) the effective radius of truck tires in the 20" to 22.5" diameter rim sizes is on the order of 1.6 times the effective radius of passenger car tires which are in the 14" and 15" diameter rim sizes.

The general torque equation, at the locked wheel condition, is:

$$T_b = \frac{F_x}{K_x} F_z + F_x R_{eff} \qquad (1)$$

If we consider, as a reference condition, those measurements performed at rated load, then

$$\frac{F_z}{K_x} = \text{Constant, } C, \tag{2}$$

for truck or passenger car tires. Substituting C into Equation (1) gives

$$T_b = F_x(C + R_{eff}) \tag{3}$$

Given that, for passenger car tires, $C \approx .09\ R_{eff_{car}}$ (as deduced from Reference [2]), and

$$R_{eff_{truck}} \approx 1.6\ R_{eff_{car}}$$

then,

$$C \approx .056\ R_{eff_{truck}}$$

Accordingly, we speculated that the error induced in truck tire longitudinal force measurements, as scaled from torque recordings, is less than the 9% maximum reported for passenger car tires, and may be on the order of 6%, if tangential stiffness is the primary determinant of this property. To check this hypothesis, static measurements were made at HSRI on two of the test sample tires, following the full-scale test program. Reference values of longitudinal force were applied at the ground plane of a standing tire using a fluid bearing for frictionless support. The "error," described below, was obtained for each tire at different values of vertical load.

$$F_x \text{ error}(\%) = \frac{\frac{T_b(\text{measured})}{R_s} - F_x(\text{applied})}{F_x(\text{applied})} \times 100$$

The maximum errors achieved in each case are tabulated below:

TABLE 1

	Vertical Load			
Tire Size	3500 lbs	5000 lbs	6500 lbs	8000 lbs
9 x 20/E (rated load, 4610)	3%	3.7%	4.2%	--
11 x 22.5/F (rated load, 5430)	<1%	<1%	1.3%	2.4%

While these few static tests do not constitute a rigorous examination of the mechanism involved, we suggest that a pragmatic approach can be adopted in adjusting the data reported herein to account for the upward bias which resides in the normalized longitudinal force measures. It is estimated that the data may be biased from .5% to 6% of the reported value of μ, with higher load levels accounting for higher errors and, conversely, with lower levels of error associated with lighter loading.

1.3.1. VERTICAL LOAD ACCURACY. Since the longitudinal force measure is normalized through the relation $\mu_x = F_x/F_z$, the accuracy of μ_x is determined, in part, by the accuracy of the measurement of vertical load, F_z. As a consequence of the load cell "seating" anomaly, alluded to earlier, an uncertainty

exists in the value of F_z, as shown in Figure 3. This limitation in absolute accuracy is coupled in the table below with the previously discussed bias error and presented as maximum-high-side and low-side errors in μ_x, i.e., μ_x(measured) = μ_x(actual) $\pm \frac{\%\ \text{error}}{100} \times \mu_x$(actual).

TABLE 2

	Uncertainty in Absolute Value of μ_x	
Vertical Load	+% (High Side Error)	-% (Low Side Error
2000 lbs	+22%	-11%
3000 lbs	+18%	- 9%
4000 lbs	+14%	- 6%
5000 lbs	+10%	- 4%
6000 lbs	+ 9%	- 3%
7000 lbs	+ 9%	- 2%
8000 lbs	+ 8%	- 2%
9000 lbs	+ 8%	- 1%
10000 lbs	+ 8%	- 1%
11000 lbs	+ 7%	- 1%
12000 lbs	+ 7%	- 1%

It is believed that the change in load cell fastening condition which gave rise to the large indicated change in the F_z calibration involved an anomaly which occurred either completely before or completely after the test program. This hypothesis is supported by a reference pair of tests (involving ten lockup cycles each) made on a 10.00 x 20/F tire early in the baseline tests, and at the end of the series. The "before" and "after" values of the respective peak and slide "μ_x's" were seen to be within 0.02 units of one another (substantially within the run-to-run variations). Thus it is postulated that the absolute F_z

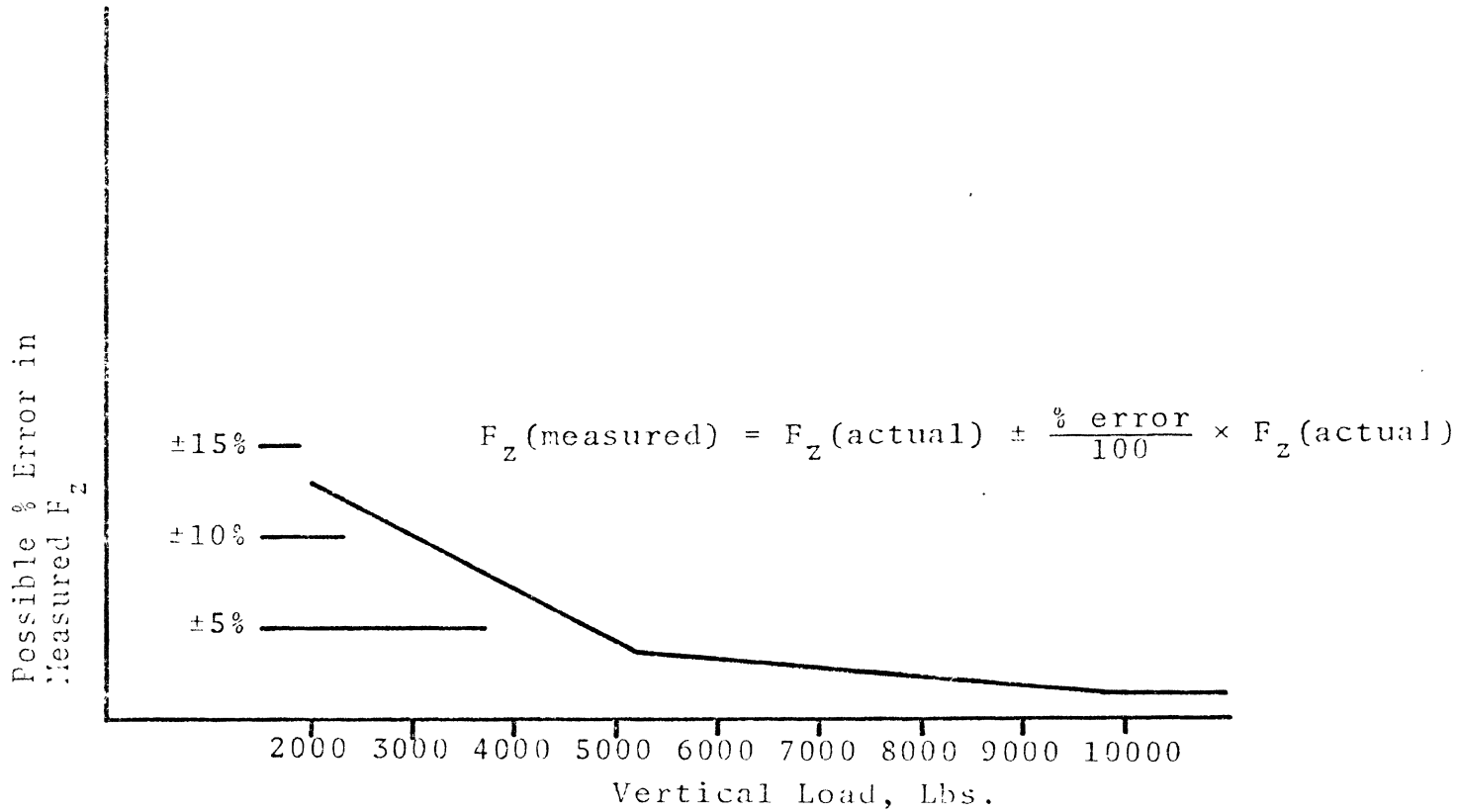

Figure 3. Vertical load error tolerances

measures are all actually biased to one polarity of the Figure 3 error scale, most likely the negative side (given our understanding of the load cell anomaly) such that the likely high/low error estimates in μ_x are listed below.

TABLE 3

Vertical Load	%, (High Side Error)	%, (Low Side Error)
2000	+22%	+15%
3000	+18%	+12%
4000	+14%	+ 8%
5000	+10%	+ 5%
6000	+ 9%	+ 4%
7000	+ 9%	+ 3%
8000	+ 8%	+ 3%
9000	+ 8%	+ 2%
10000	+ 8%	+ 2%
11000	+ 7%	+ 2%
12000	+ 7%	+ 2%

The tolerances of Table 3 can be applied to a given data sample by first noting the vertical load level of the test, and then subtracting the indicated percentage error from the reported value of μ_x. For example, a tire which showed a μ peak value on dry asphalt of 0.89, when loaded to 6000 lbs F_z, would be corrected to read within the range defined by:

$$\frac{.89}{1.04} = .855 \text{ (high value)}$$

$$\frac{.89}{1.09} = .817 \text{ (low value)}$$

Since a given percentage error applies to all data taken at a given value of vertical load, peak to slide ratios and relative velocity sensitivities are unaffected by this error problem. The sensitivity of peak and slide μ_x performance to vertical load, however, must be corrected by the application of the Table 3 adjustments.

2.0 RESULTS OF THE BASELINE TESTING PROGRAM

2.1 BASELINE DATA PRESENTATION

Longitudinal shear force measurements were made on a set of eight truck tires covering the sizes indicated below:

8.25 x 20/E	Rated load, 4050 lbs.
9.00 x 20/E	Rated load, 4610 lbs.
10.00 x 20/F	Rated load, 5430 lbs.
11.00 x 22.5 /F	Rated load, 5430 lbs.
11.00 x 20/F	Rated load, 6290 lbs.
12.00 x 20/G	Rated load, 7000 lbs.
12.00 x 22.5/F	Rated load, 5920 lbs.
15.00 x 22.5/H	Rated load, 8460 lbs.

All tires were of cross-bias ply construction and highway rib tread pattern.

The data deriving from these tests are summarized in Table 4, in their uncorrected form. The μ-slip histories which are associated with each set of data in Table 4 are presented in Appendix 1. Strictly speaking, these data are qualified by the error tolerances described in Table 2. As discussed, however, we propose the Table 3 corrections as the most likely set of bounds for absolute interpretations. Thus a tabulation of high and low values for μ_p and μ_s is presented in Table 5, representing the application of Table 3 corrections to the baseline data. Table 5 presents the high and low limits which we feel specify the range of confidence in the values of μ_x.

TABLE 4

SUMMARY OF UNCORRECTED BASELINE DATA

Tire	20 mph Wet Jennite			40 mph Dry Asphalt			60 mph Dry Asphalt		
	F_z	μ_p	μ_s	F_z	μ_p	μ_s	F_z	μ_p	μ_s
	2010	.60	.36	1942	1.11	.59	2012	.95	.59
8.25-20/E	3984	.59	.31	4066	.92	.50	4043	.86	.53
	5675	.54	.27	5883	.86	.47	5936	.75	.46
	2571	.48	.25	2745	.97	.49	2609	.88	.49
9.00-20/E	4826	.53	.28	4929	.87	.45	4927	.78	.44
	6918	.49	.27	7006	.79	.41	7116	.66	.38
	3079	.56	.35	3079	1.01	.54	3138	1.00	.54
10.00-20/F	5601	.63	.31	5550	.89	.47	5662	.82	.48
	8407	.49	.29	8800	.73	.41	8362	.73	.43
	2740	.54	.36	3081	.87	.51	———	———	———
11.00-22.5/F	5380	.48	.25	5364	.88	.49	5507	.79	.48
	8376	.40	.23	8218	.68	.45	8214	.66	.44
	3240	.50	.33	3431	.85	.55	———	———	———
11.00-22/F	6542	.51	.30	6529	.87	.48	———	———	———
	9812	.41	.24	———	———	———	8344	.76	.46
	3820	.49	.27	3875	.95	.53	3859	.84	.53
12.00-20/G	7359	.42	.23	5544	.88	.48	5529	.87	.49
	11248	.37	.20	———	———	———	———	———	———
	3274	.52	.30	———	———	———	3369	.94	.52
12.00-22.5/F	5959	.52	.31	6078	.87	.46	6036	.81	.46
	9293	.42	.23	7830	.76	.42	7821	.76	.43
	4501	.45	.22	4353	.99	.53	4414	.86	.49
15.00-22.5/H	8749	.42	.22	6597	.87	.43	———	———	———
	13519	.36	.20	———	———	———	———	———	———

TABLE 5

SUMMARY OF BASELINE DATA CORRECTED PER THE TABLE 3 ERROR RANGE ESTIMATES

Tire	20 mph - Wet Jennite				40 mph - Dry Asphalt				60 mph - Dry Asphalt			
		μ_p		μ_s		μ_p		μ_s		μ_p		μ_s
	F_z	Hi -- Lo		Hi -- Lo	F_z	Hi -- Lo		Hi -- Lo	F_z	Hi -- Lo		Hi -- Lo
8.25-20/E	2010	.52	--.49	.31 --.30	1942	.97	--.91	.51 --.48	2012	.83	--.78	.51 --.48
	3984	.55	--.52	.29 --.27	4066	.85	--.75	.46 --.44	4043	.80	--.75	.49 --.46
	5675	.52	--.50	.26 --.25	5883	.83	--.79	.45 --.43	5936	.72	--.69	.44 --.42
9.00-20/E	2571	.42	--.40	.22 --.21	2745	.86	--.81	.43 --.41	2609	.78	--.73	.43 --.41
	4826	.50	--.48	.27 --.25	4929	.83	--.79	.43 --.41	4927	.74	--.71	.42 --.40
	6918	.48	--.45	.26 --.25	7006	.77	--.72	.40 --.38	7116	.64	--.61	.37 --.35
10.00-20/F	3079	.50	--.47	.31 --.30	3079	.90	--.86	.48 --.46	3138	.89	--.85	.48 --.46
	5601	.61	--.58	.30 --.28	5550	.86	--.82	.45 --.43	5662	.79	--.75	.46 --.44
	8407	.48	--.45	.28 --.27	8800	.71	--.68	.40 --.38	8362	.71	--.68	.42 --.40
11.00-22.5/F	2740	.48	--.45	.32 --.30	3081	.77	--.73	.45 --.43	----------			
	5380	.46	--.44	.24 --.23	5364	.84	--.80	.47 --.45	5507	.75	--.72	.46 --.44
	8376	.39	--.37	.22 --.21	8218	.66	--.63	.44 --.42	8214	.64	--.61	.43 --.41

TABLE 5 (Continued)

Tire	20 mph - Wet Jennite F_z	μ_p Hi -- Lo	μ_s Hi -- Lo	40 mph - Dry Asphalt F_z	μ_p Hi -- Lo	μ_s Hi -- Lo	60 mph - Dry Asphalt F_z	μ_p Hi -- Lo	μ_s Hi -- Lo
	3240	.45 --.43	.30 --.28	3431	.77 --.73	.50 --.47		----------	
11.00-22/F	6542	.50 --.47	.29 --.28	6529	.84 --.80	.47 --.44		----------	
	9812	.40 --.38	.24 --.22		----------		8344	.75 --.70	.45 --.43
	3820	.45 --.43	.25 --.24	3875	.88 --.83	.49 --.46	3859	.78 --.74	.49 --.46
12.00-20/G	7359	.40 --.39	.22 --.21	5544	.85 --.81	.46 --.44	5529	.83 --.80	.47 --.45
	11248	.36 --.35	.20 --.19		----------			----------	
	3274	.47 --.44	.27 --.26		----------		3369	.85 --.80	.47 --.44
12.00-22.5/F	5959	.50 --.48	.30 --.28	6078	.84 --.80	.44 --.42	6036	.78 --.74	.44 --.42
	9293	.41 --.39	.22 --.21	7830	.74 --.70	.41 --.39	7821	.74 --.70	.42 --.40
	4501	.42 --.41	.21 --.20	4353	.93 --.89	.50 --.48	4414	.81 --.77	.46 --.44
15.00-22.5/h	8749	.41 --.39	.21 --.20	6597	.84 --.80	.42 --.39		----------	
	13519	.35 --.34	.20 --.19		----------			----------	

2.2 DISCUSSION OF RESULTS AND BASIC FINDINGS

A direct observation which can be made from the presented data concerns the large peak-to-slide ratio exhibited by all tires in the sample—even on dry paved surfaces. This property, which contrasts markedly with passenger car tire performance, is felt to constitute a valid representation of a commercial tire characteristic which is of great significance to limit stopping distance performance.

Another finding which we feel to be supported in the data concerns a significant, though not universally exhibited, sensitivity of shear force potential to vehicle velocity. Extending the velocity sensitivity indications which appear in the baseline data, an extra set of data was taken using a 10.00 x 20/F tire over a large range of velocities, including a few very low speed runs. The results are plotted in Figure 4 in terms of corrected μ_p and μ_s. We would speculate that the very large increase in shear force potential at velocities near zero is a potentially contributing factor to the violent terminal behavior exhibited by many trucks at the conclusion of a limit stopping test.

An observation of vertical load sensitivity can be made from the data shown in Figure 5 which indicates the load sensitivity on dry asphalt of the 9:00 x 20/E tire. Since this tire was one whose F_x versus torque relation was measured in the laboratory (see Table 1), a total correction in F_x was achieved. The F_z condition was evaluated using the negative polarity error limits shown in Figure 3. The F_z influence described in the Figure 5 cross plot shows a sensitivity of normalized longitudinal force to load which results in a nearly equal percentage loss in both μ_p and μ_s over the range examined.

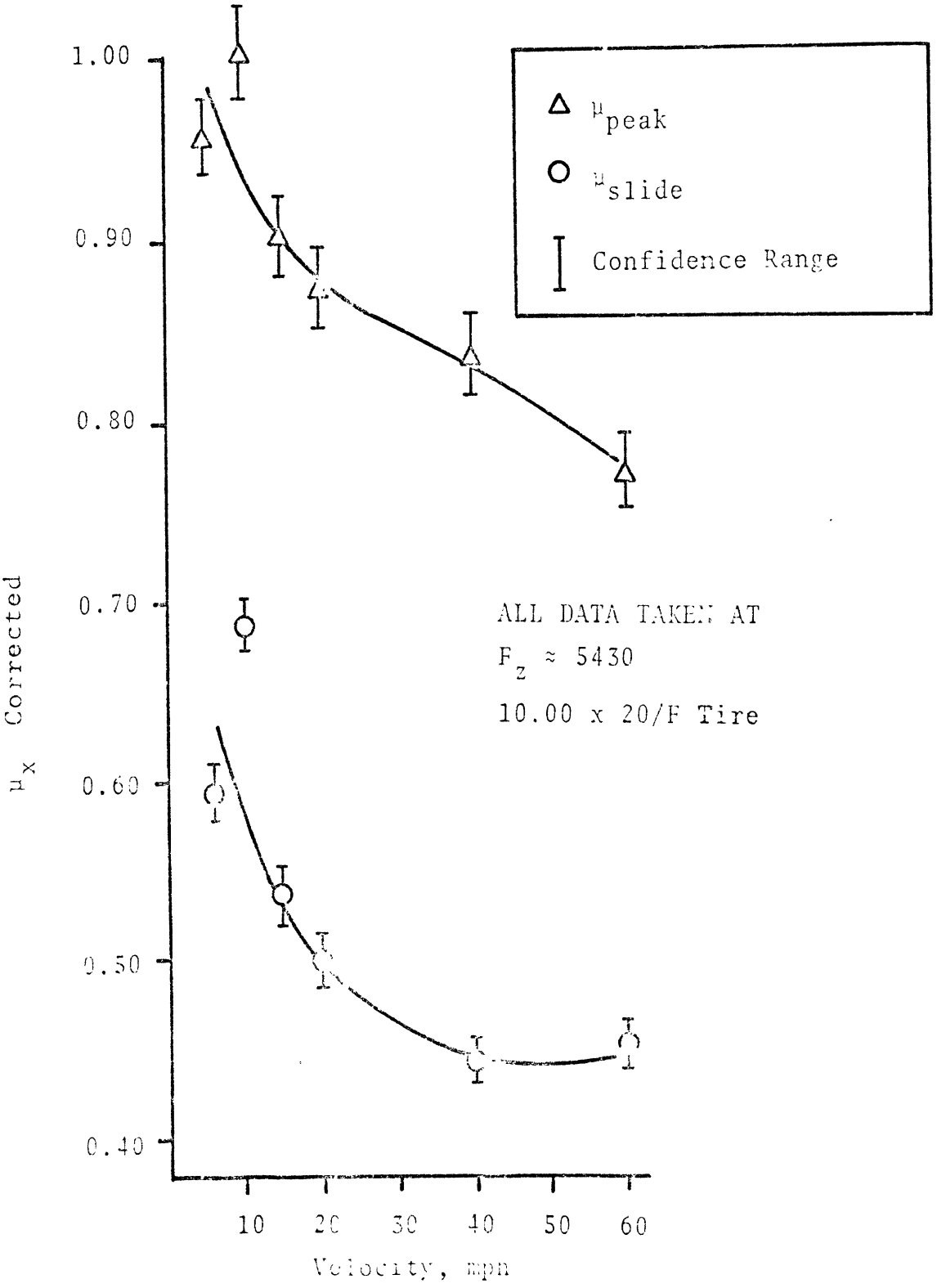

Figure 7. Velocity sensitivity data.

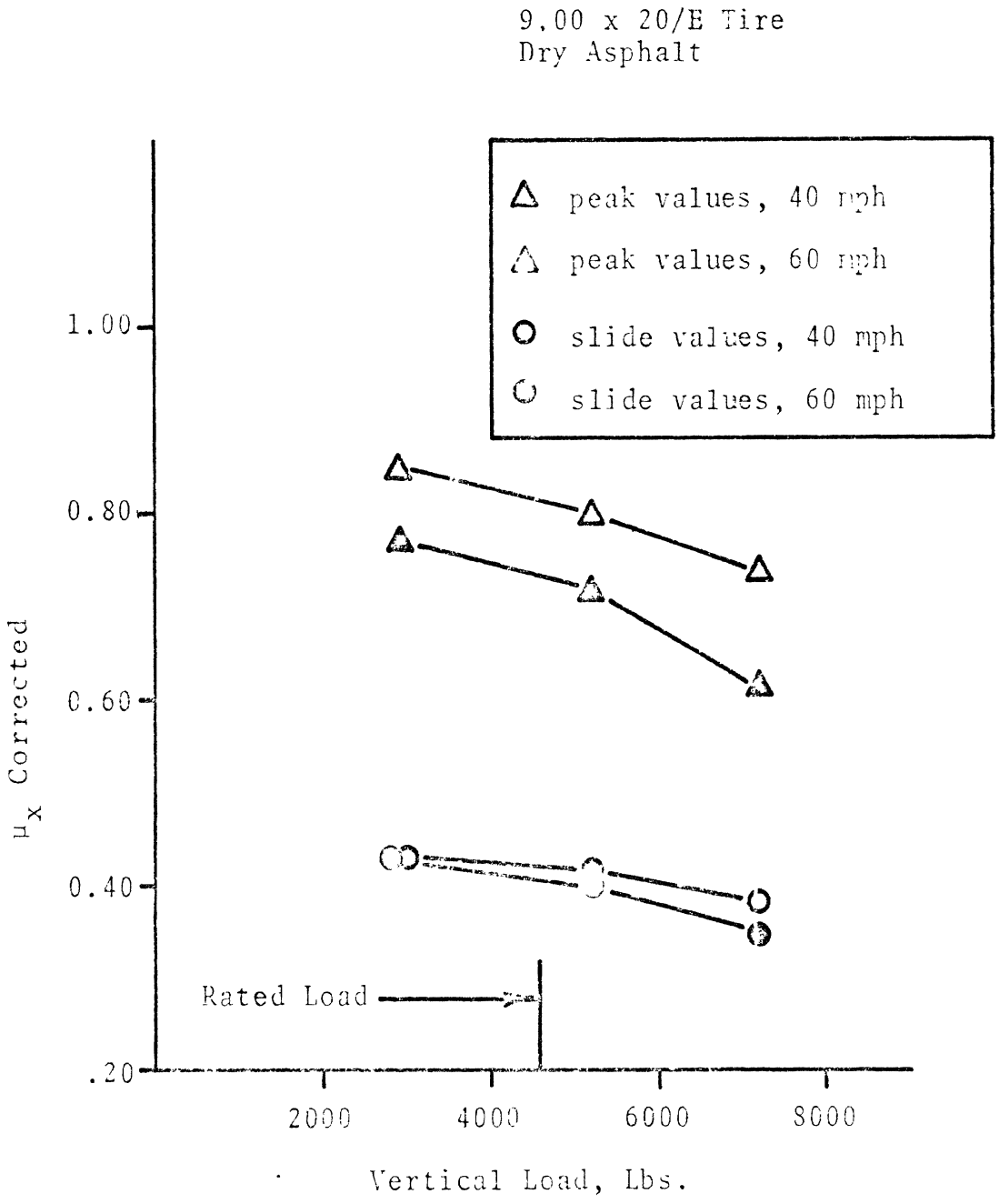

Figure 5. Example of vertical load sensitivity. (Values corrected using Table 1 measurements for this tire and Figure 3—negative polarity error limit).

A rather remarkable consistency in μ_p and μ_s was observed over the eight-tire sample for the rated load condition on dry asphalt at 40 mph (for which a full set of eight data points is available). For each tire the mean corrected values of μ_p and μ_s are presented in Table 6, showing a very narrow range of both peak and slide values. Although all but the 10.00 x 20 tire were made by the same manufacturer, one might have anticipated a much broader spread in dry friction performance, if one were to extrapolate from passenger car tire experience [5]. Despite this consistency in normalized shear force performance near rated load, varying load sensitivities are apparent across the tire sample such that consistency at other load levels is not comparable to that shown in Table 6.

TABLE 6

Tire	μ_{peak}	μ_{slide}
8.25 x 20/E	80	45
9.00 x 20/E	81	42
10.00 x 20/F	84	44
11.00 x 22.5/F	82	46
11.00 x 20/F	82	45
12.00 x 20/G	83	45
12.00 x 22.5/F	82	43
15.00 x 22.5/H	82	40

With regard to the μ_x versus slip histories presented in Appendix 1, the most notable peculiarity in shape concerns the slim, narrow-slip-range peaks which occur on dry surfaces as opposed to the broad, and rather flat, peaks which are measured on the wet coated asphalt. These curve-shape characteristics are completely reversed from that normally observed with passenger car tires [6].

While the fidelity of the curve shape at large slip values ($s > 75\%$) is not as high quality as it is in the low slip range of these data, there is an inflection at high slip in many of the dry asphalt data curves which is intriguing; and, we believe, factual. As shown in Figure 6, the abrupt change in slope which occurs near $s = 85\%$ accounts for a large additional decrement in μ_x. Thus it would appear that a large "price" is paid in sustaining the lockup condition itself, while the mid-slip range imposes losses in force production which are not as severe as the high "peak-to-slide" ratios would suggest. It is presumed that the indicated high slip inflection derives from some thermal sensitivity to the localized heating of the near-lockup condition.

2.3 CONCLUDING REMARKS

Although we have, unfortunately, found it necessary to qualify certain aspects of the data presented herein, it does appear that a number of meaningful observations can be drawn. Given the current limitations in available data describing the longitudinal (or any other) shear force characteristics of truck tires, the measurements reported here are felt to be useful in filling an existing need. They suggest that the commercial vehicle tire, to the extent represented in our sample, is quite unlike the passenger car tire in many of the characteristics which are relevant to the limit braking performance of highway vehicles. Certain properties are at such variance with our current models of longitudinal traction mechanics that serious efforts must be undertaken to examine the matter in depth.

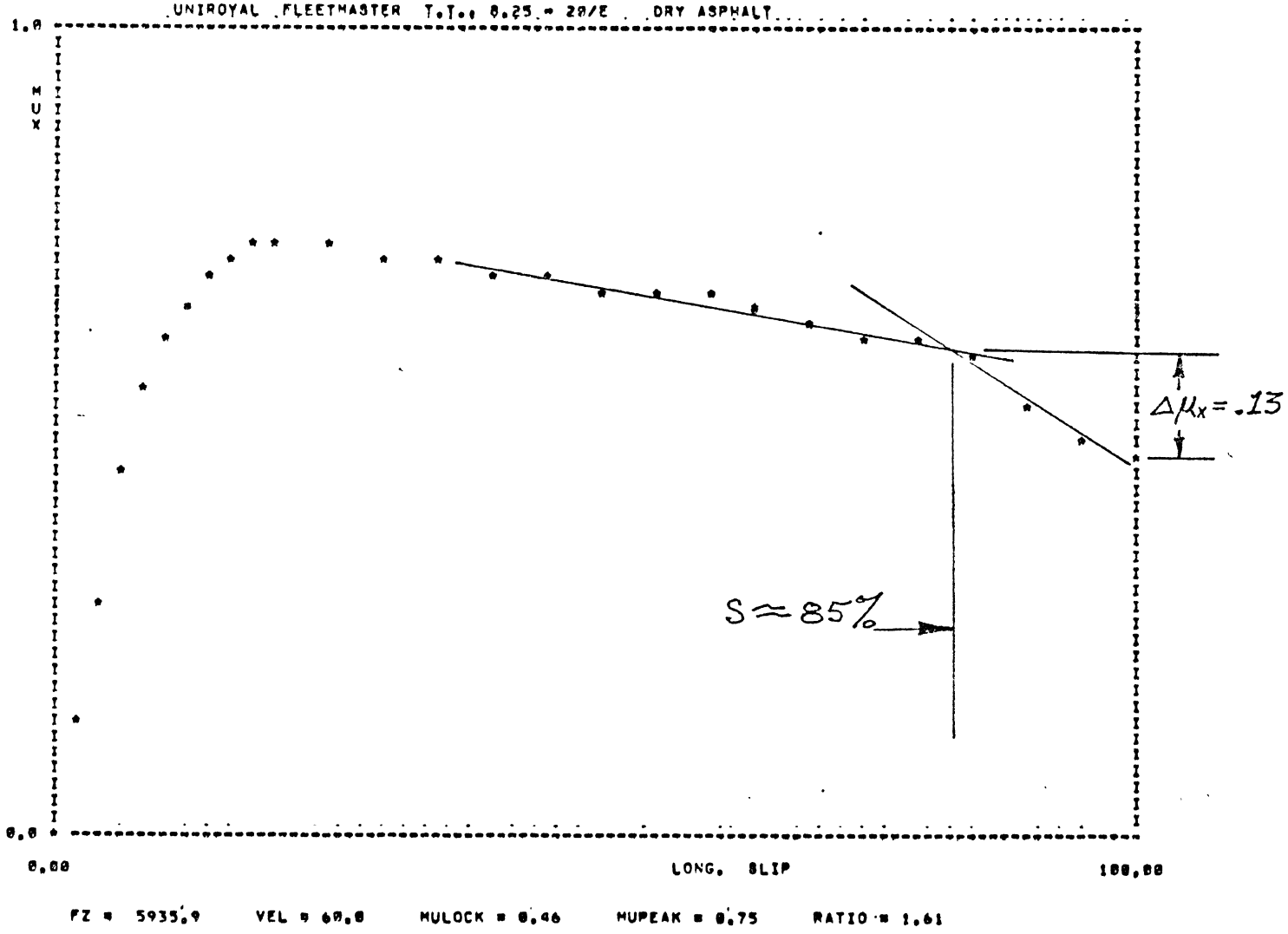

Figure 6. Example of high-slip inflection in dry pavement μ_x-slip history.

The data presented are seen as only indicators of certain qualitative relationships. These indications must be pursued with measurements of broader samples of tires—under more comprehensive sets of conditions. Presumably, as the HSRI machine becomes perfected, and as other appropriately equipped agencies undertake extensive measurement and subsequent publication, this lightly-touched area of tire mechanics will be developed into the technology which is needed in predicting commercial vehicle braking performance.

APPENDIX 1

PRINT-PLOT DISPLAYS OF μ-SLIP HISTORIES

In this appendix, individual μ-slip histories are presented as outputted through a digital line printer. The graduation of the ordinate scale provides a print increment every 0.02 units of "μ_x". The graduation of the abscissa scale provides a print increment for each 1% slip. The printed header at the top of the graph indicates the tire sample and the surface for which the data applies. The print out located below each graph indicates the vertical load and velocity conditions under which the data were obtained, and also lists the value of μ at 100% slip (MULOCK) and the peak value of μ (MUPEAK). Also, the ratio of MUPEAK/MULOCK is printed.

The data graphs are arranged by tire sample with each tire's data presented in the following sequence:

1)	20 mph wet jennite	F_{z1}
2)		F_{z2}
3)		F_{z3}
4)	40 mph dry asphalt	F_{z1}
5)		F_{z2}
6)		F_{z3}
7)	60 mph dry asphalt	F_{z1}
8)		F_{z2}
9)		F_{z3}

In the 72-point matrix of data, defined by eight tires times nine conditions, there are a total of nine (9) missing points as were indicated in Table 4.

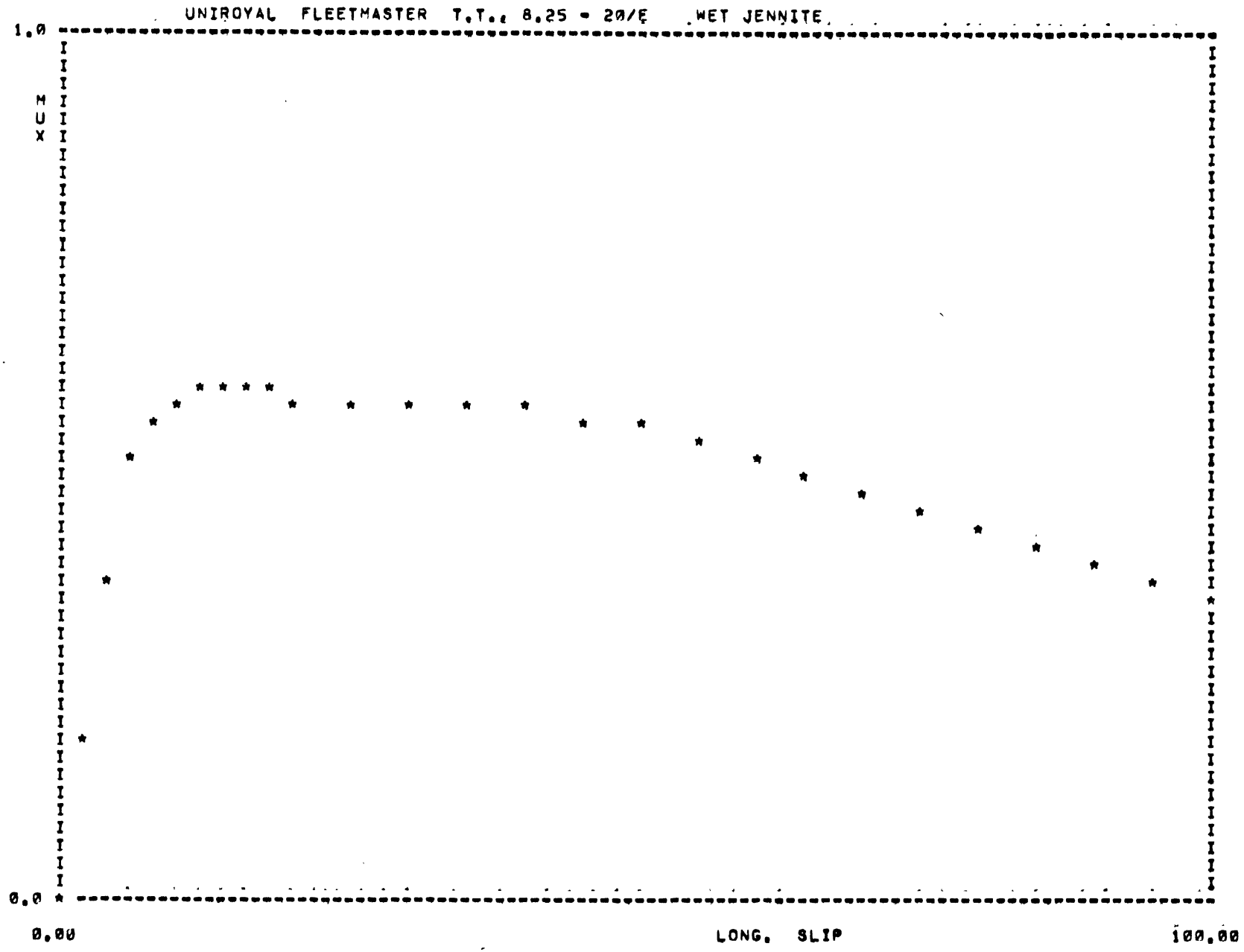

FZ = 2010.5 VEL = 20.0 MULOCK = 0.36 MUPEAK = 0.60 RATIO = 1.67

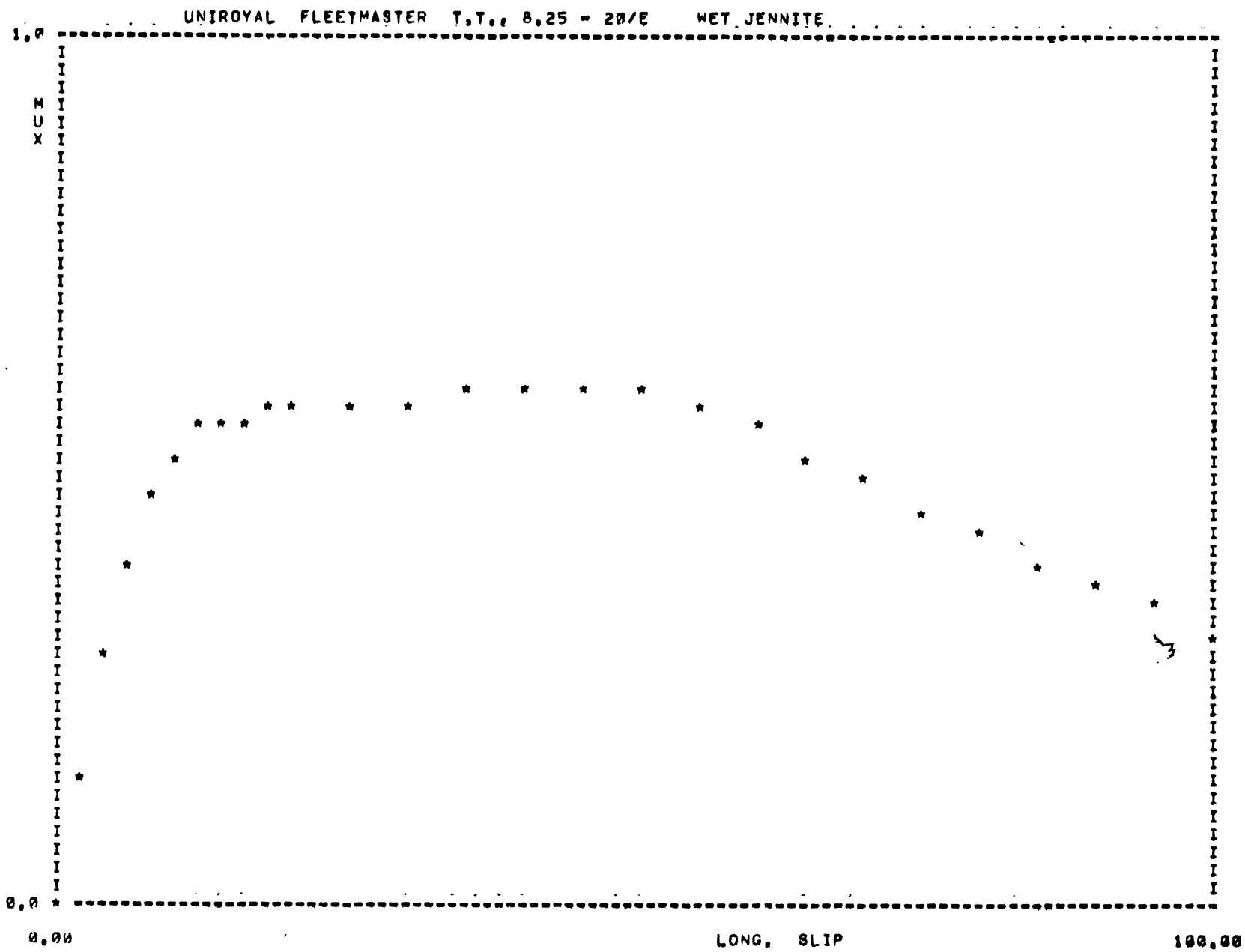

FZ = 3984,9 VEL = 20,0 MULOCK = 0,31 MUPEAK = 0,59 RATIO = 1,92

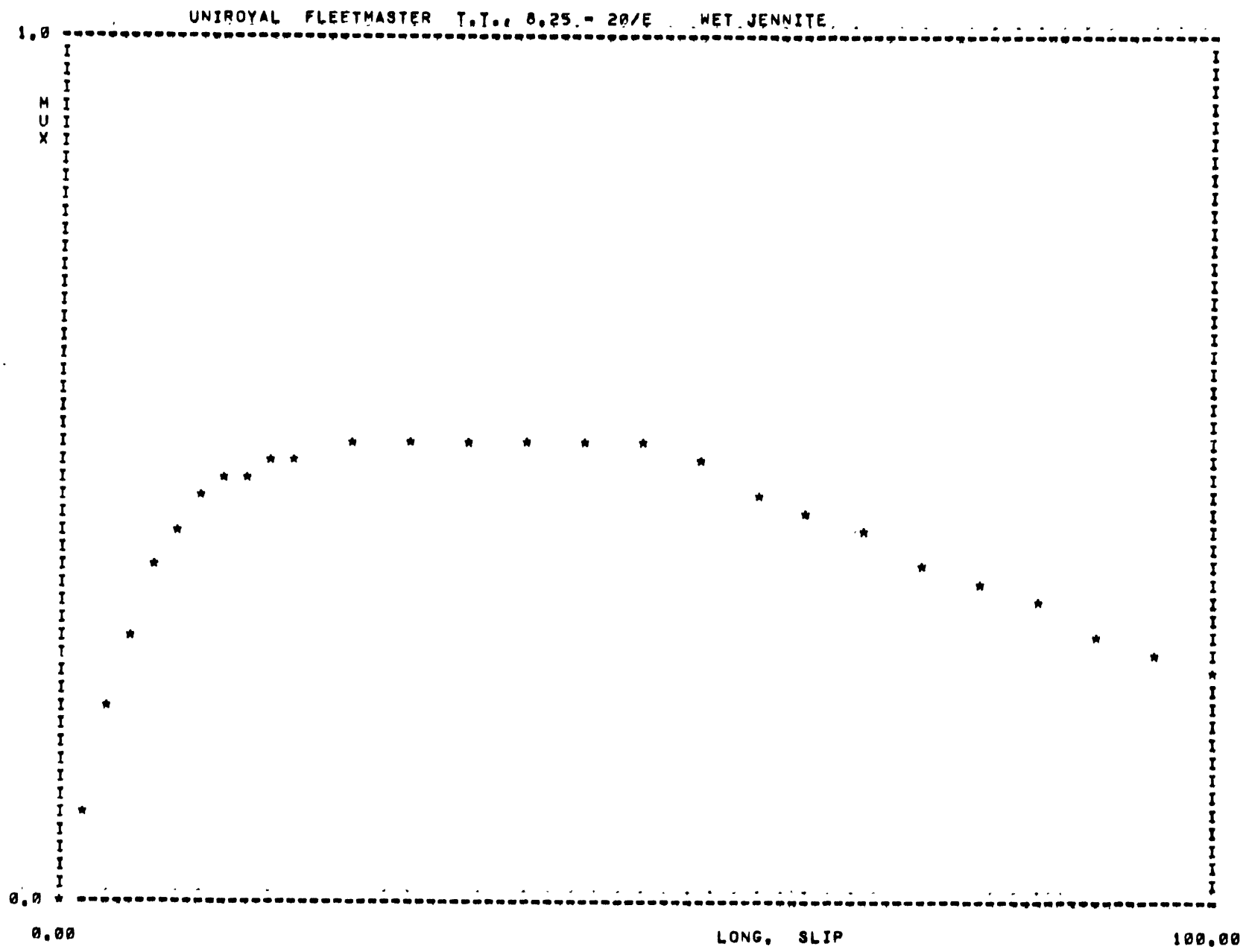

FZ = 5675.3 VEL = 20.0 MULOCK = 0.27 MUPEAK = 0.54 RATIO = 2.02

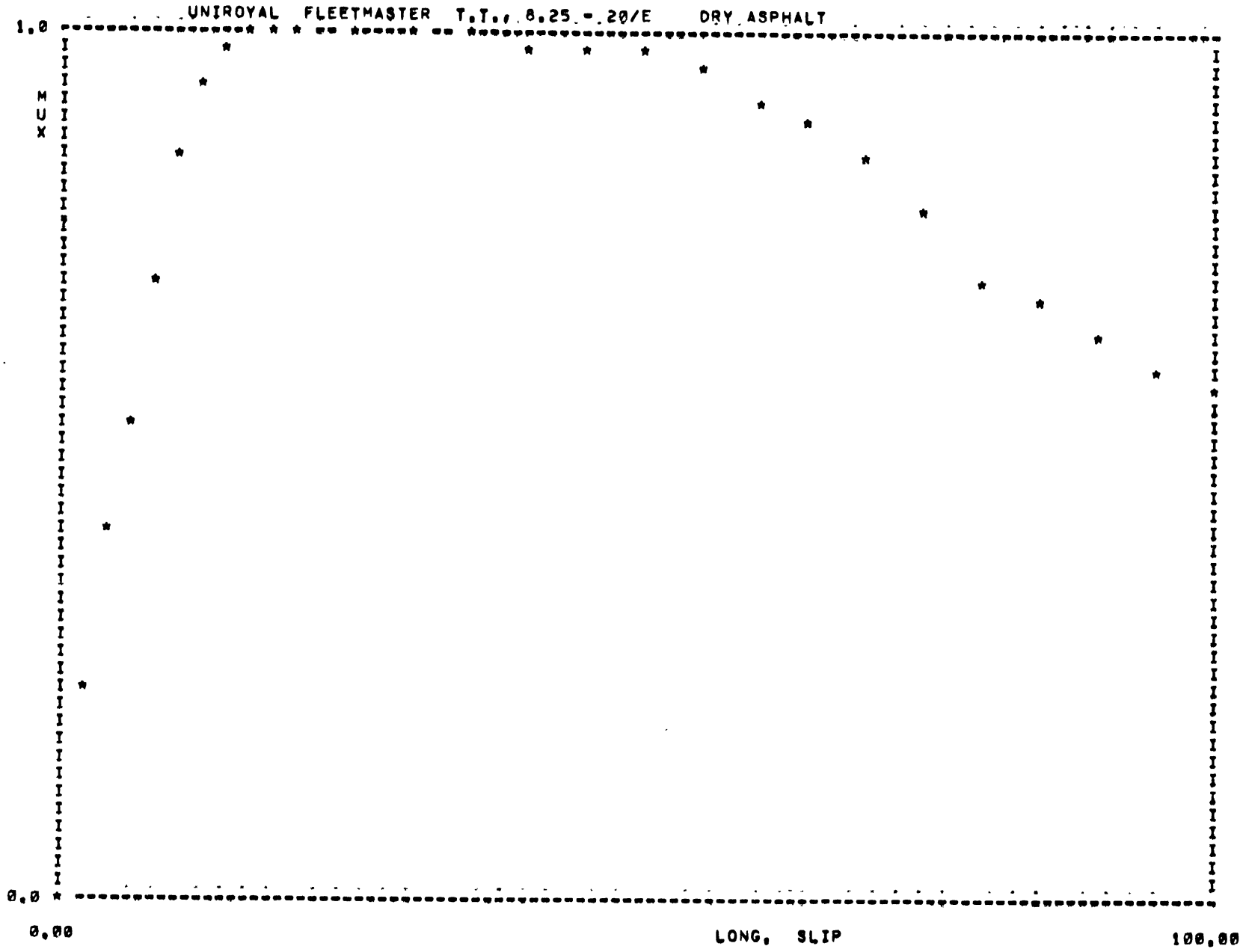

FZ = 1942.3 VEL = 40.0 MULOCK = 0.59 MUPEAK = 1.11 RATIO = 1.89

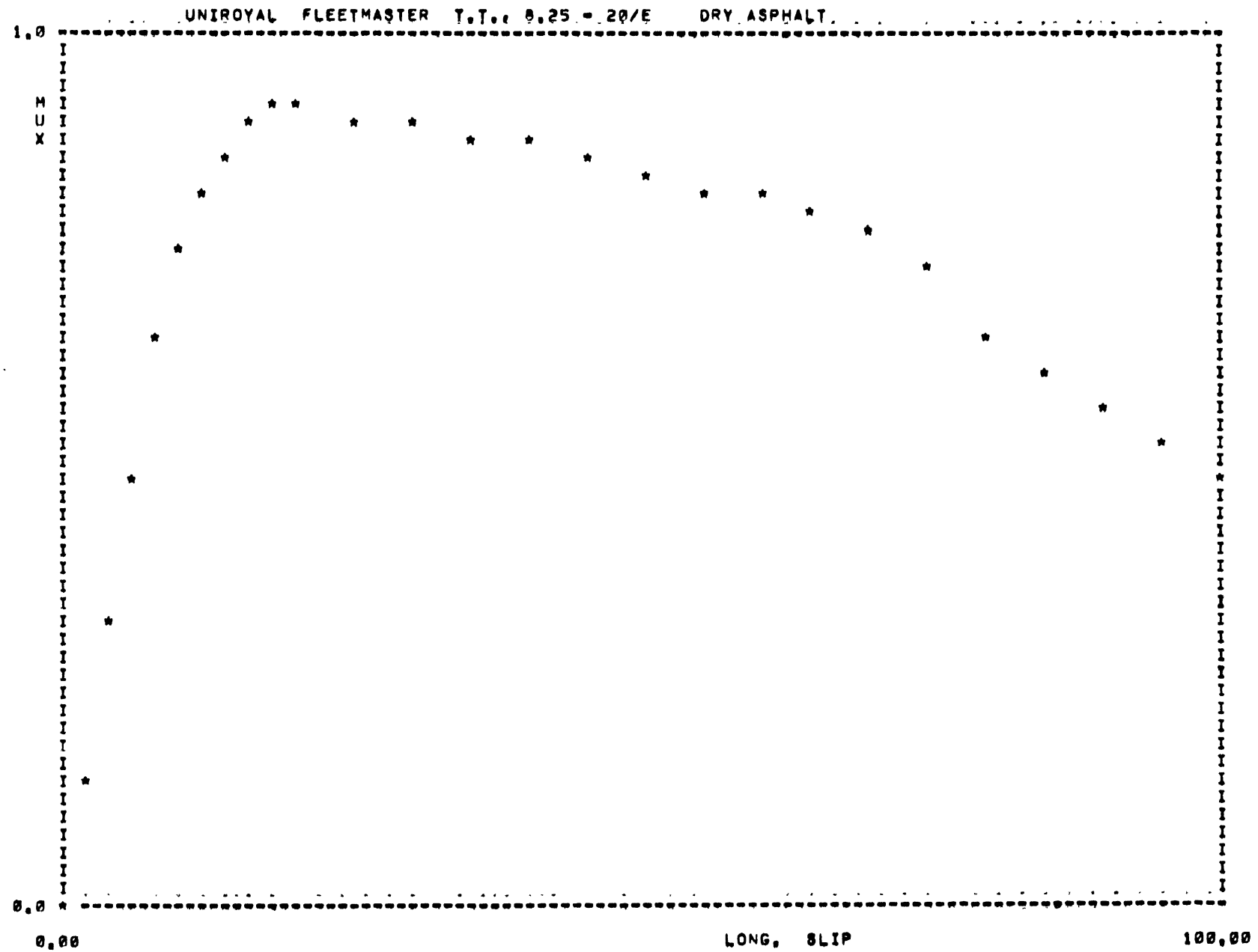

FZ = 4066.7 VEL = 40.0 MULOCK = 0.50 MUPEAK = 0.92 RATIO = 1.85

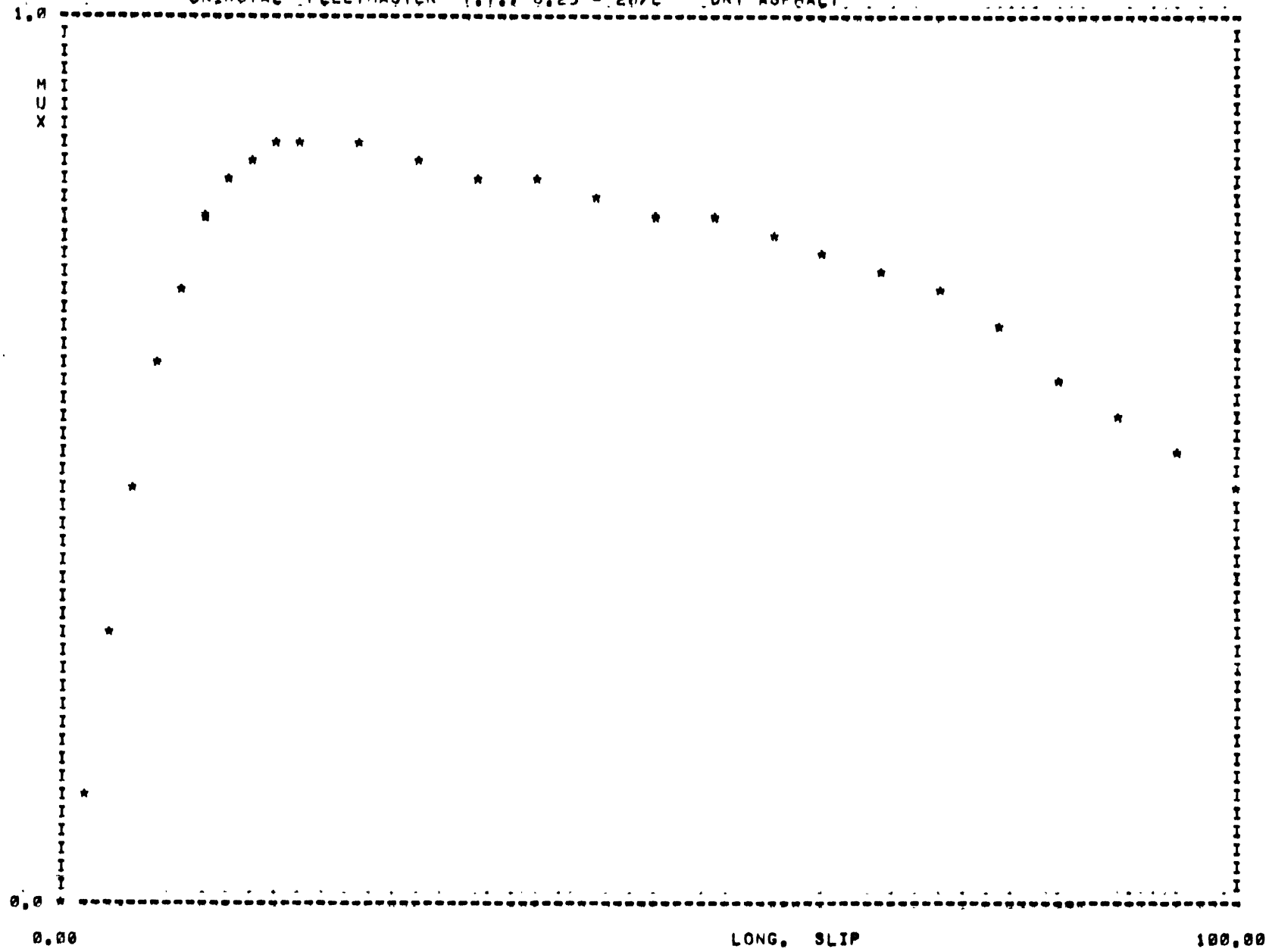

FZ = 5883.6 VEL = 40.0 MULOCK = 0.47 MUPEAK = 0.86 RATIO = 1.83

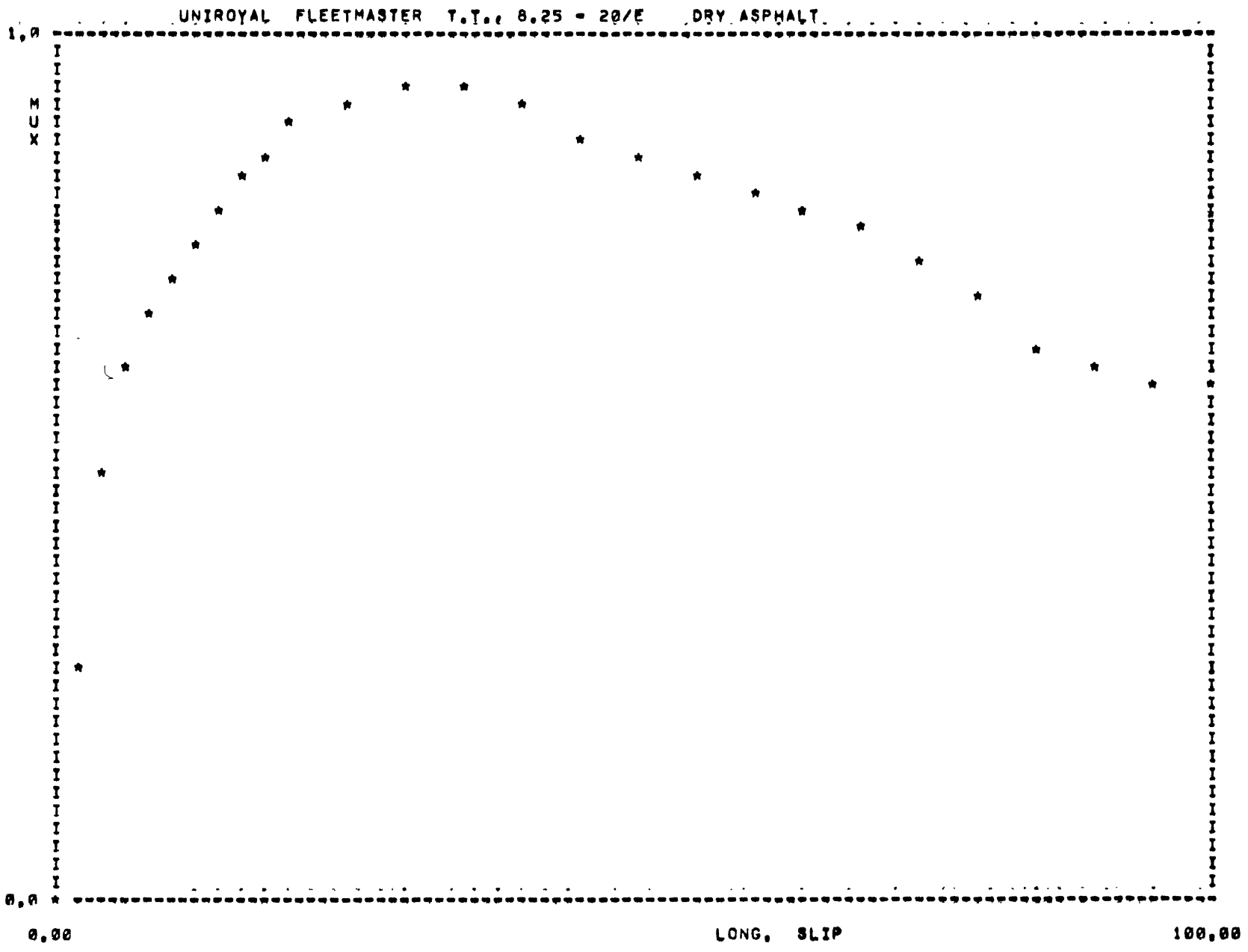

FZ = 2012.2 VEL = 60.0 MULOCK = 0.59 MUPEAK = 0.95 RATIO = 1.60

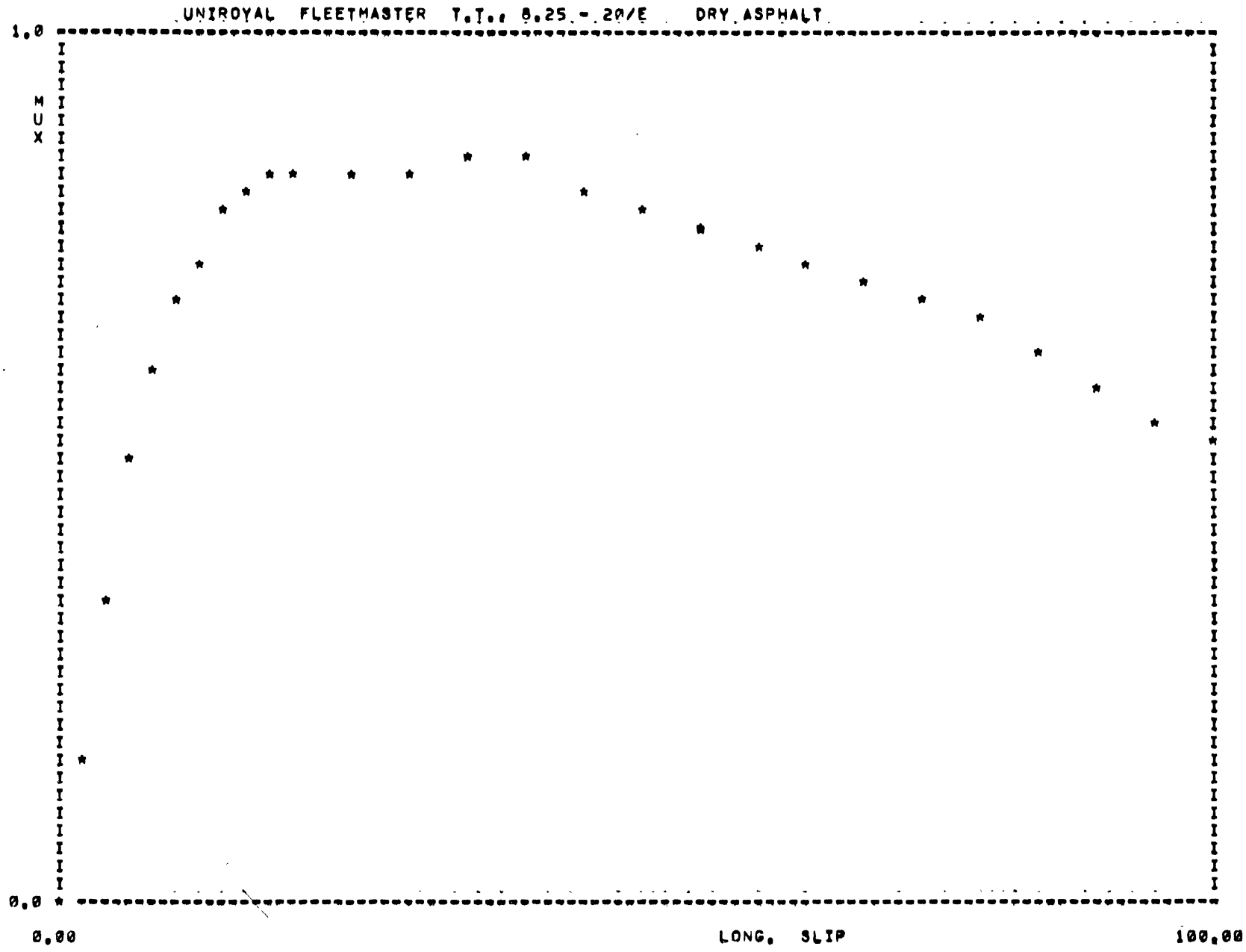

FZ = 4043.8 VEL = 60.0 MULOCK = 0.53 MUPEAK = 0.86 RATIO = 1.62

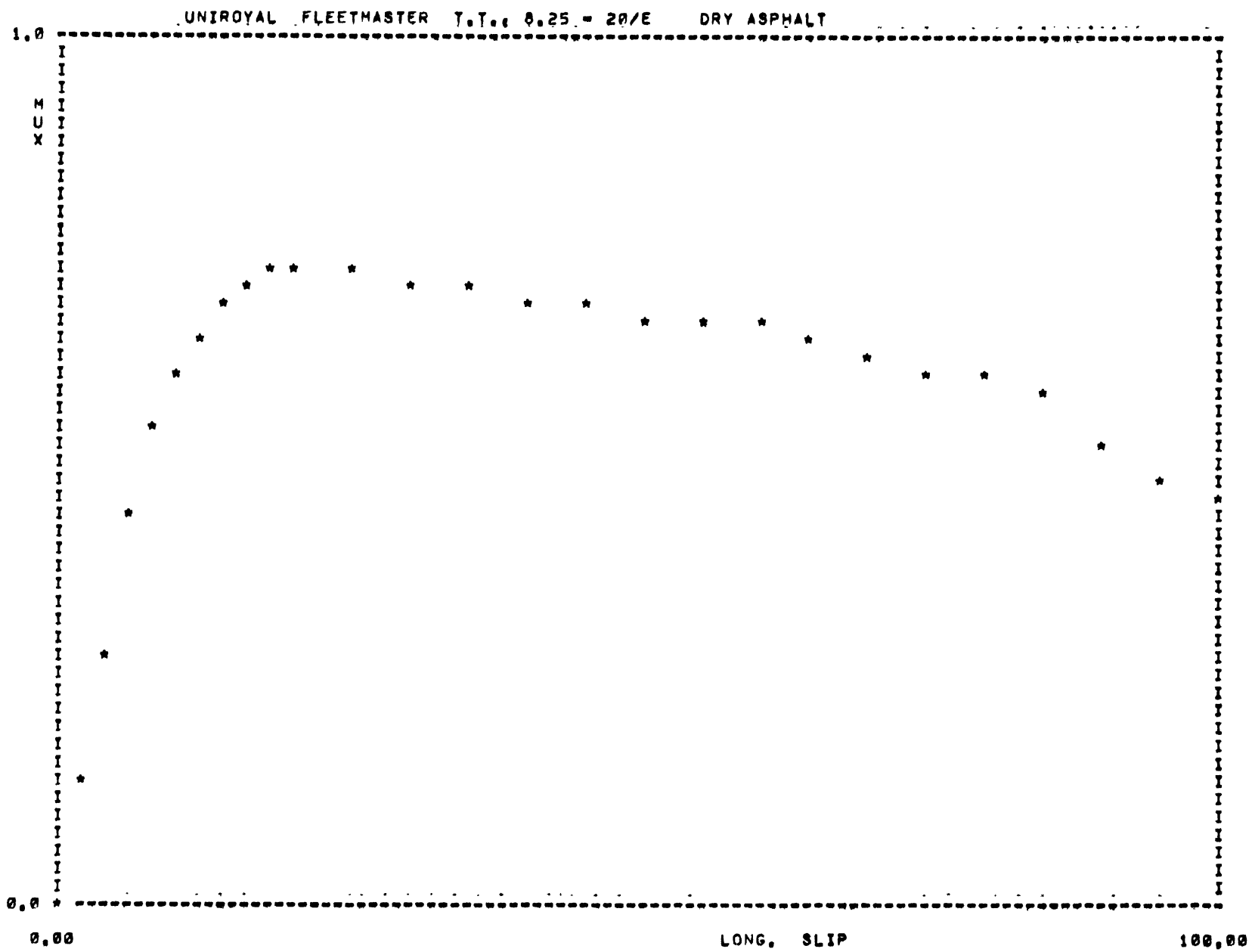

FZ = 5935.9 VEL = 60.0 MULOCK = 0.46 MUPEAK = 0.75 RATIO = 1.61

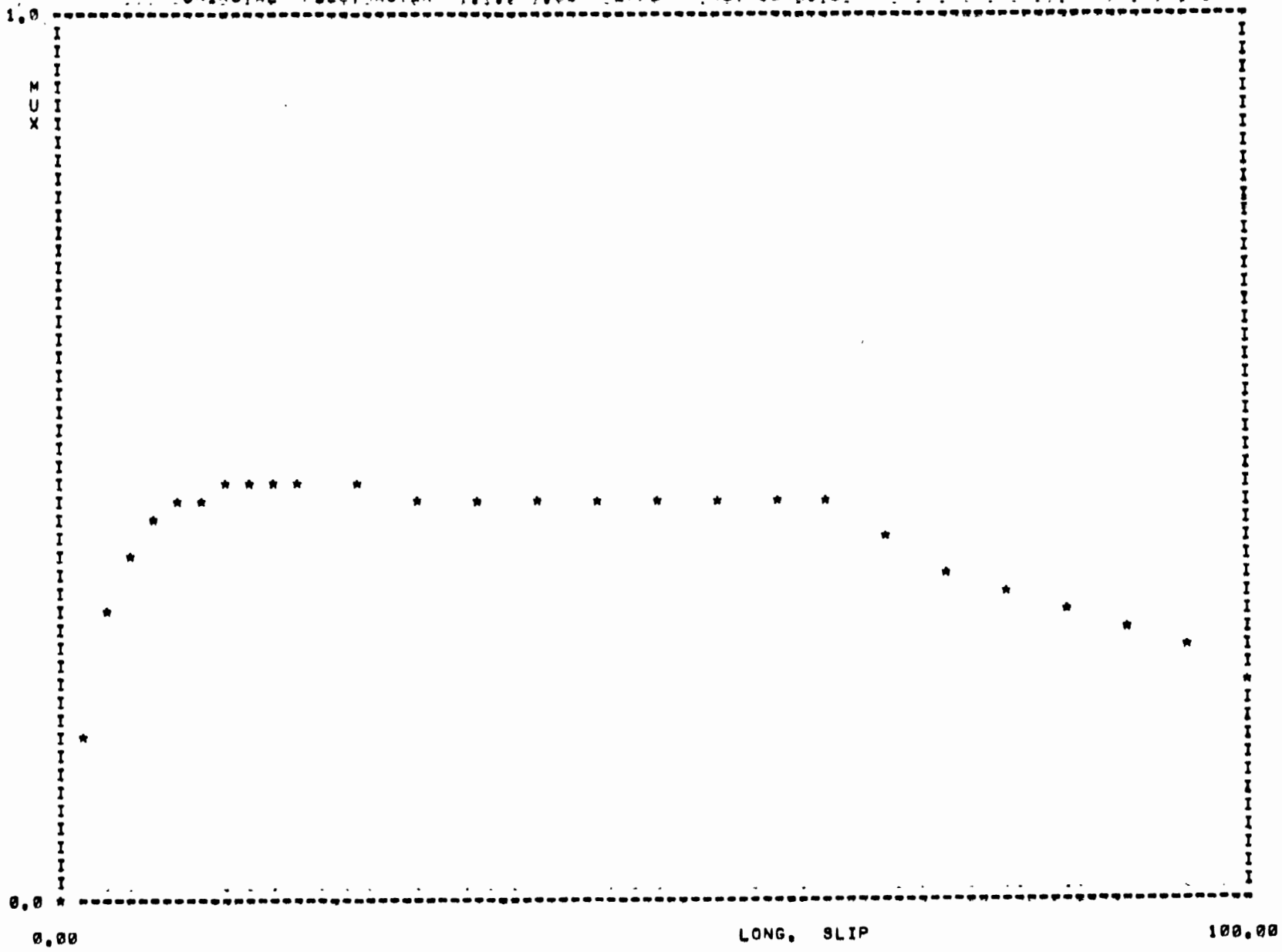

FZ = 2571.2 VEL = 20.0 MULOCK = 0.25 MUPEAK = 0.48 RATIO = 1.90

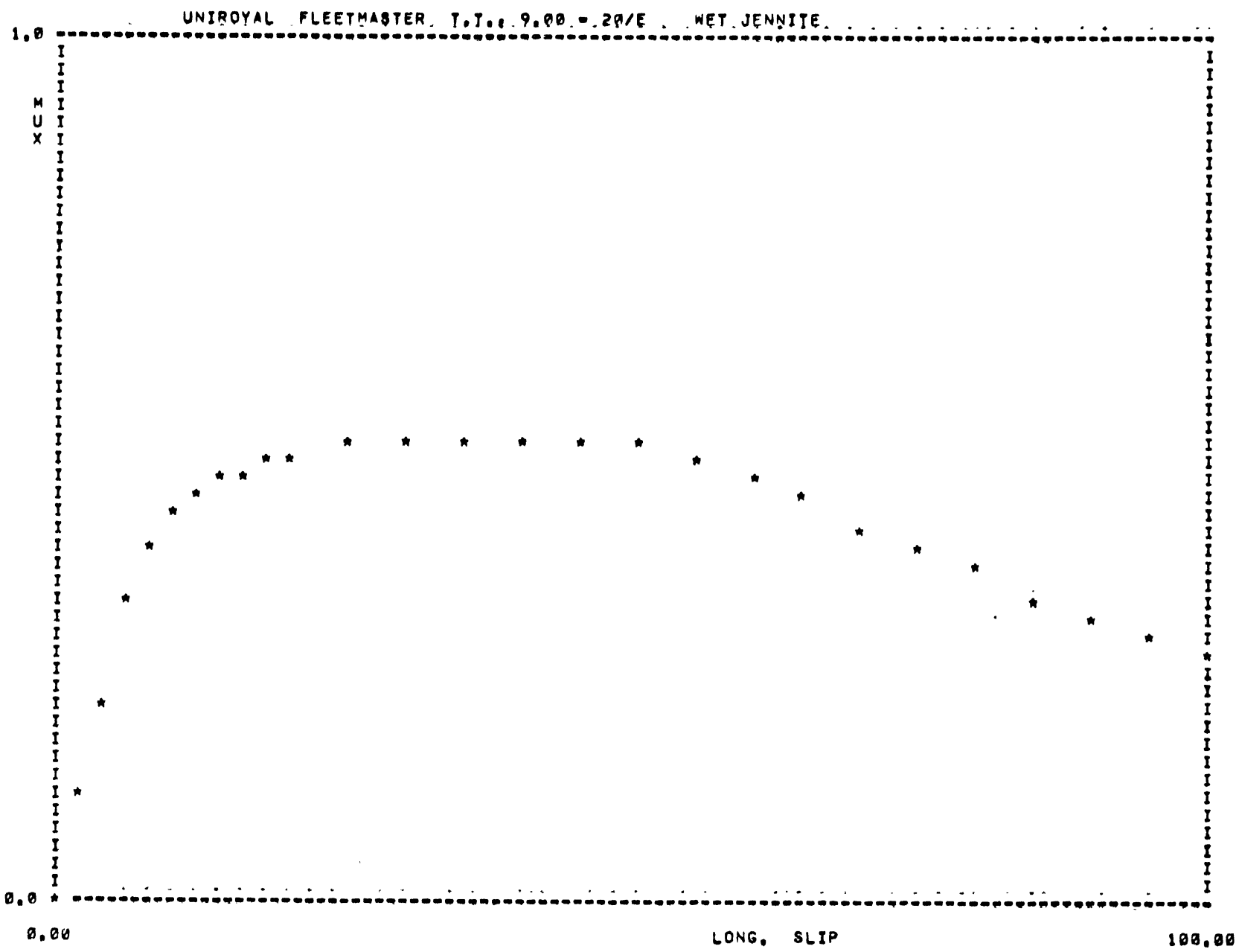

FZ = 4826.3 VEL = 20.0 MULOCK = 0.28 MUPEAK = 0.53 RATIO = 1.89

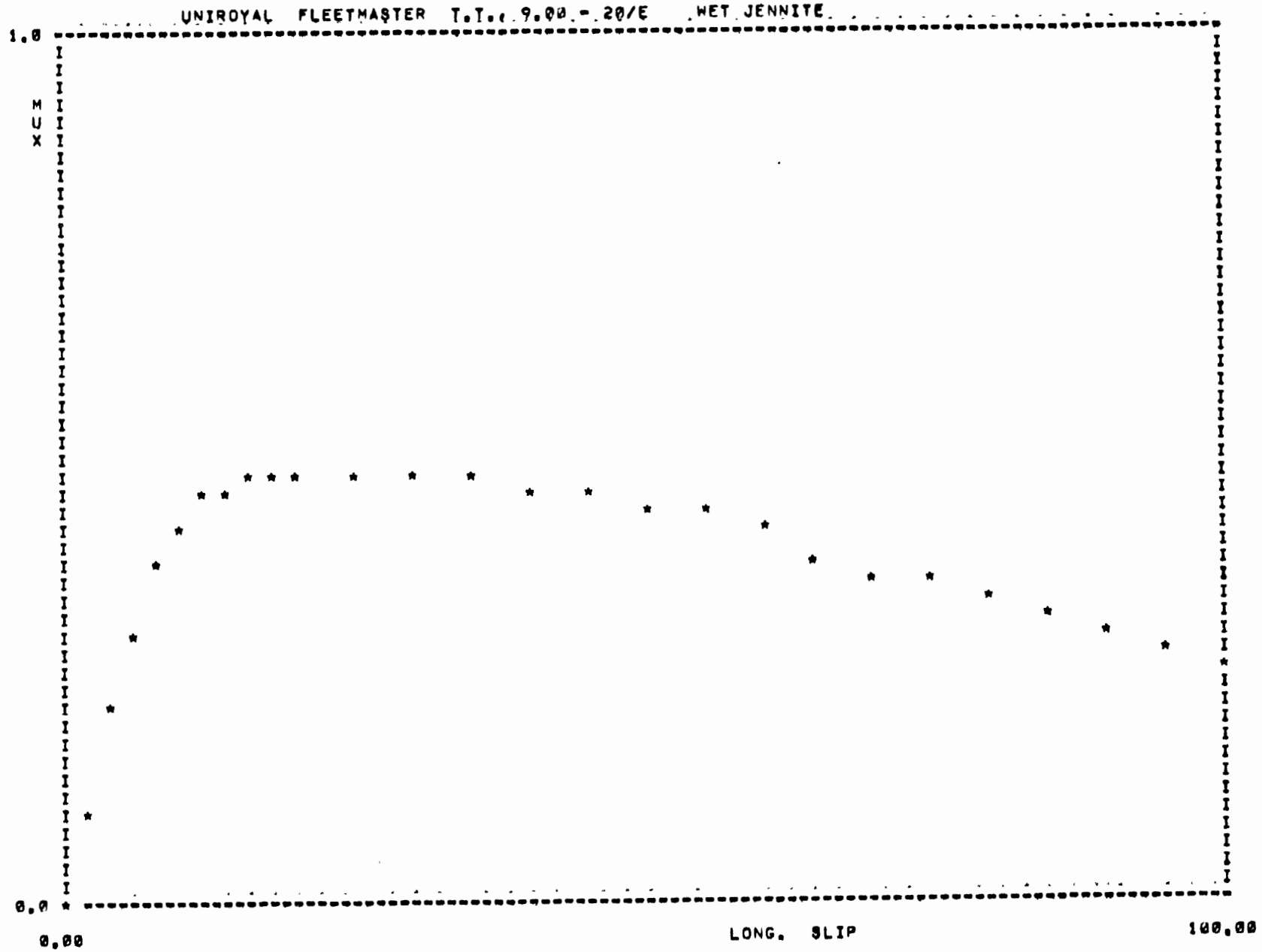

FZ = 6918.2 VEL = 20.0 MULOCK = 0.27 MUPEAK = 0.49 RATIO = 1.86

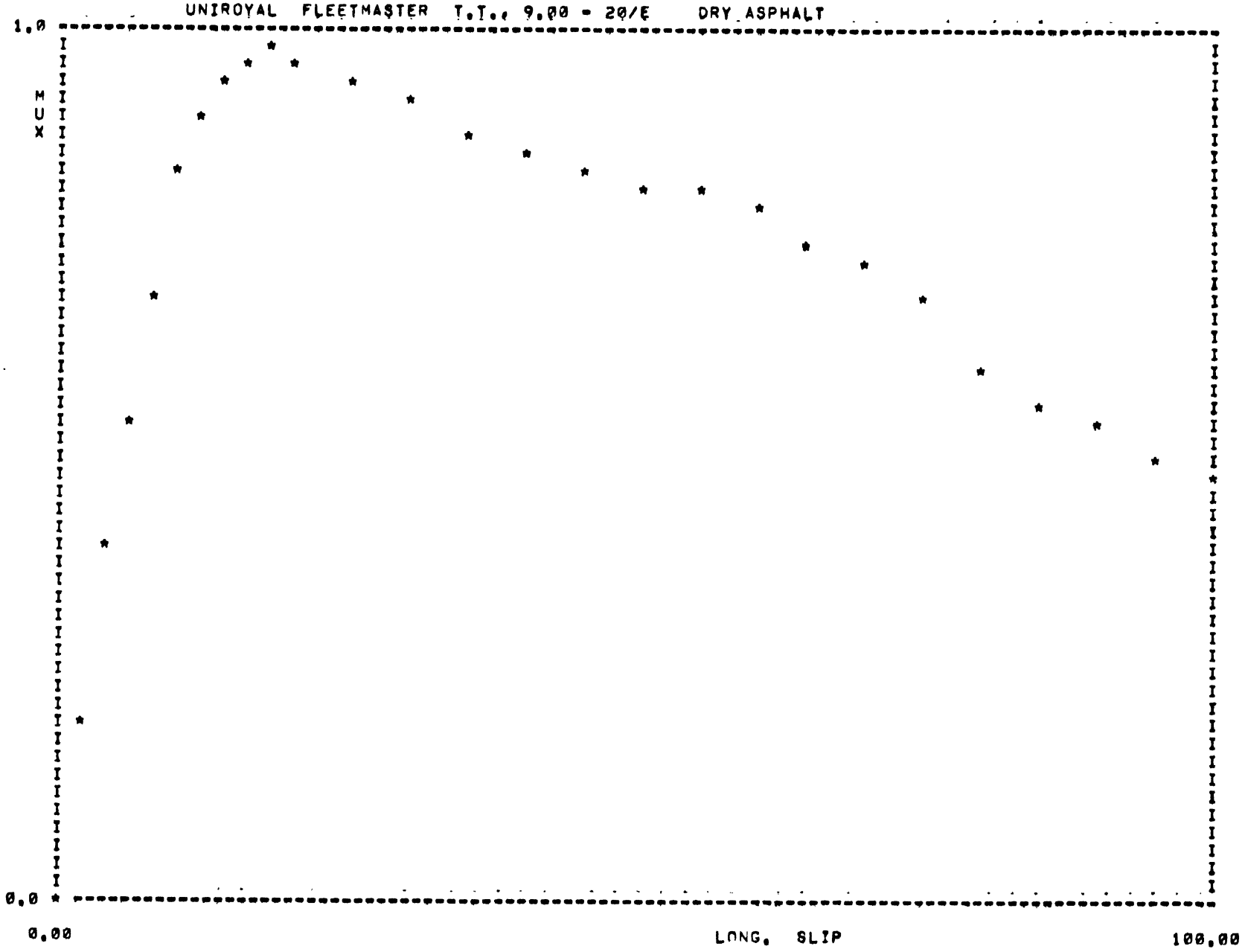

FZ = 2745.1 VEL = 40.0 MULOCK = 0.49 MUPEAK = 0.97 RATIO = 1.99

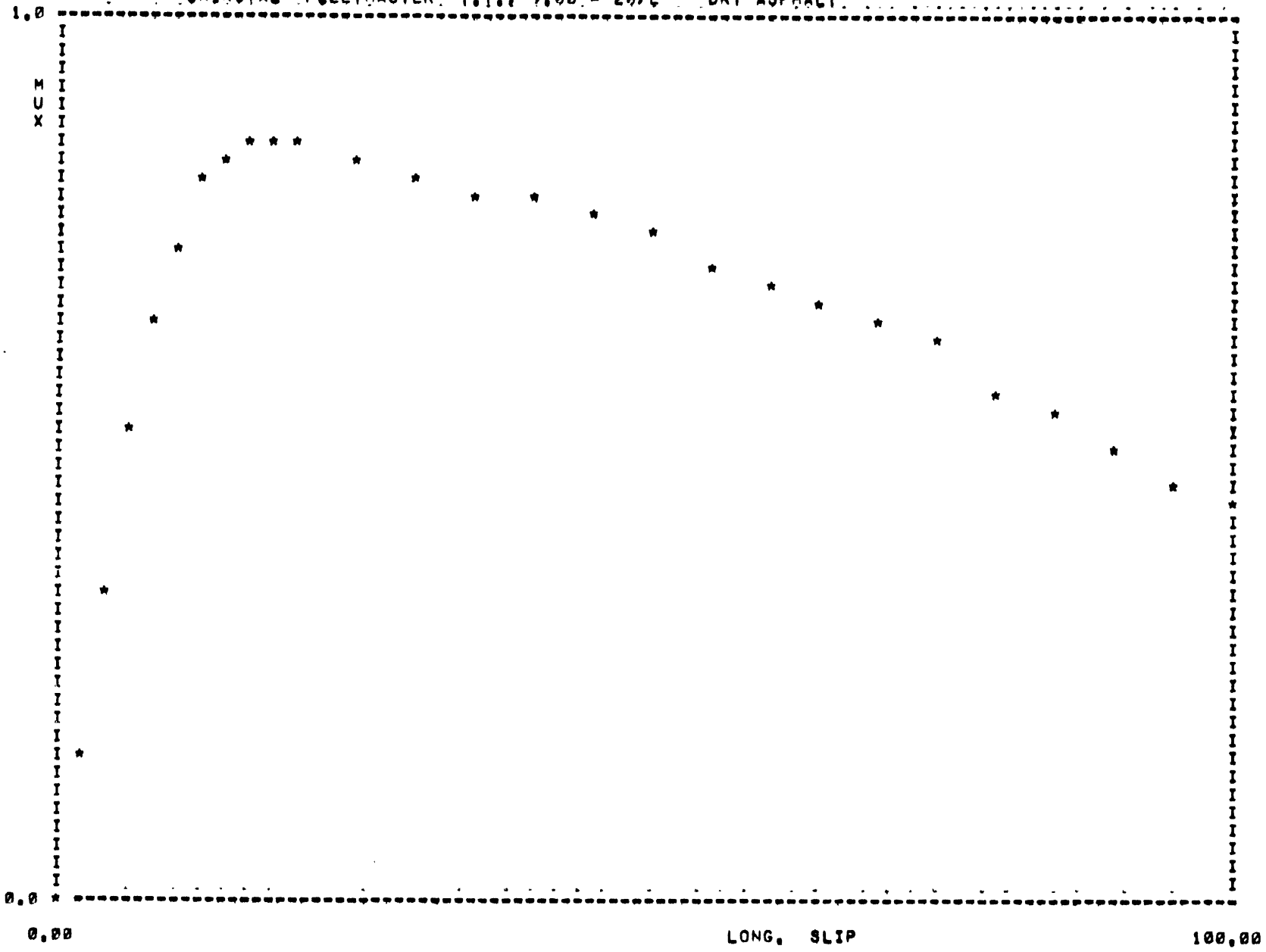

FZ = 4929.7 VEL = 40.0 MULOCK = 0.45 MUPEAK = 0.87 RATIO = 1.94

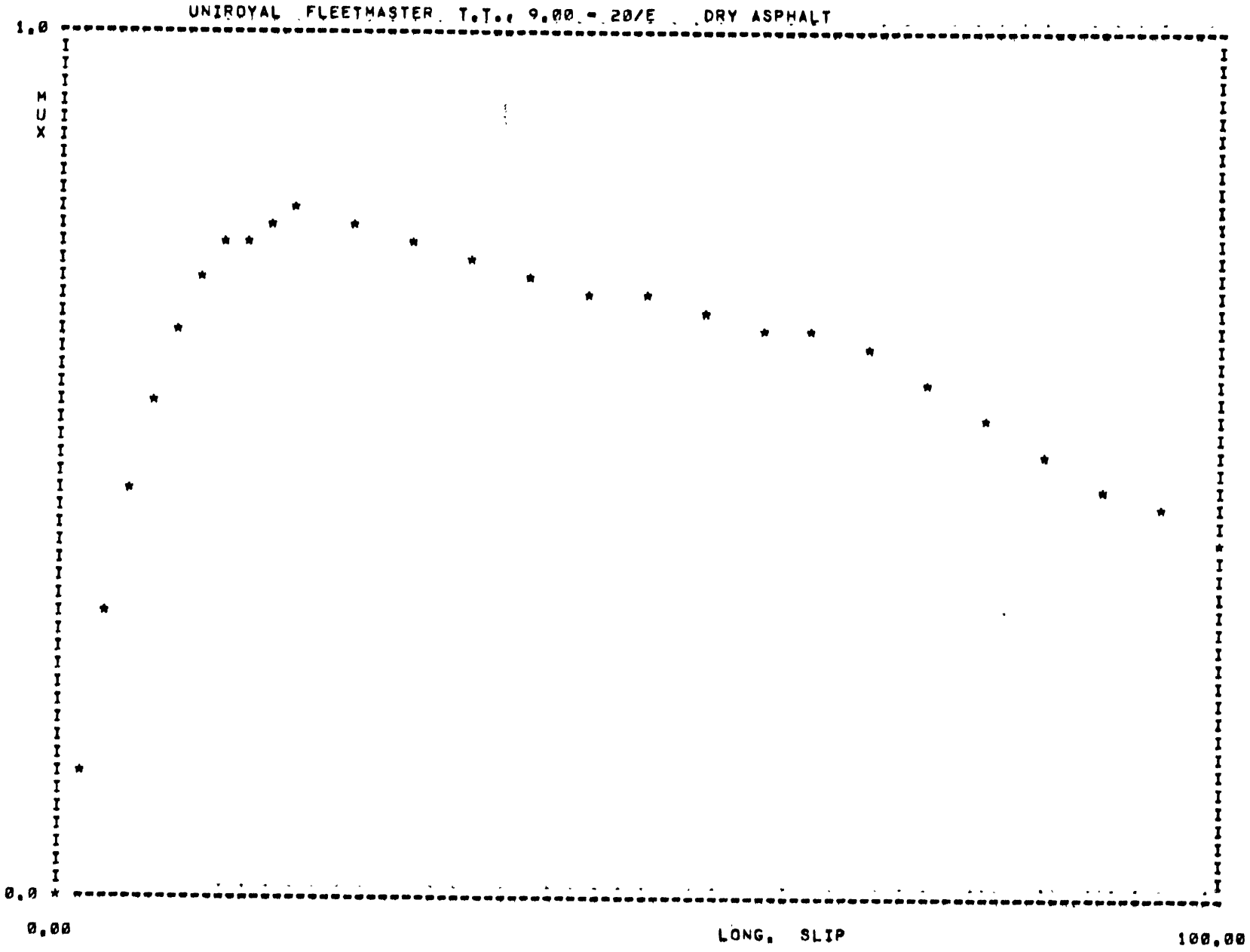

FZ = 7006.8 VEL = 40.0 MULOCK = 0.41 MUPEAK = 0.79 RATIO = 1.93

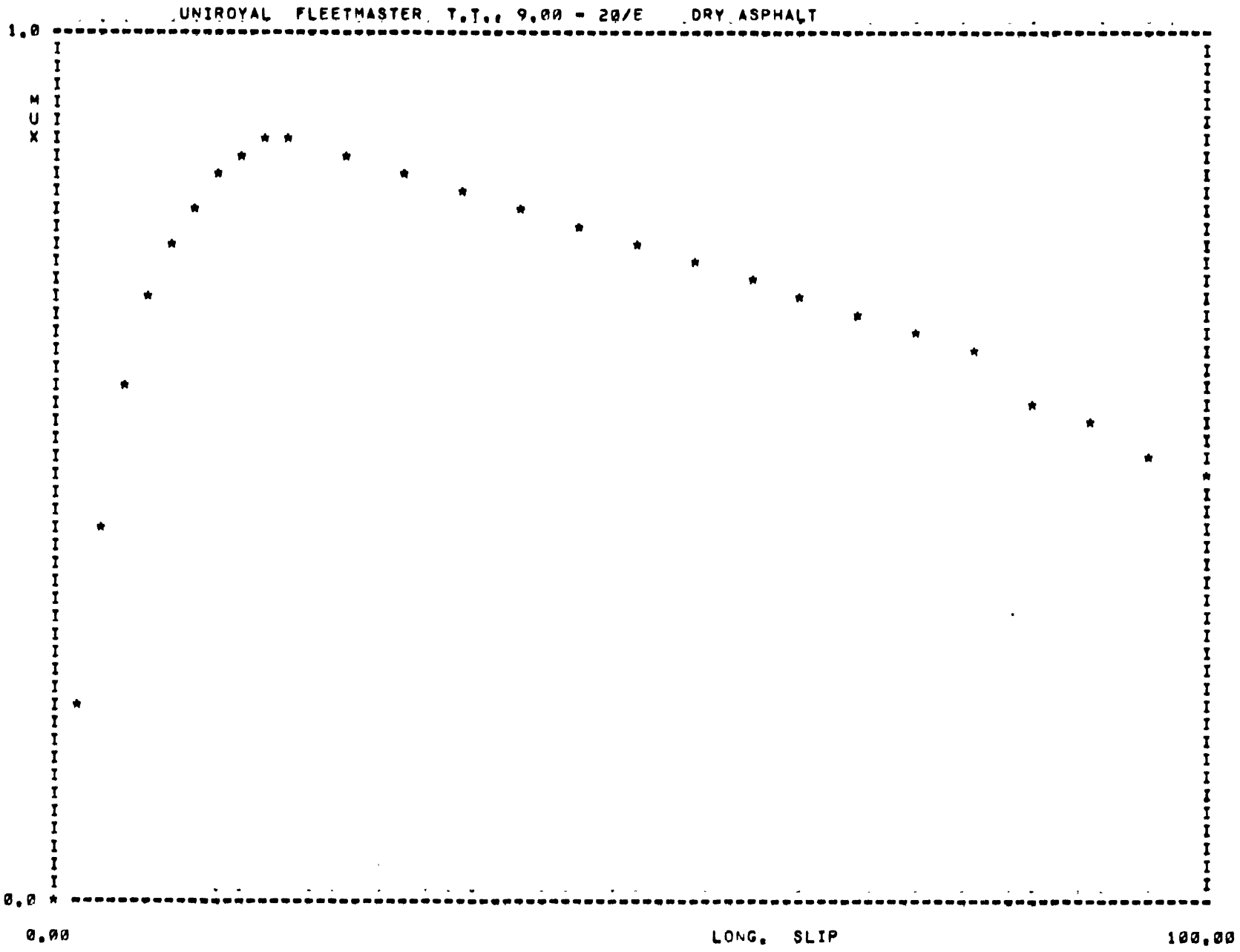

FZ = 2609.8 VEL = 60.0 MULOCK = 0.49 MUPEAK = 0.88 RATIO = 1.78

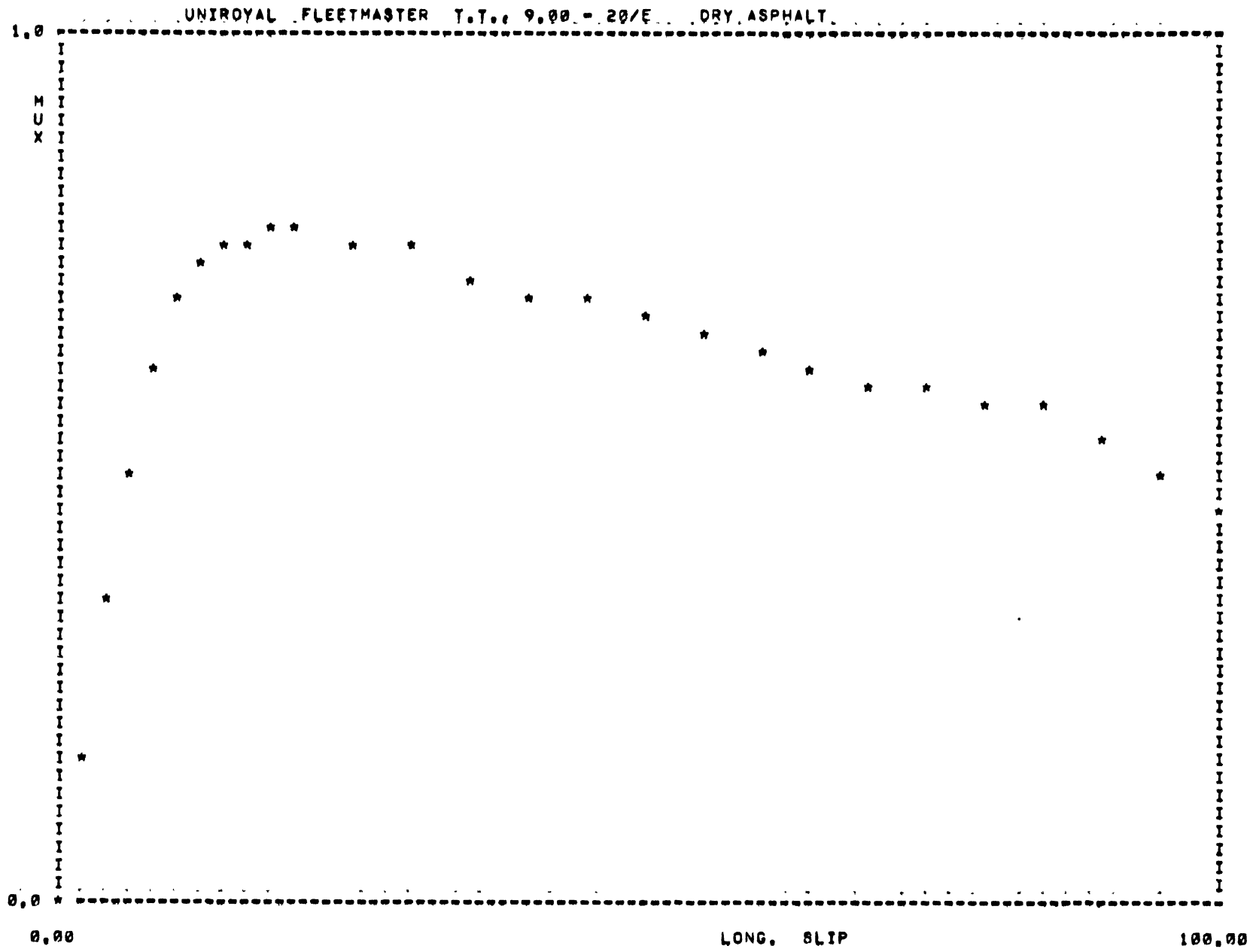

FZ = 4927.8 VEL = 60.0 MULOCK = 0.44 MUPEAK = 0.78 RATIO = 1.78

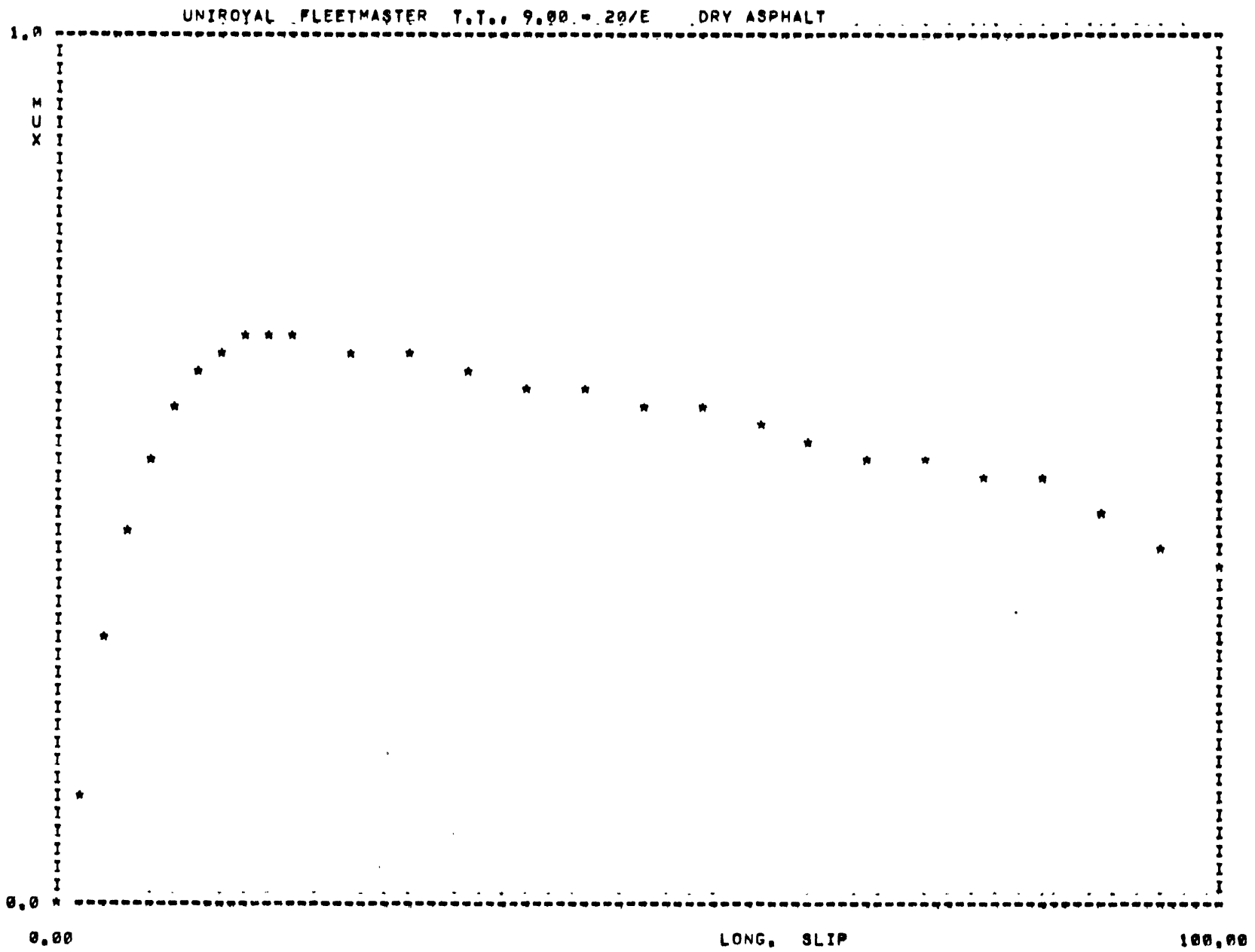

FZ = 7116.3 VEL = 60.0 MULOCK = 0.38 MUPEAK = 0.66 RATIO = 1.73

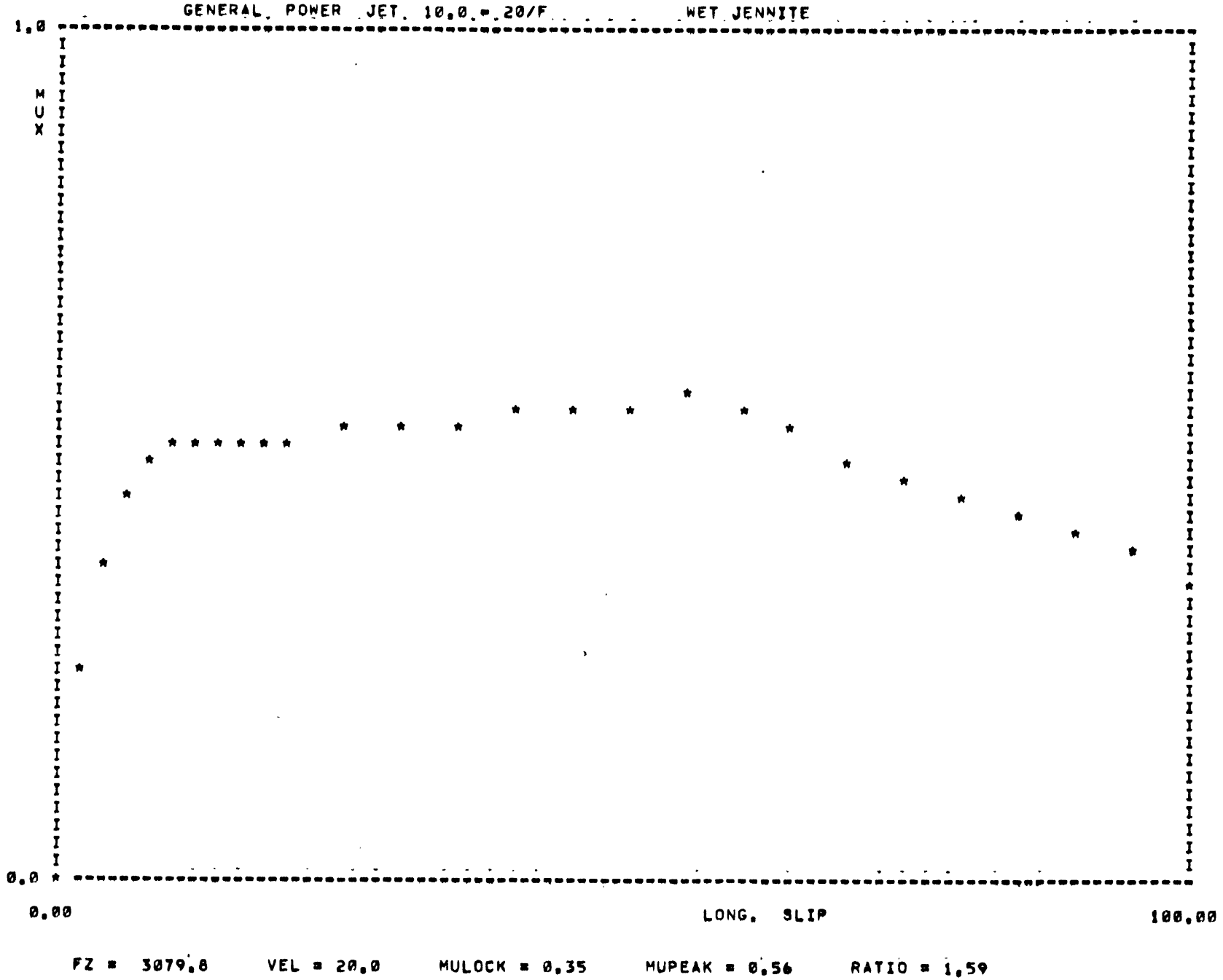

FZ = 3079.8 VEL = 20.0 MULOCK = 0.35 MUPEAK = 0.56 RATIO = 1.59

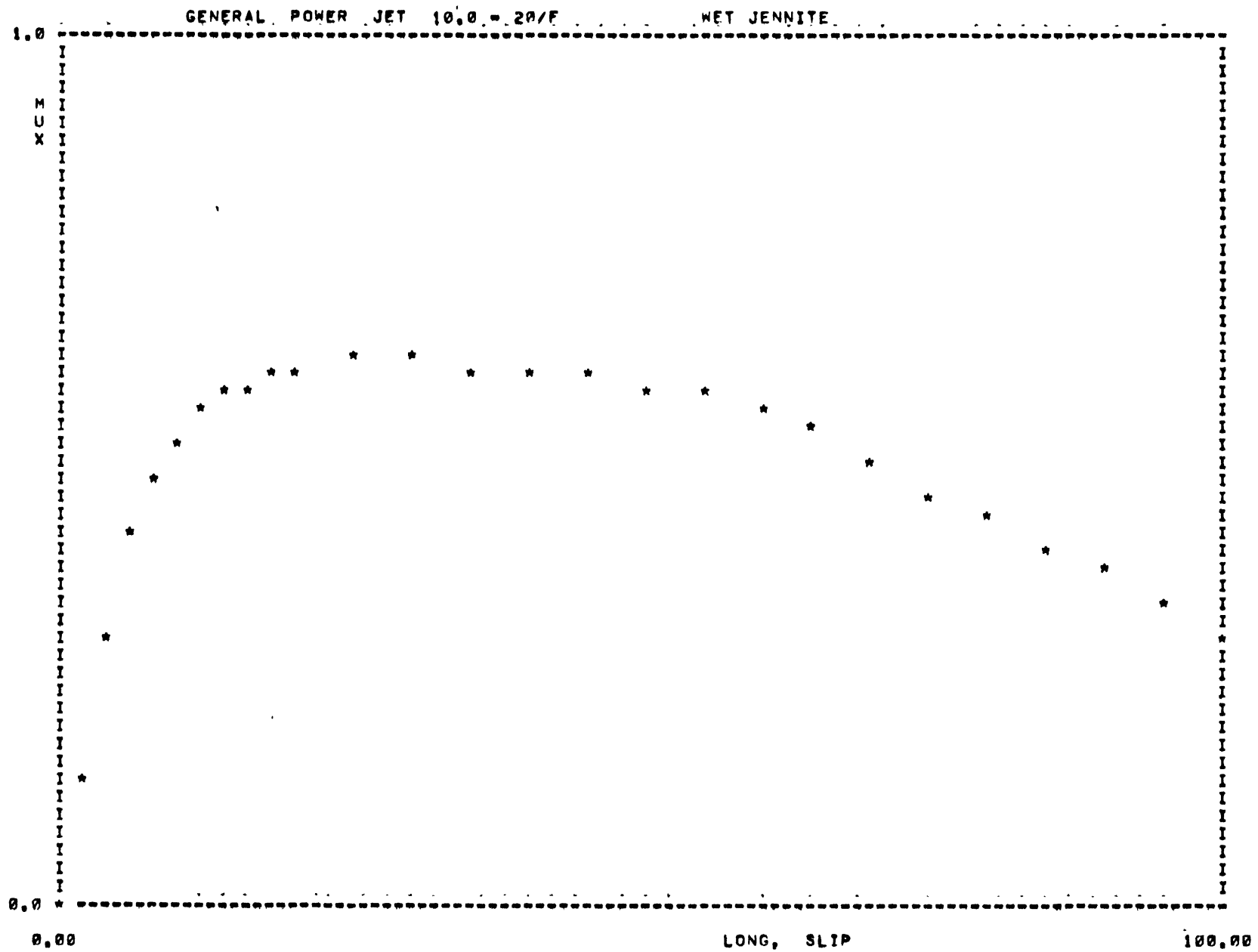

FZ = 5601.0 VEL = 20.0 MULOCK = 0.31 MUPEAK = 0.63 RATIO = 2.02

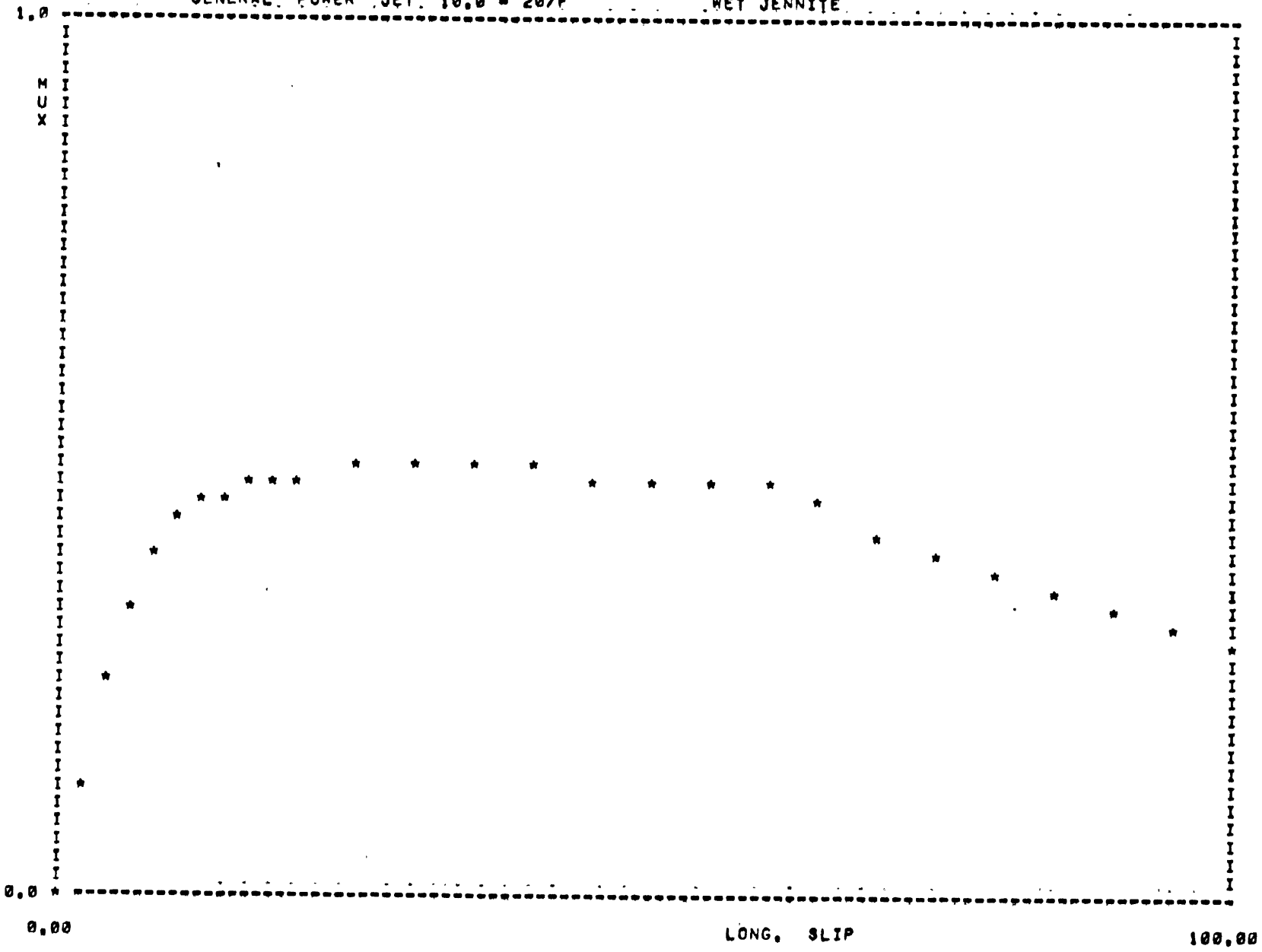

FZ = 8407.9 VEL = 20.0 MULOCK = 0.29 MUPEAK = 0.49 RATIO = 1.67

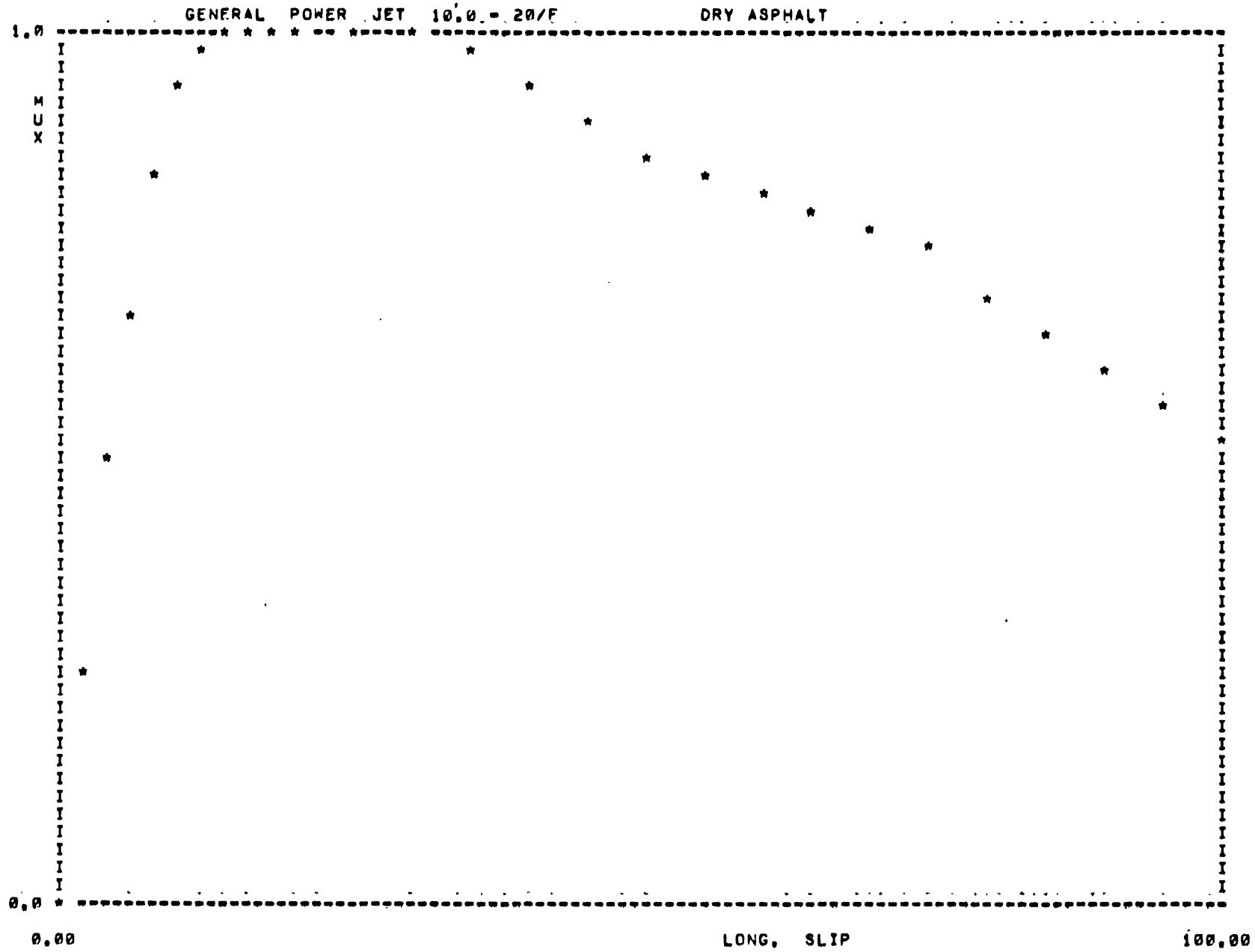

FZ = 3079.0 VEL = 40.0 MULOCK = 0.54 MUPEAK = 1.01 RATIO = 1.88

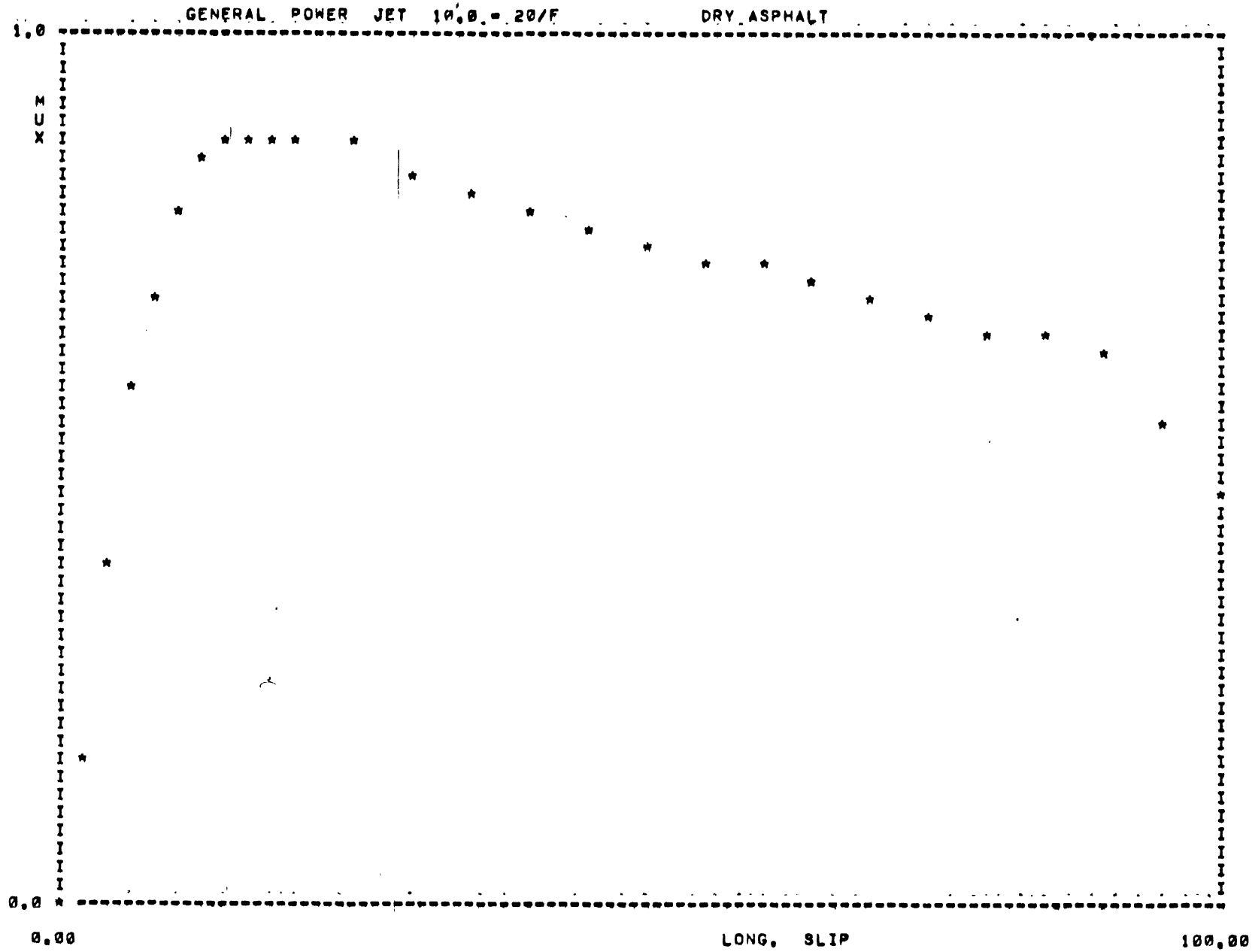

FZ = 5550.4 VEL = 40.0 MULOCK = 0.47 MUPEAK = 0.89 RATIO = 1.91

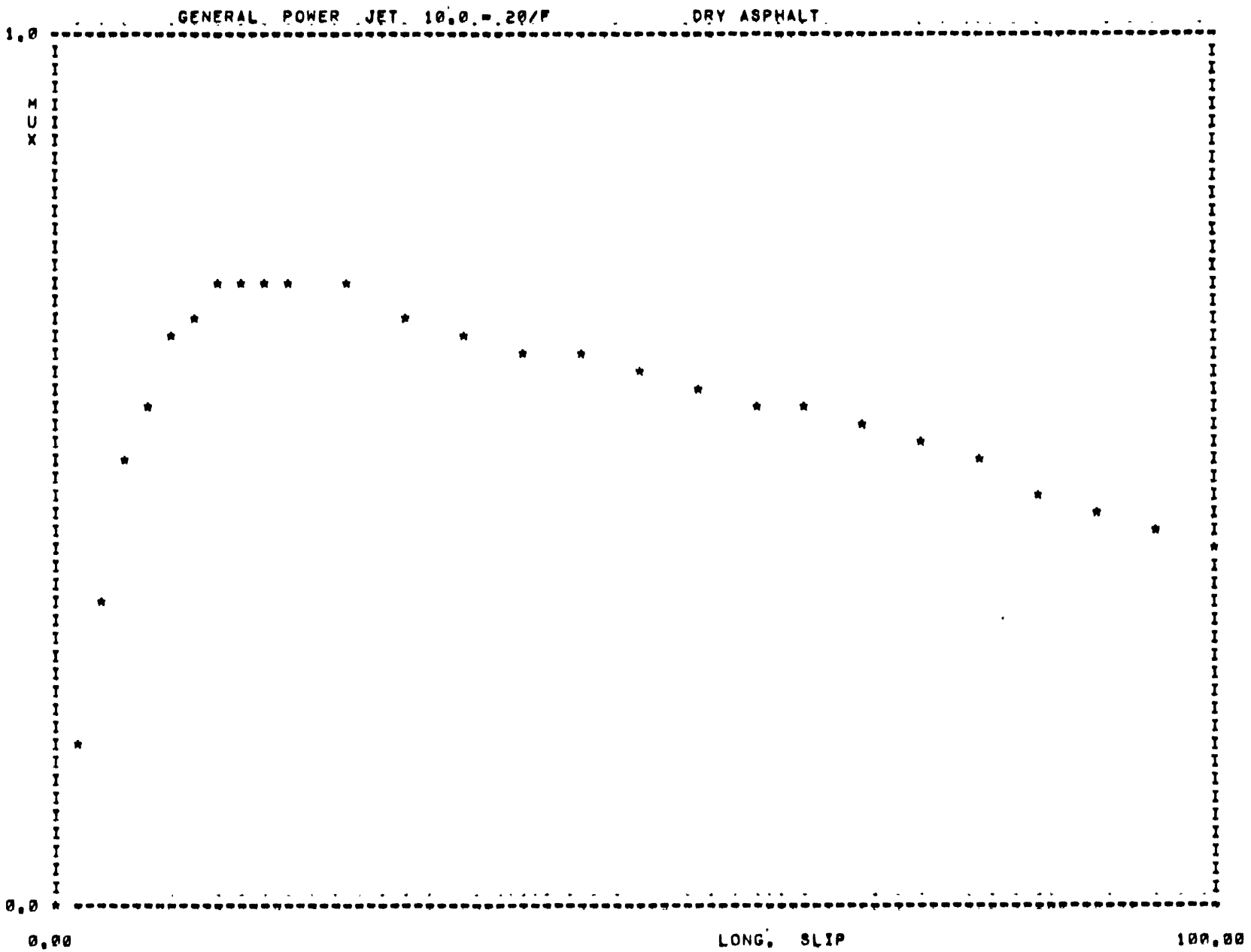

FZ = 8800.2 VEL = 40.0 MULOCK = 0.41 MUPEAK = 0.73 RATIO = 1.76

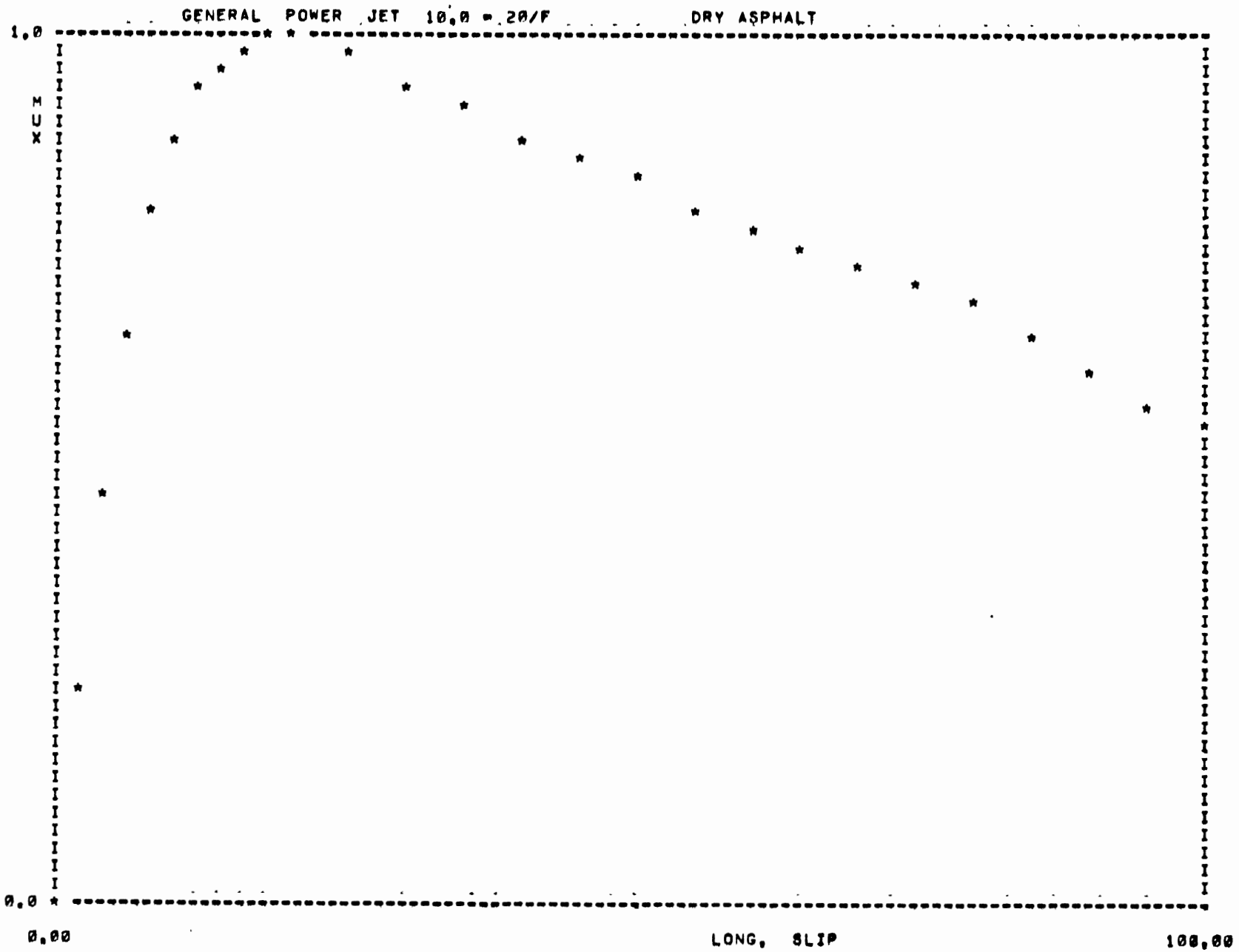

FZ = 3138,4 VEL = 60,0 MULOCK = 0,54 MUPEAK = 1,00 RATIO = 1,83

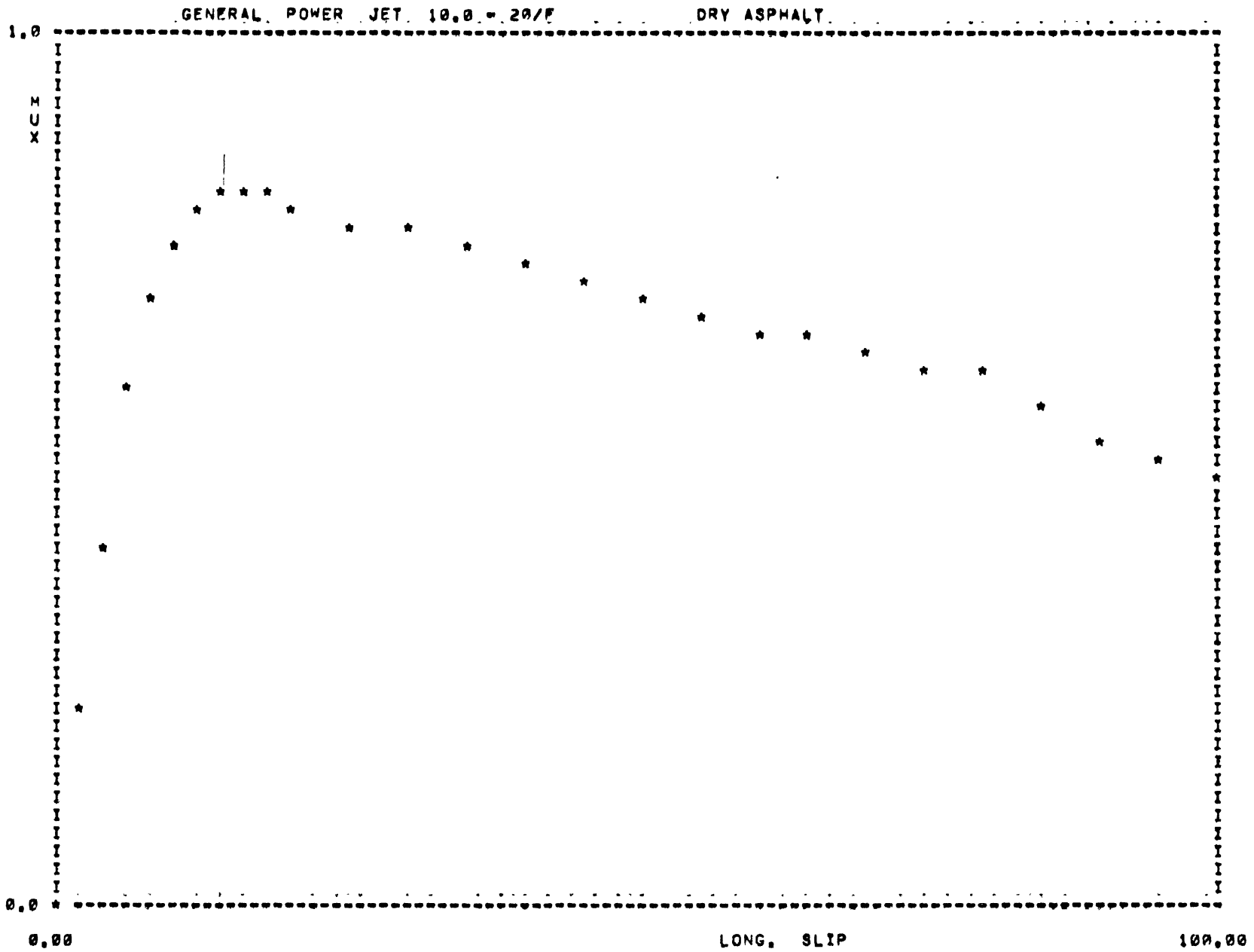

FZ = 5662.7 VEL = 60.0 MULOCK = 0.48 MUPEAK = 0.82 RATIO = 1.70

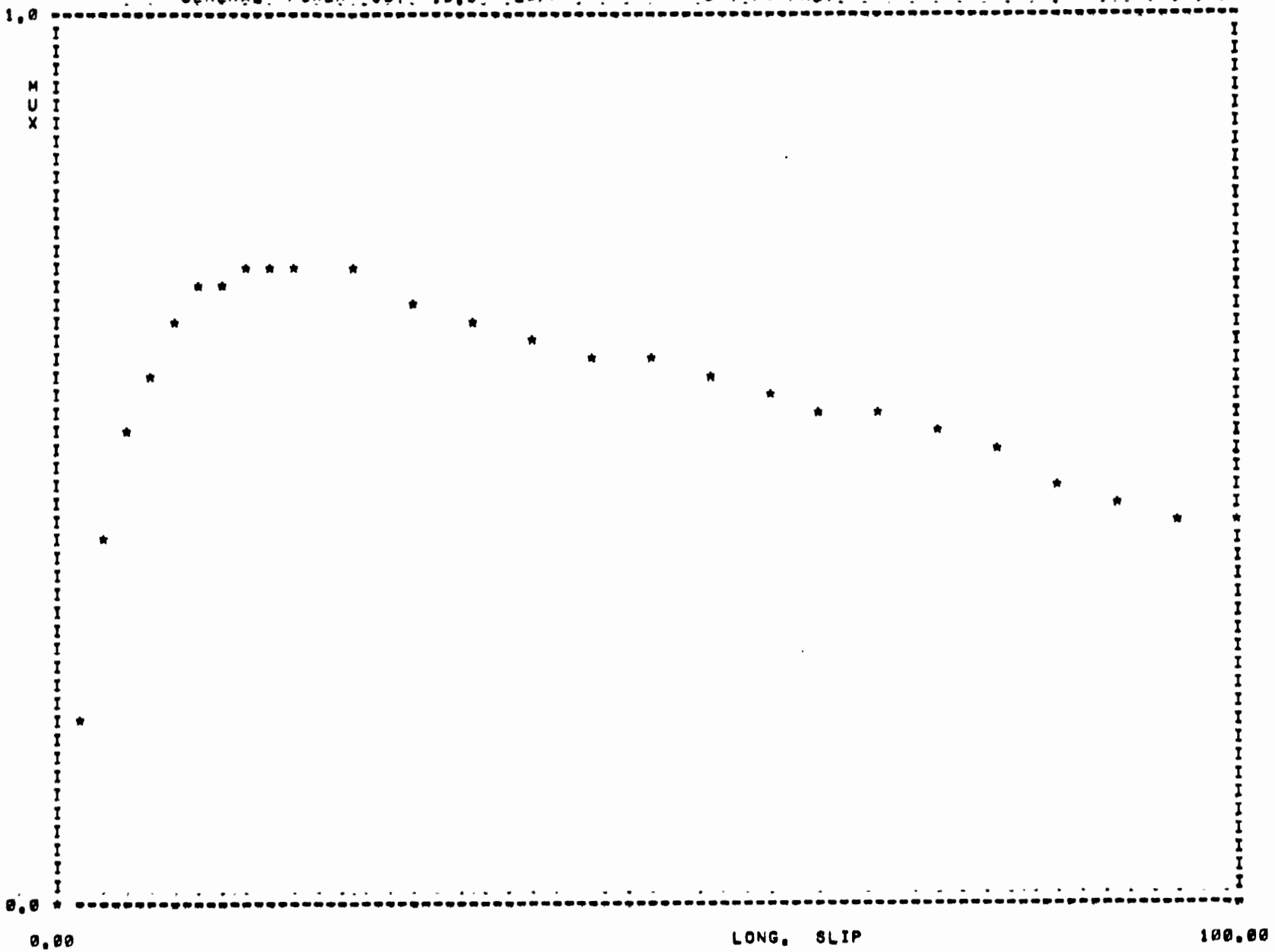

FZ = 8362.9 VEL = 60.0 MULOCK = 0.43 MUPEAK = 0.73 RATIO = 1.70

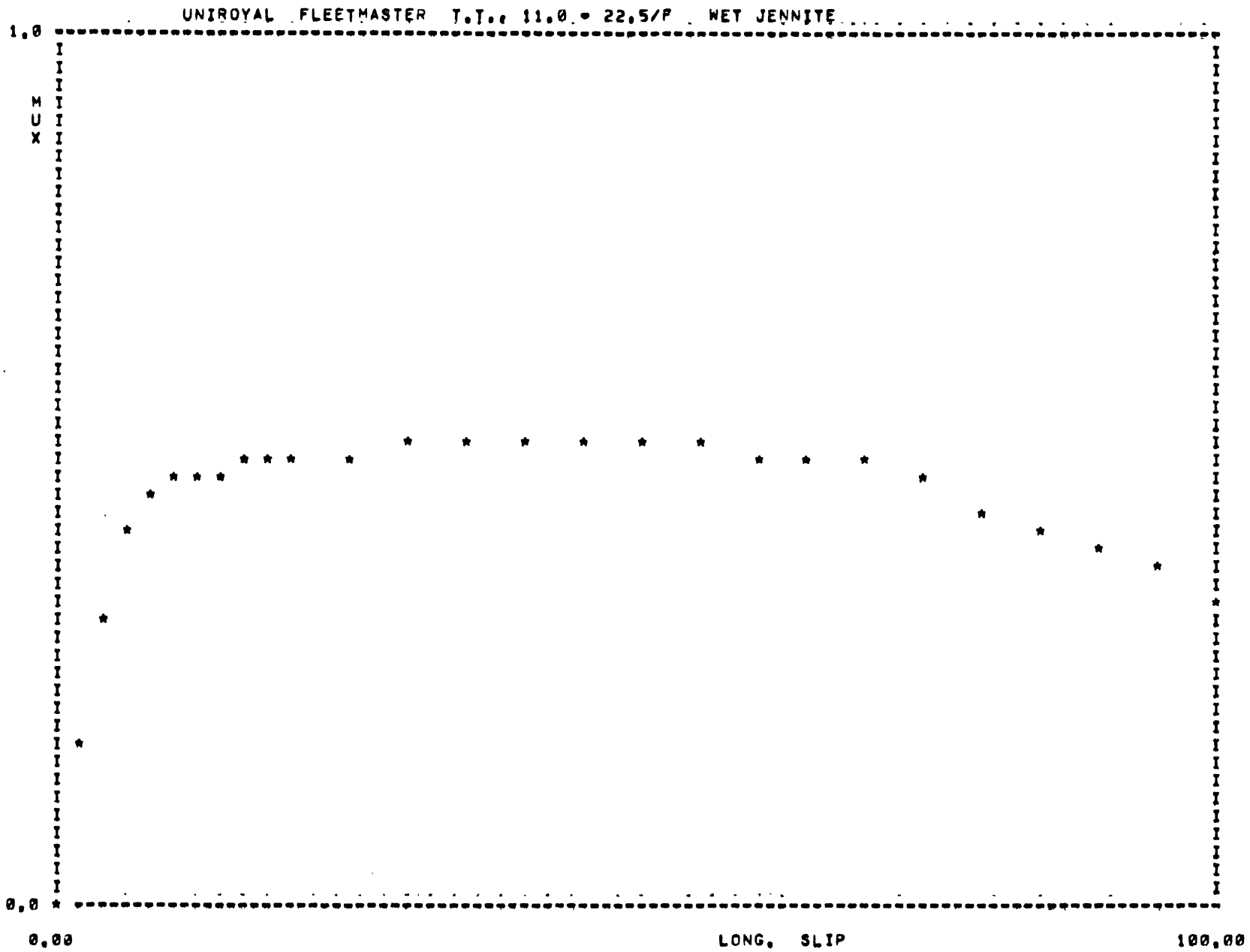

FZ = 2740.3 VEL = 20.0 MULOCK = 0.36 MUPEAK = 0.54 RATIO = 1.50

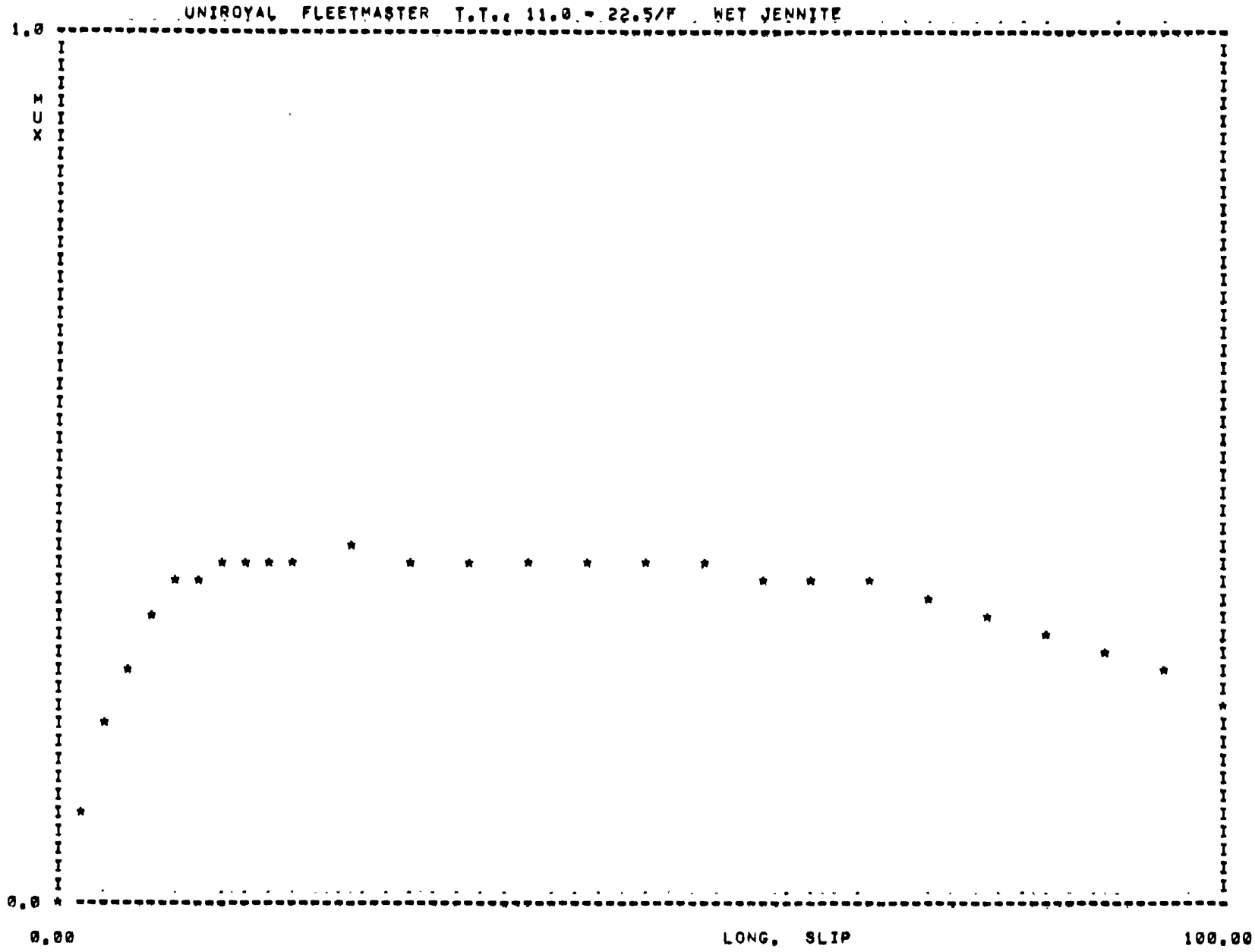

FZ = 8376.7 VEL = 20.0 MULOCK = 0.23 MUPEAK = 0.40 RATIO = 1.73

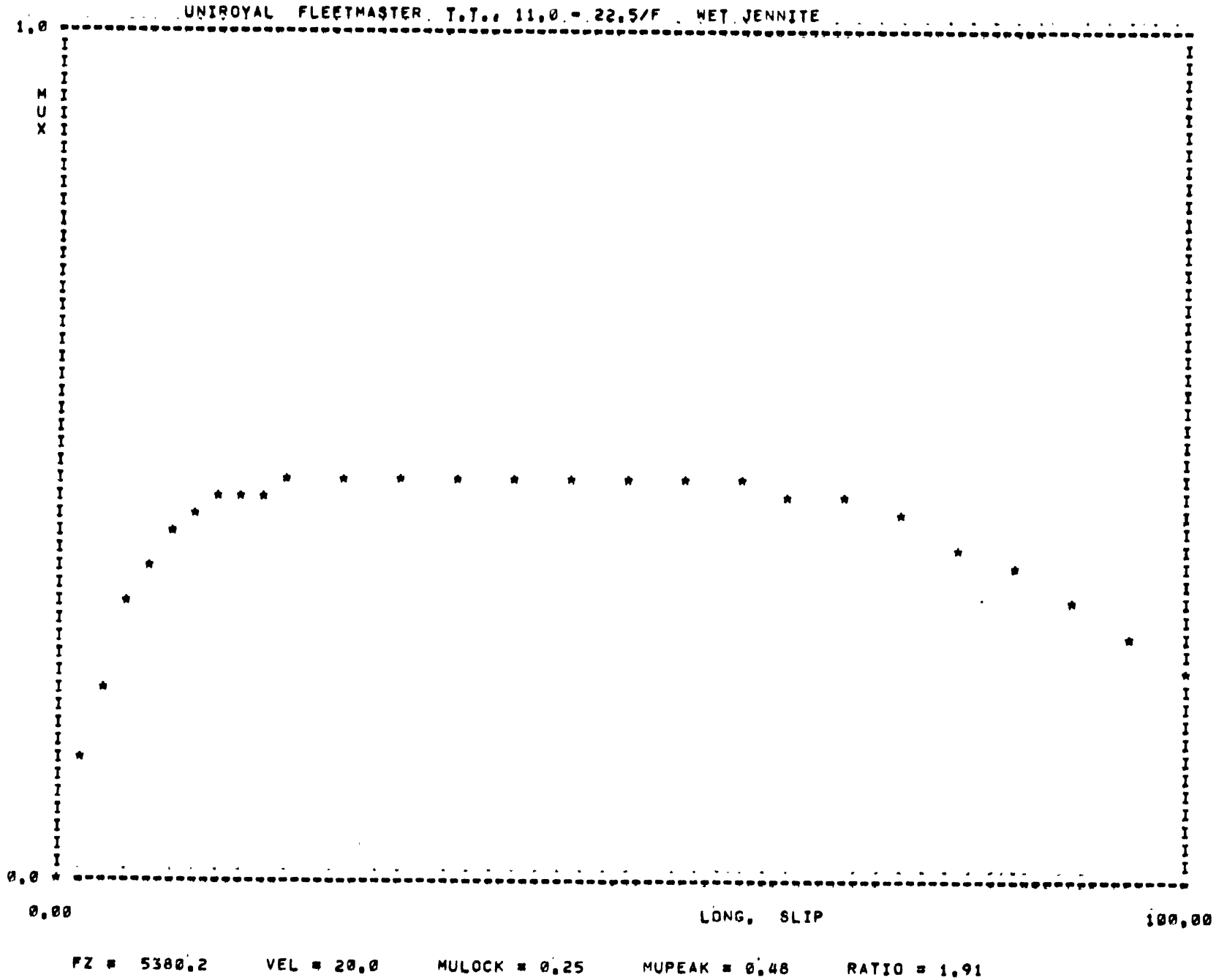

FZ = 5380.2 VEL = 20.0 MULOCK = 0.25 MUPEAK = 0.48 RATIO = 1.91

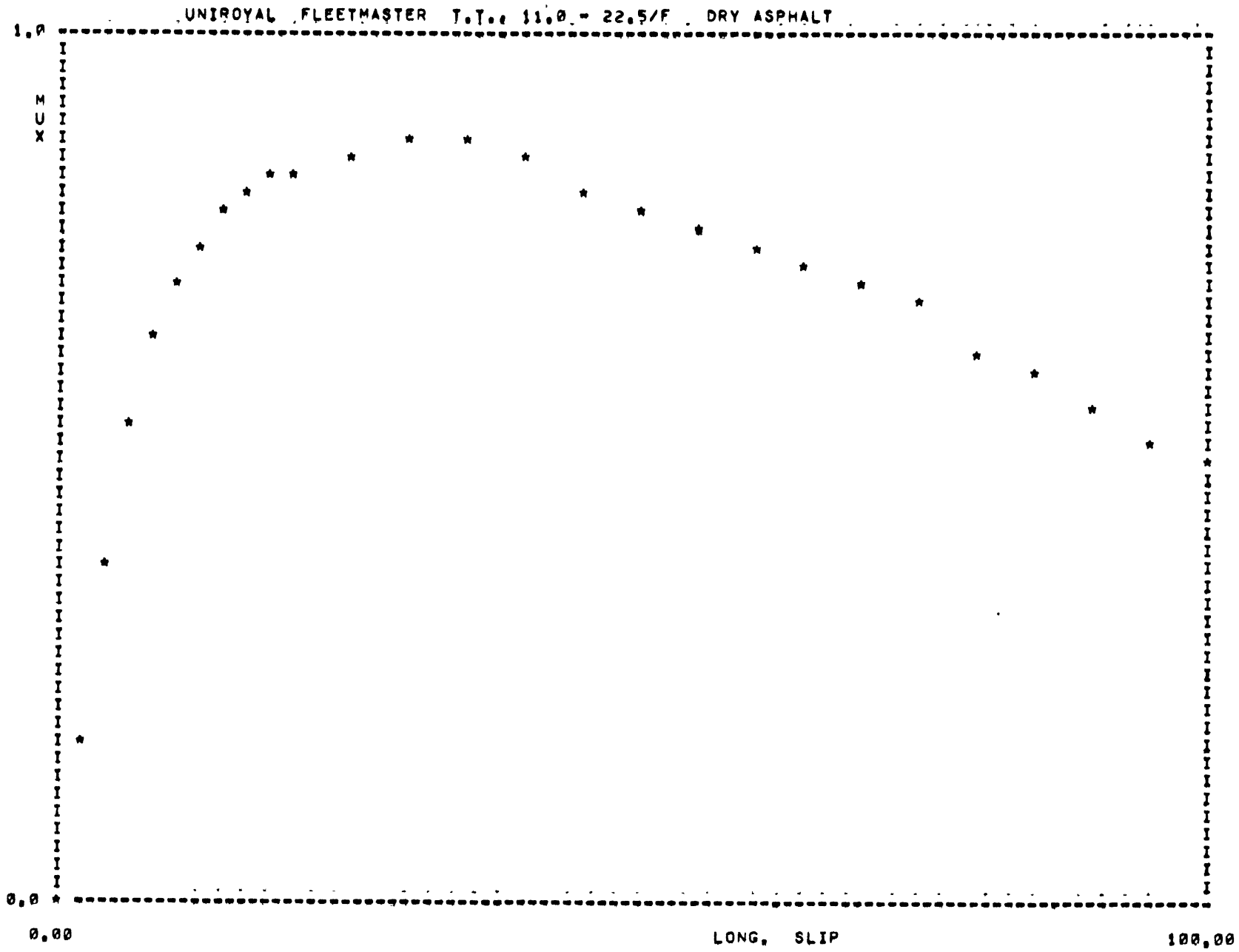

FZ = 3081.1 VEL = 40.0 MULOCK = 0.51 MUPEAK = 0.87 RATIO = 1.72

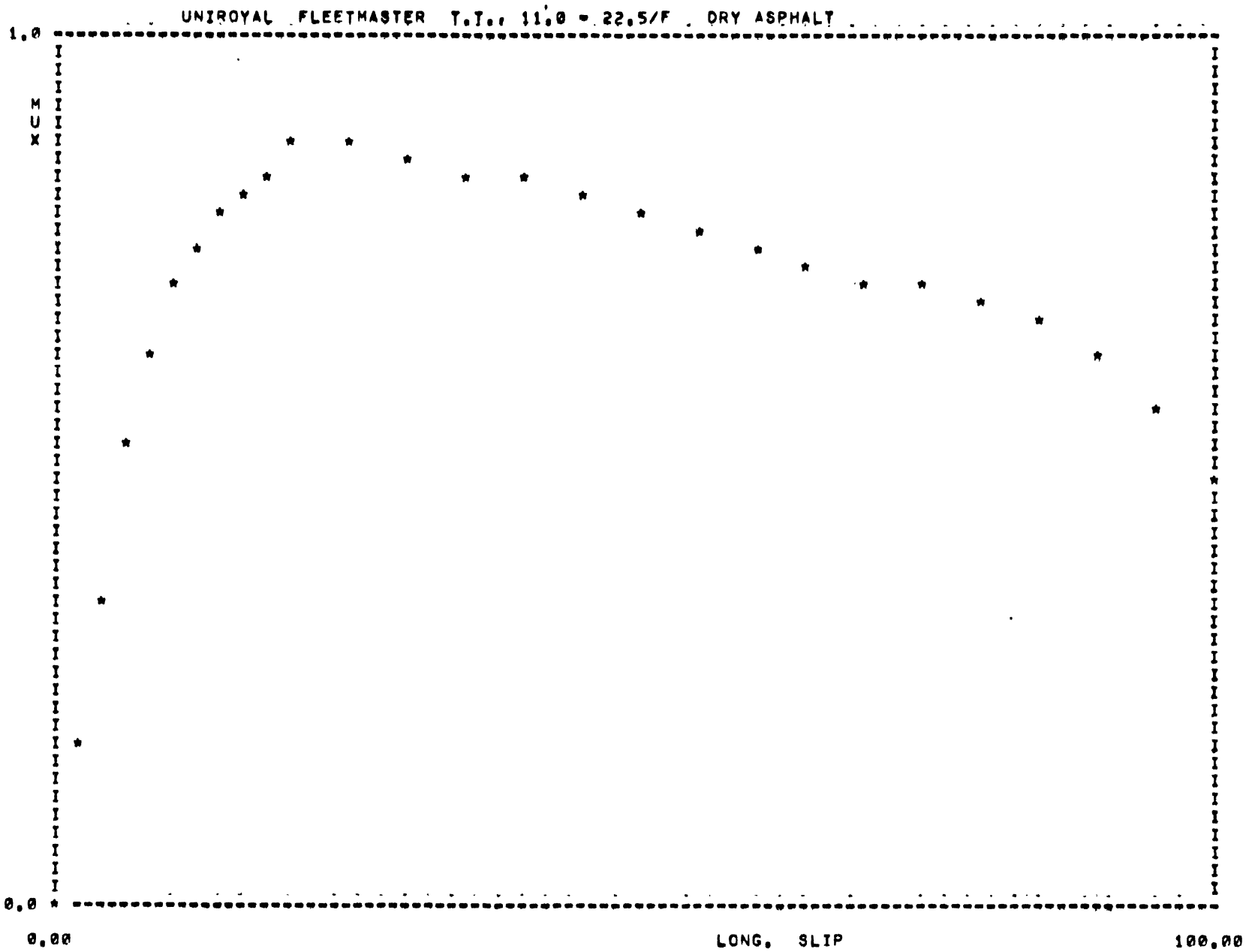

FZ = 5364.2 VEL = 40.0 MULOCK = 0.49 MUPEAK = 0.88 RATIO = 1.81

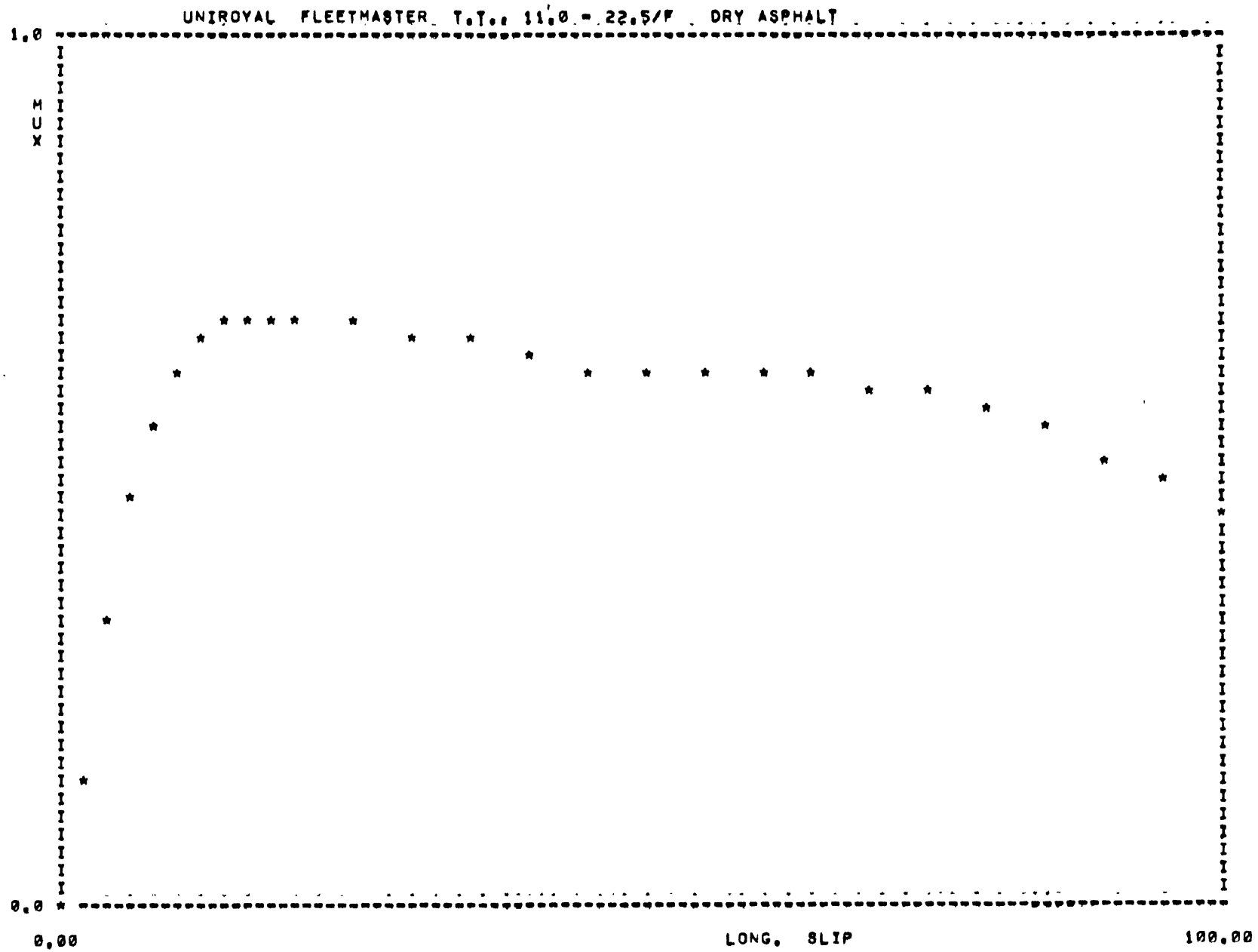

FZ = 8218.4 VEL = 40.0 MULOCK = 0.45 MUPEAK = 0.68 RATIO = 1.50

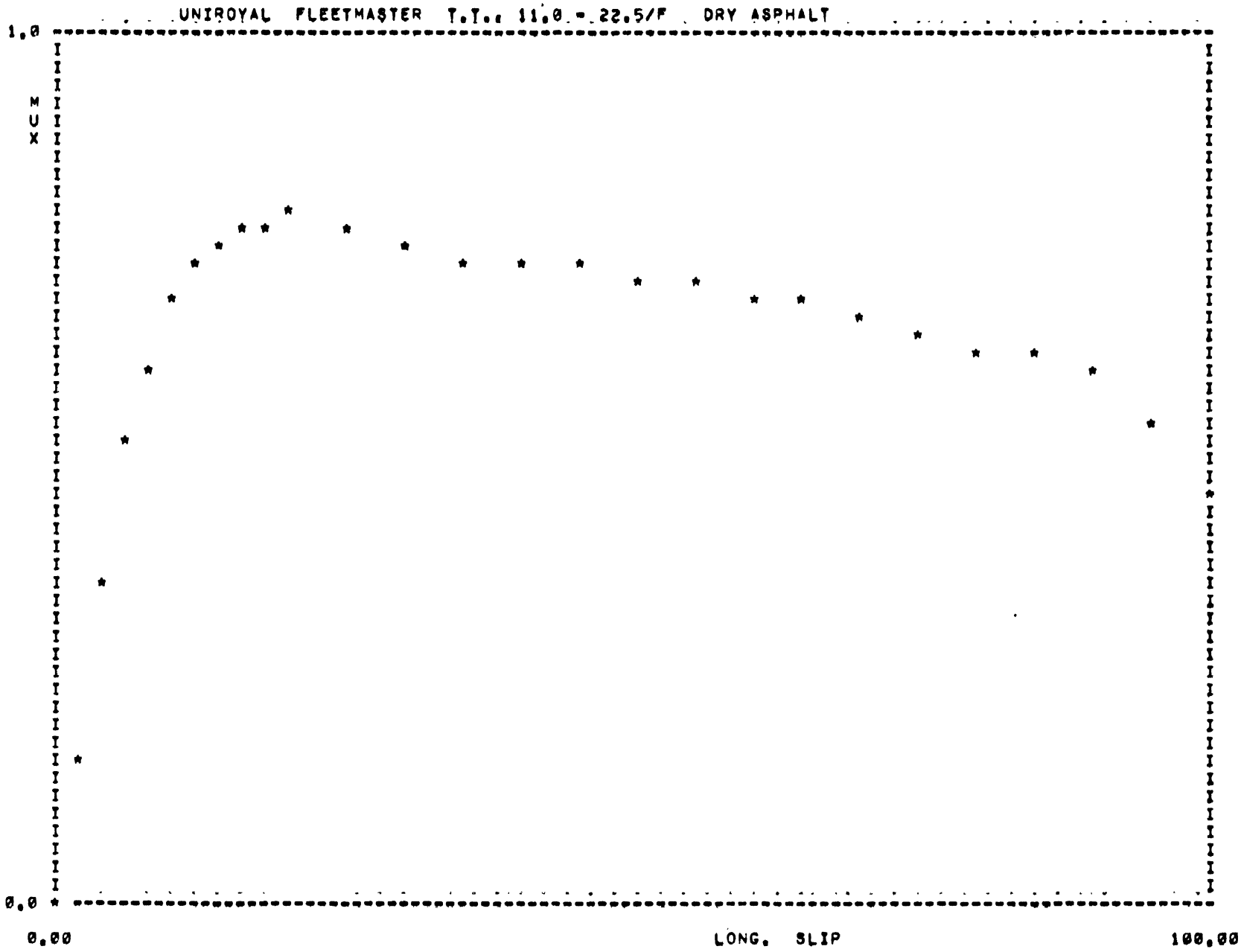

FZ = 5507.1 VEL = 60.0 MULOCK = 0.48 MUPEAK = 0.79 RATIO = 1.65

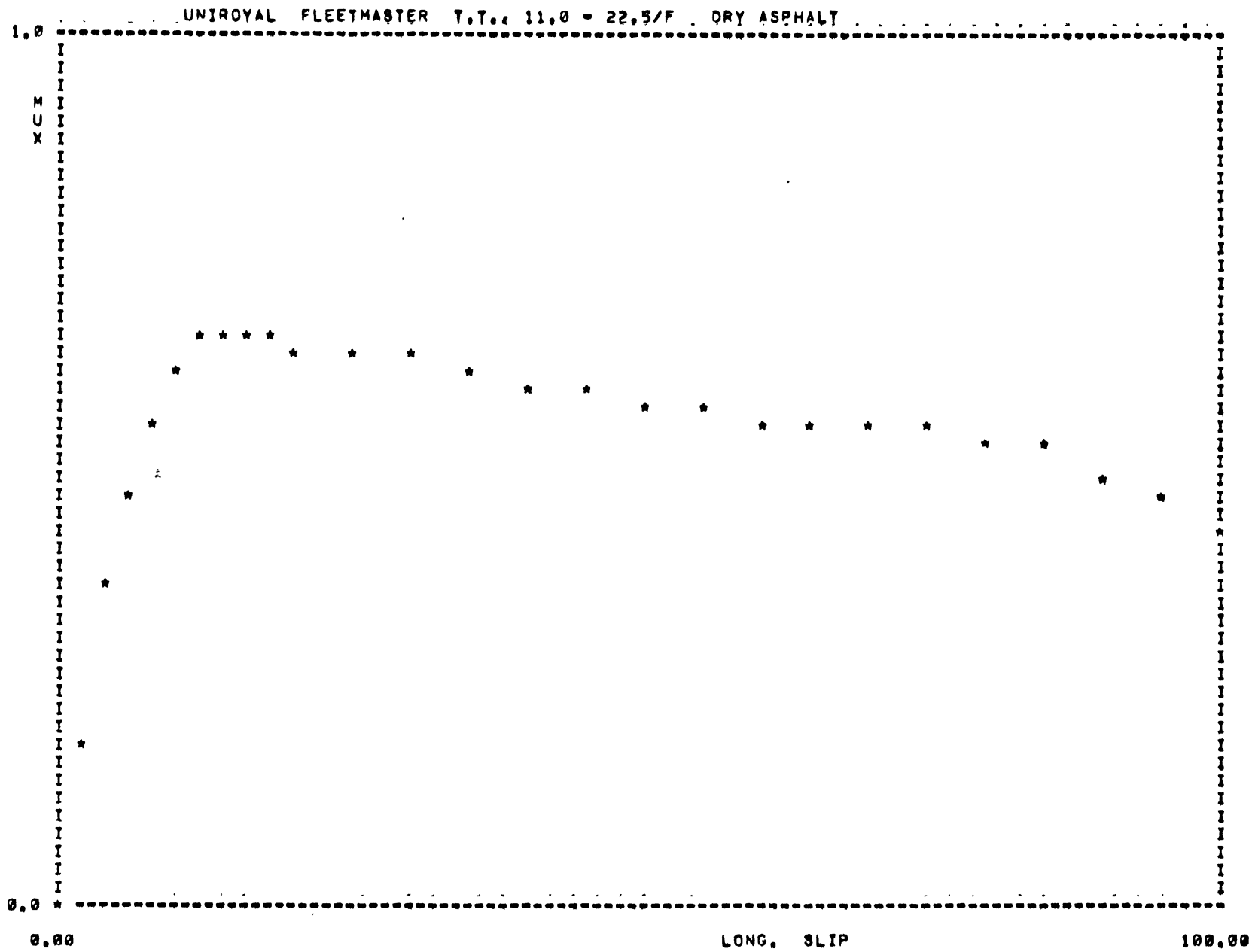

FZ = 8214.0 VEL = 60.0 MULOCK = 0.44 MUPEAK = 0.66 RATIO = 1.51

file 3

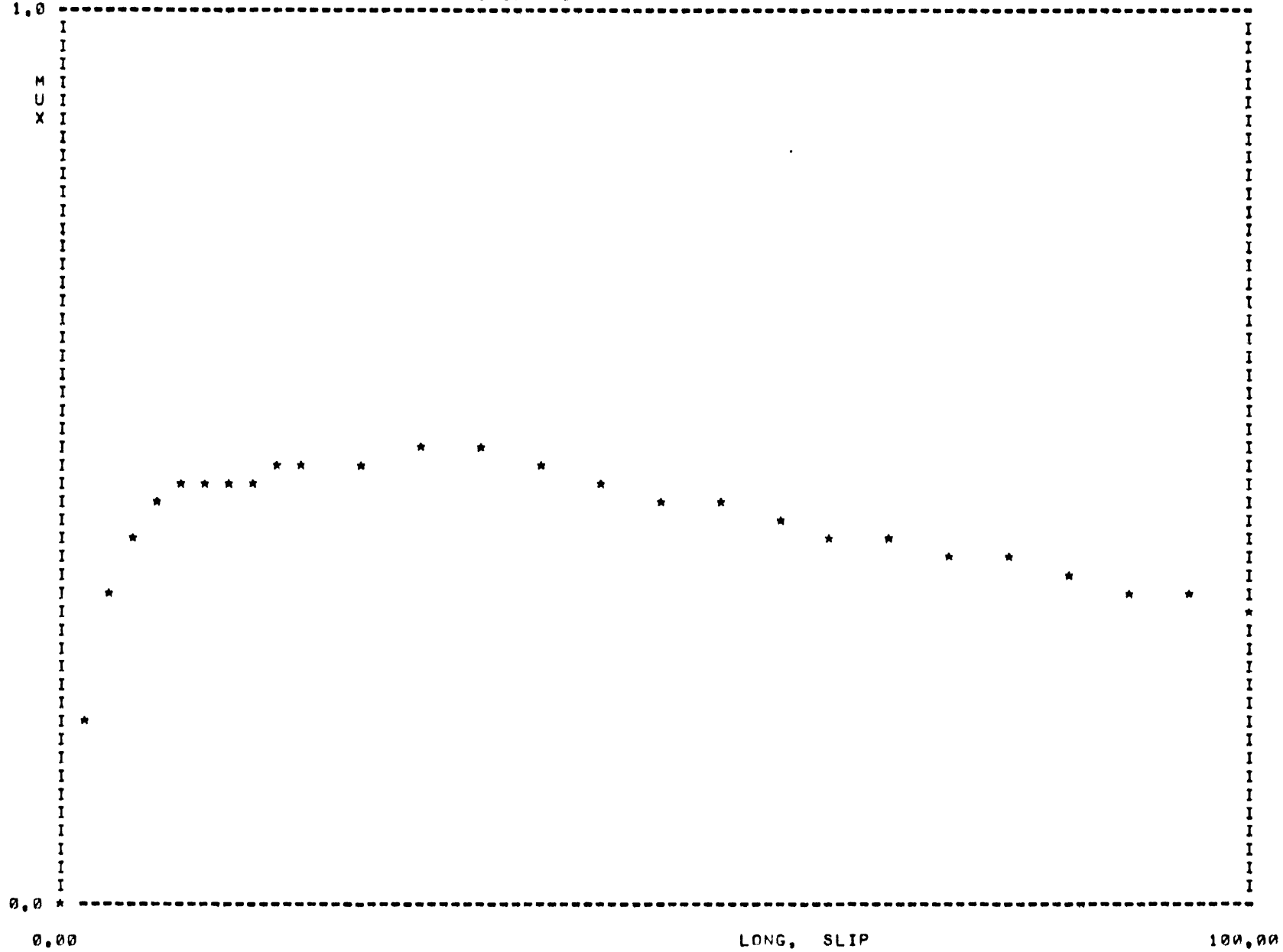

FZ = 3240.1 VEL = 20. MUPEAK = .50 MULOCK = .33 RATIO = 1.54

A = 1:lo 88

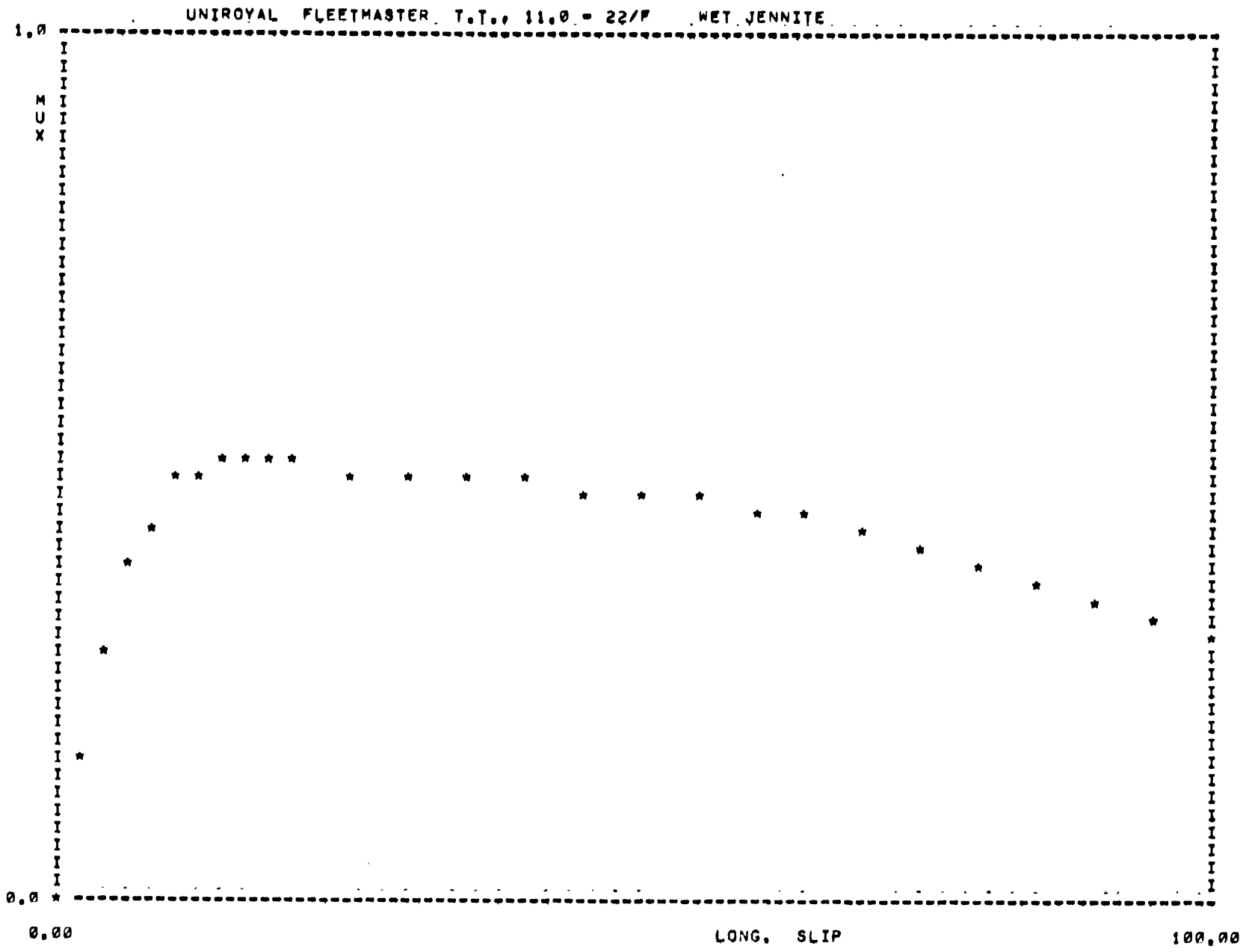

FZ = 6542.0 VEL = 20.0 MULOCK = 0.30 MUPEAK = 0.51 RATIO = 1.66

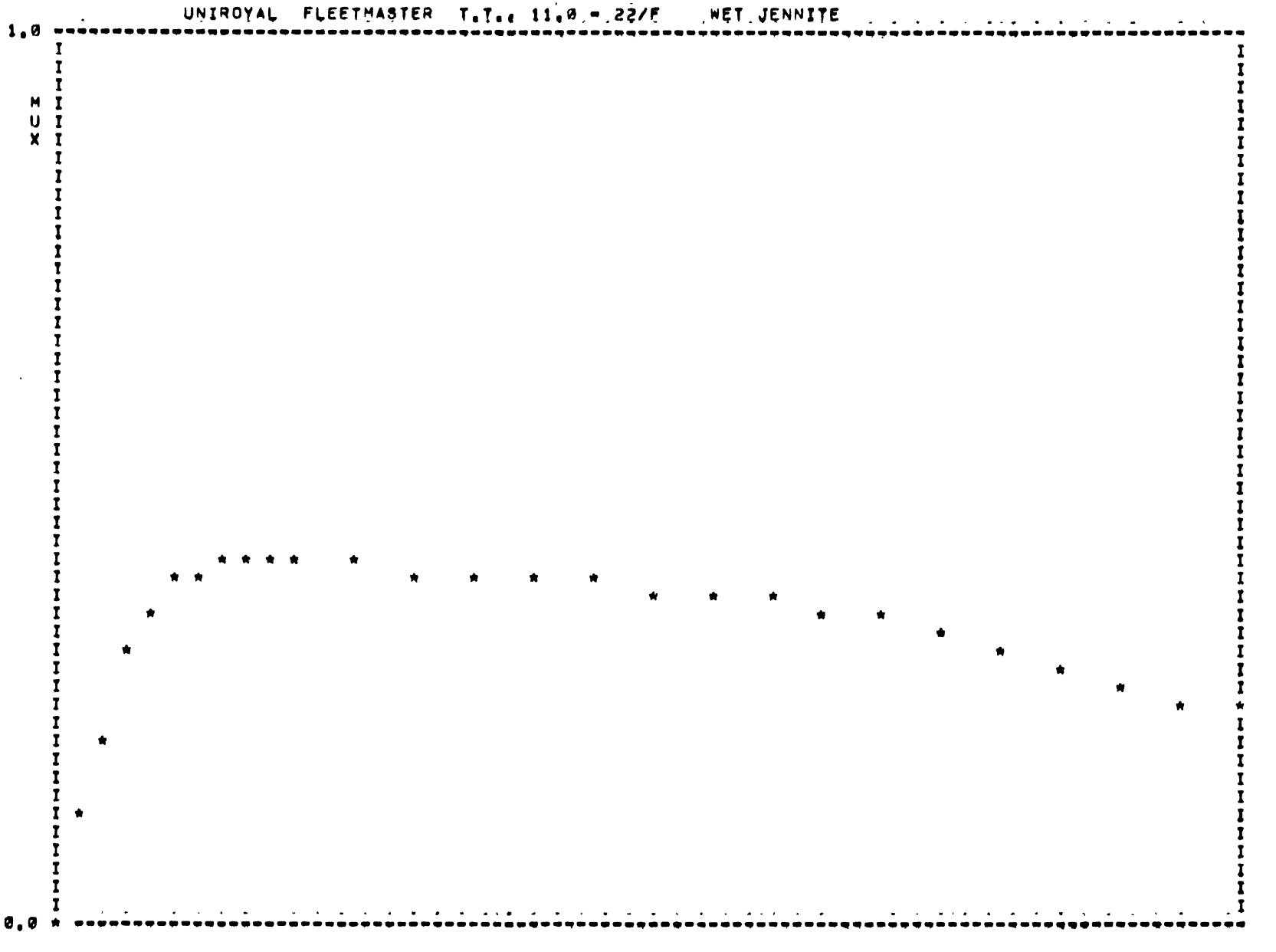

FZ = 9812.5 VEL = 20.0 MULOCK = 0.24 MUPEAK = 0.41 RATIO = 1.71

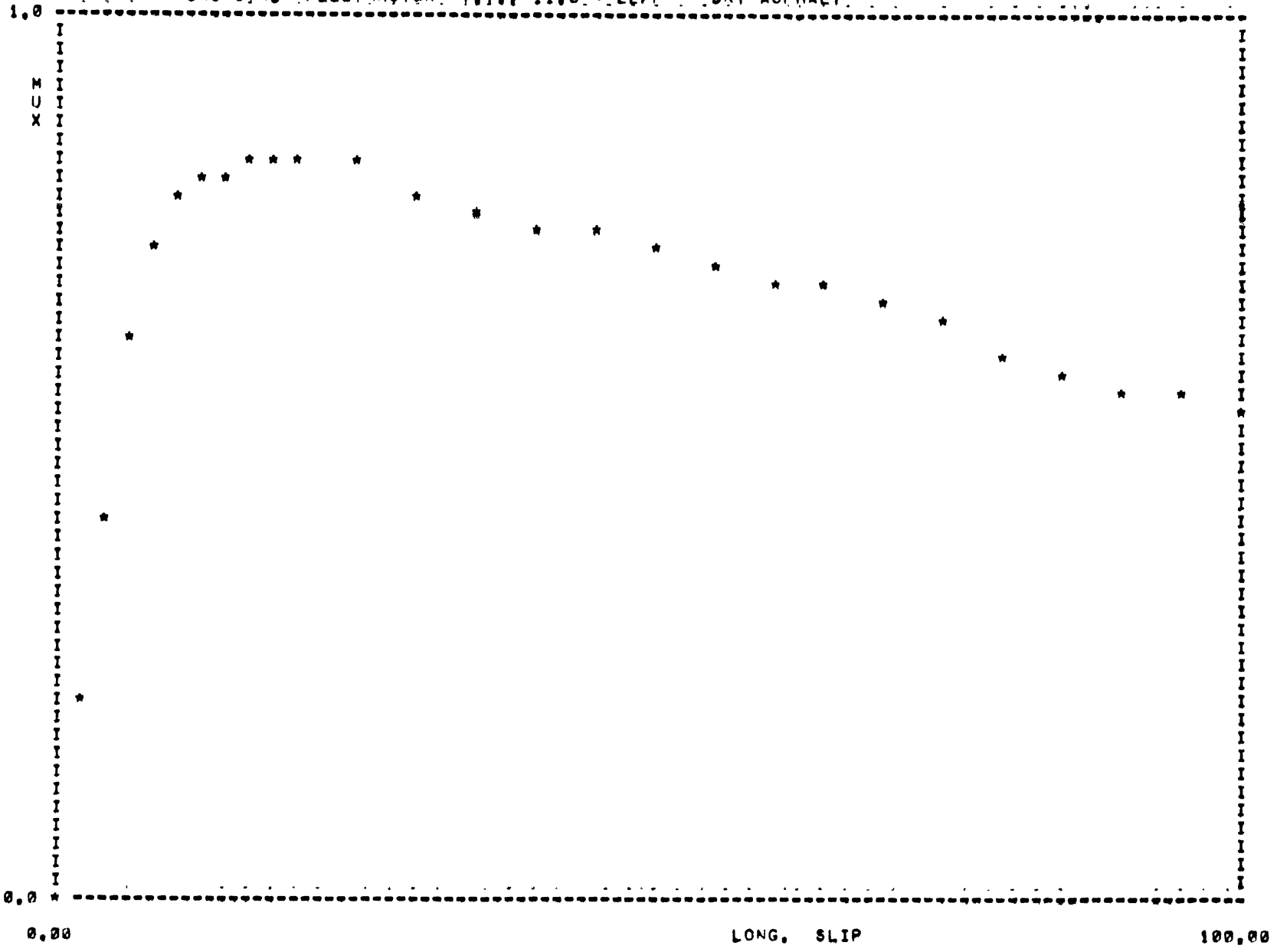

FZ = 3431.5 VEL = 40.0 MULOCK = 0.55 MUPEAK = 0.85 RATIO = 1.53

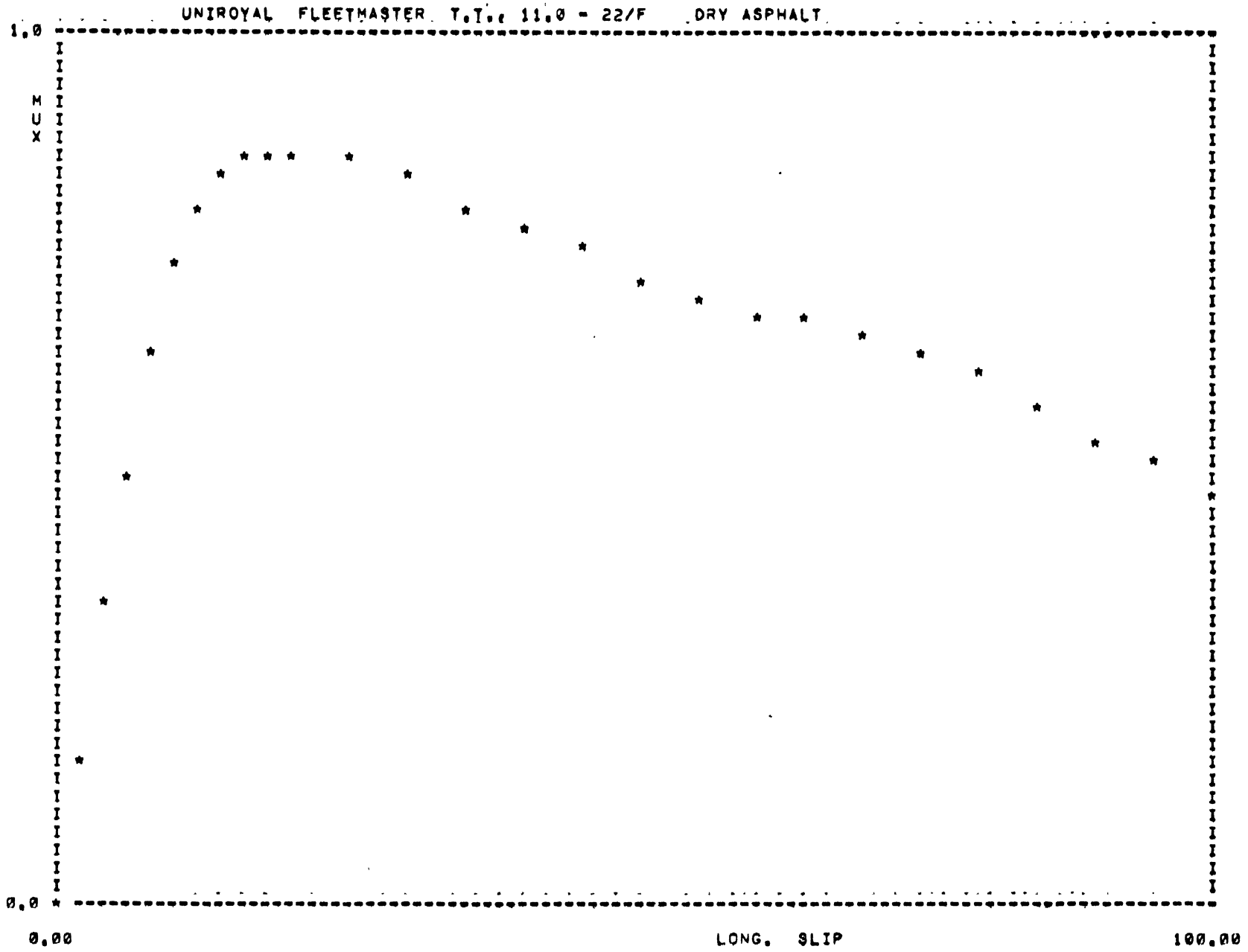

FZ = 6529.8 VEL = 40.0 MULOCK = 0.48 MUPEAK = 0.87 RATIO = 1.80

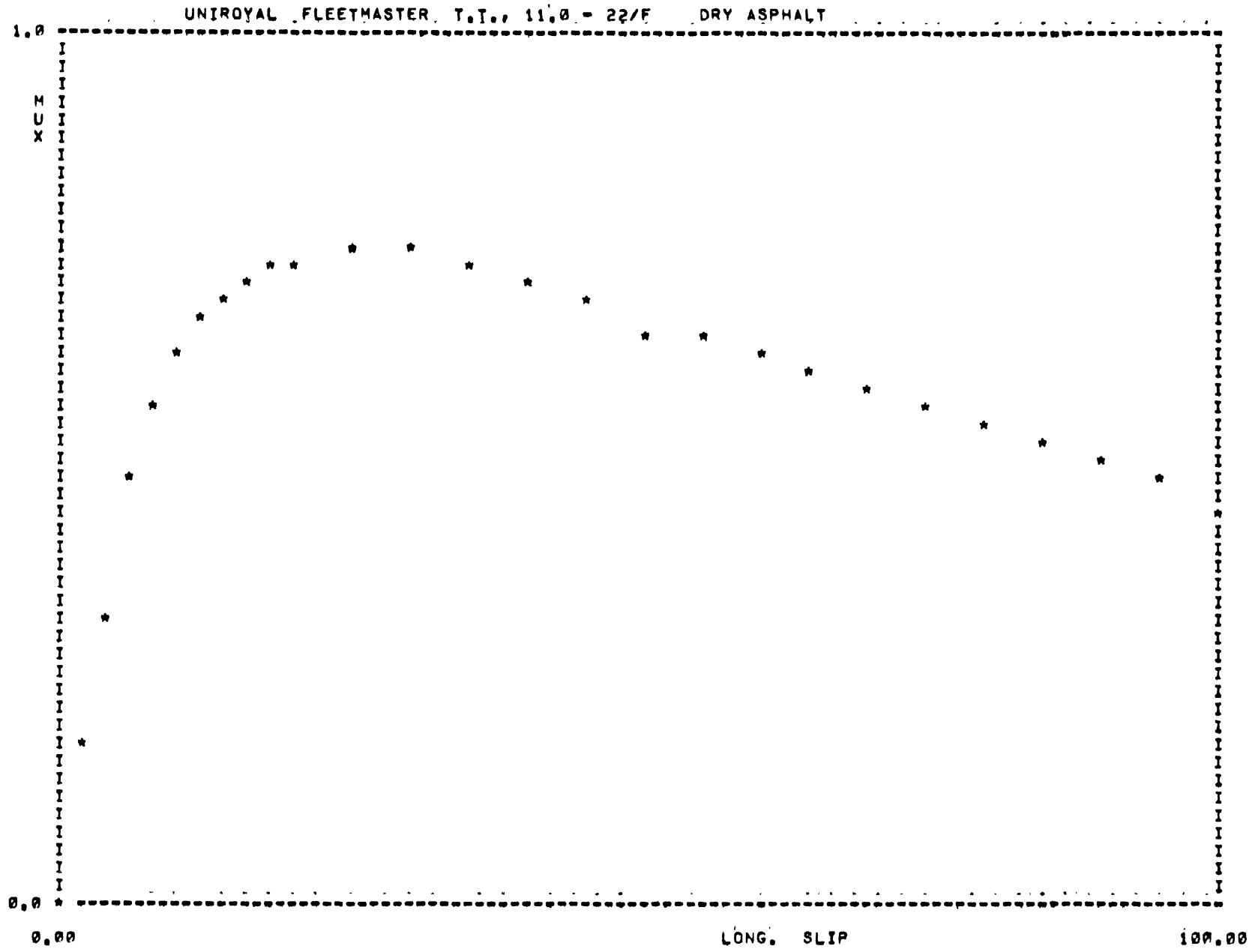

FZ = 8344.3 VEL = 60.0 MULOCK = 0.46 MUPEAK = 0.76 RATIO = 1.66

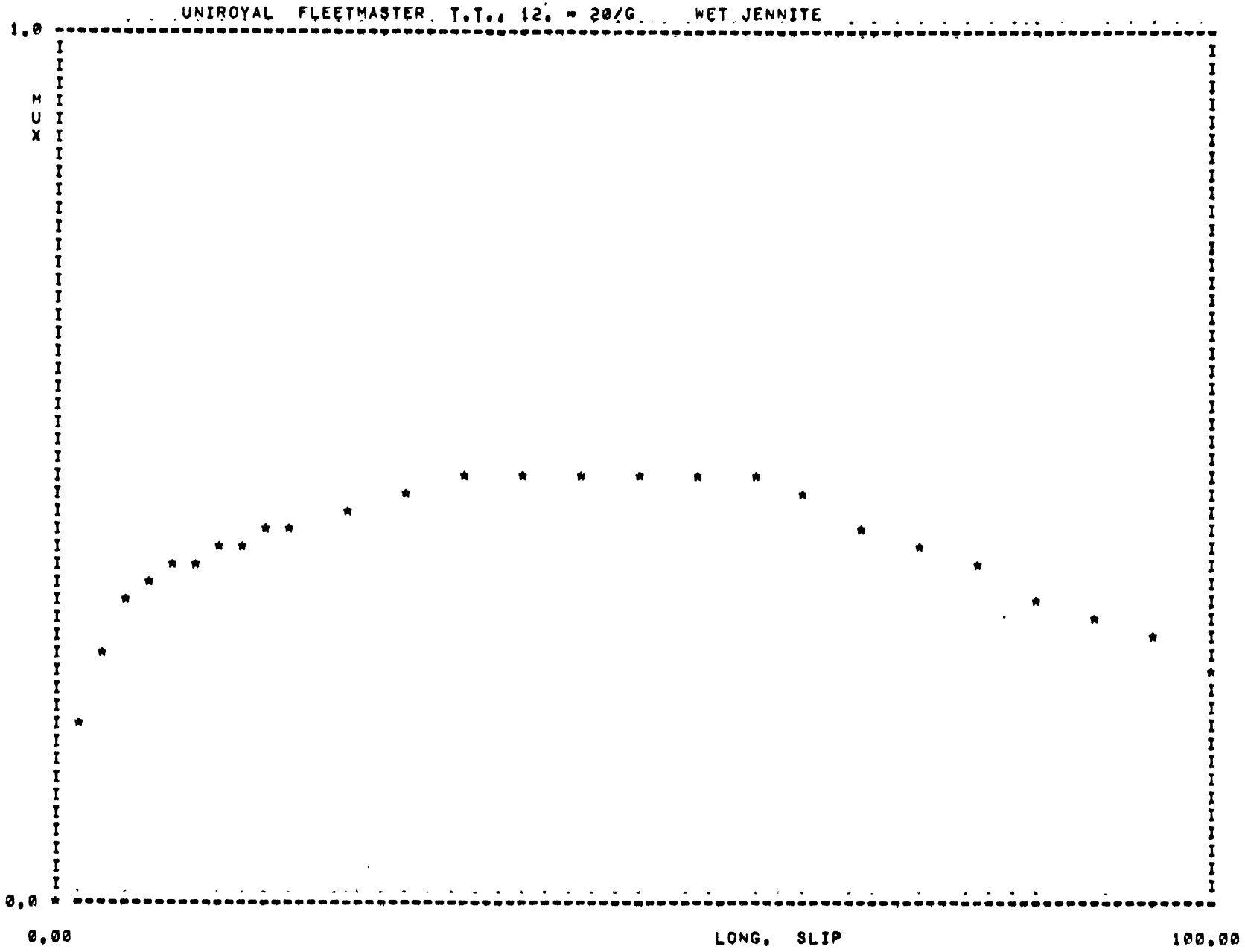

FZ = 3820.8 VEL = 20.0 MULOCK = 0.27 MUPEAK = 0.49 RATIO = 1.86

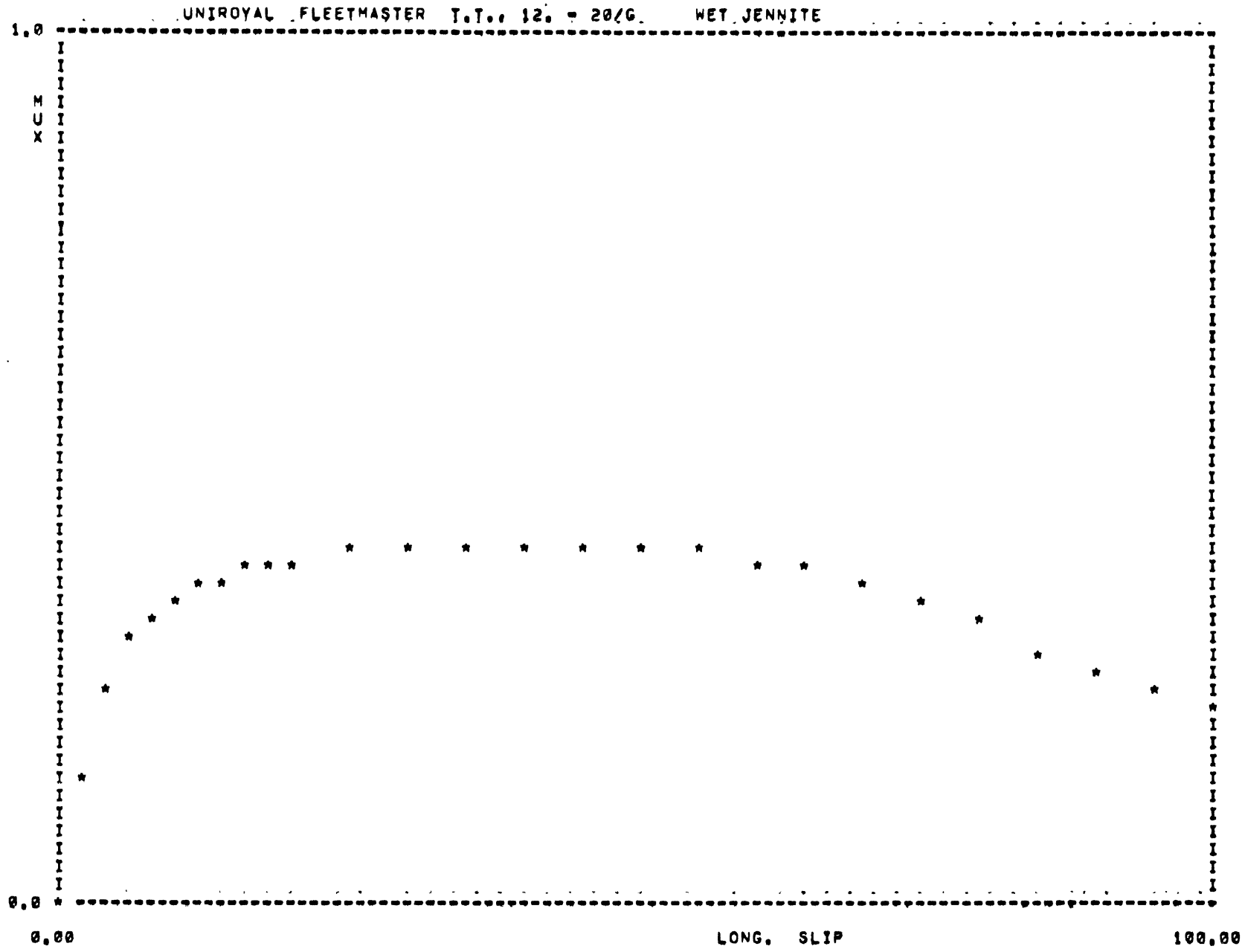

FZ = 7359.7 VEL = 20.0 MULOCK = 0.23 MUPEAK = 0.42 RATIO = 1.85

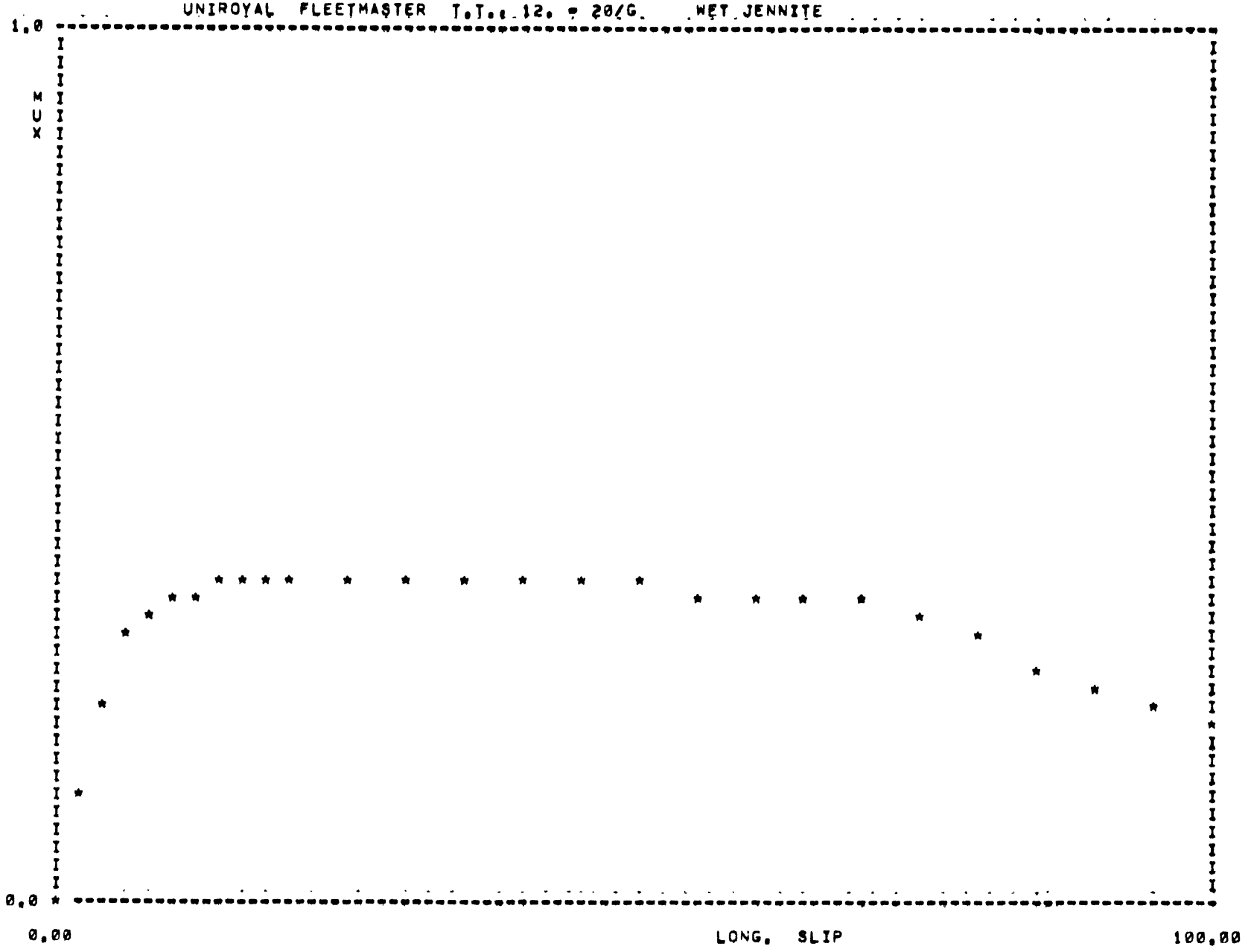

FZ = 11248.5 VEL = 20.0 MULOCK = 0.29 MUPEAK = 0.37 RATIO = 1.86

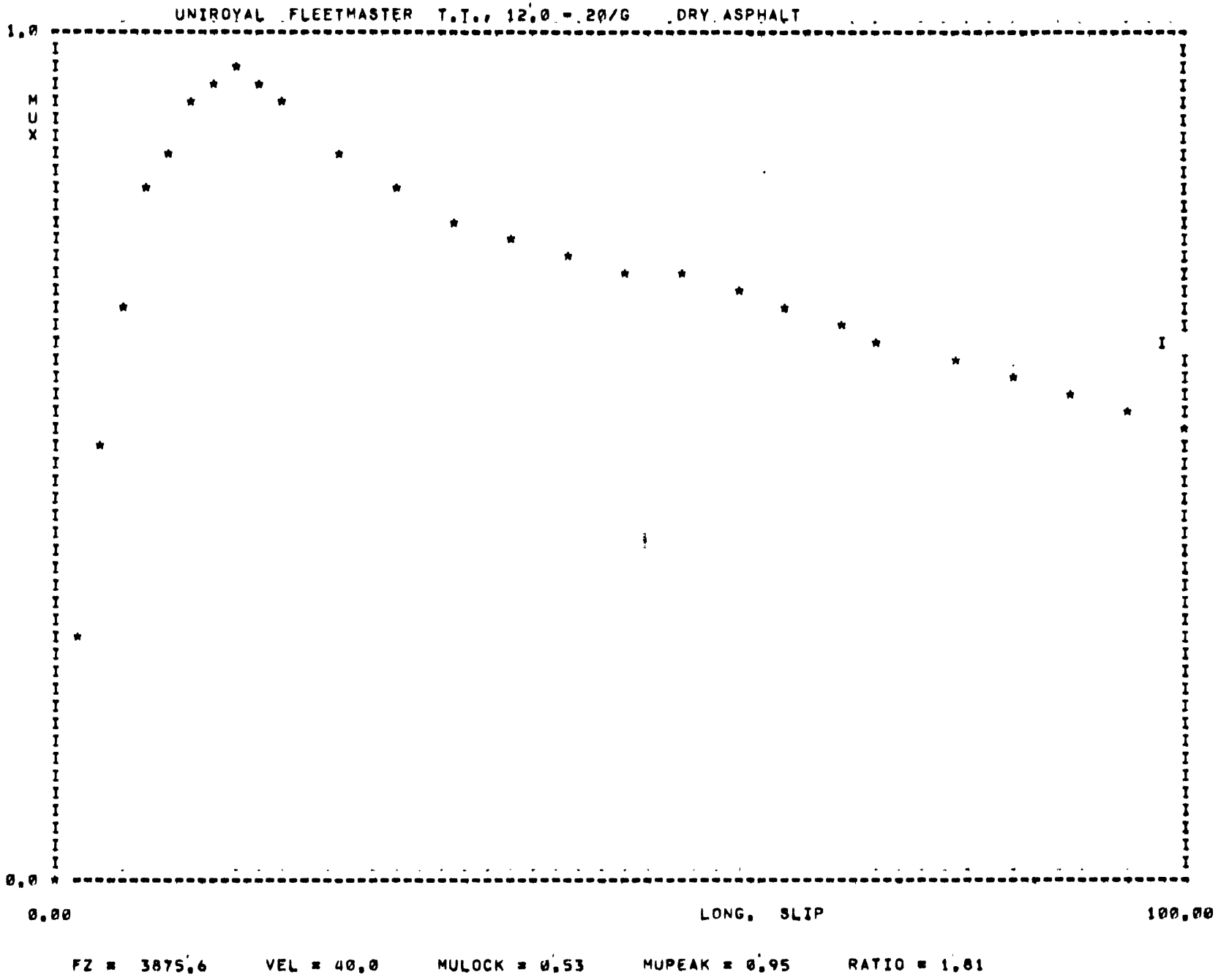
UNIROYAL FLEETMASTER T.I., 12.0 - 20/G DRY ASPHALT
1.0
MUX
0.0
0.00
LONG. SLIP
100.00
FZ = 3875.6 VEL = 40.0 MULOCK = 0.53 MUPEAK = 0.95 RATIO = 1.81

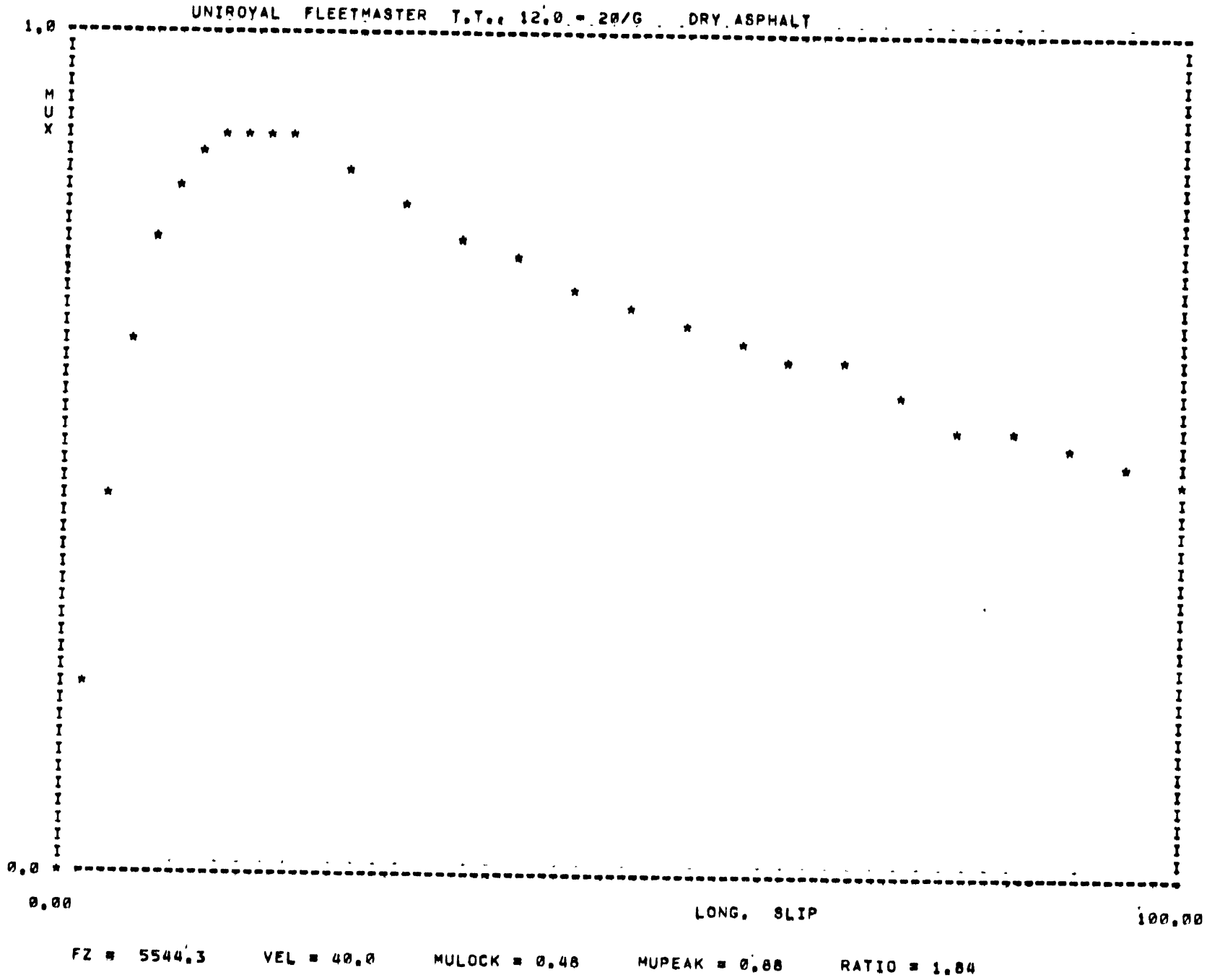
UNIROYAL FLEETMASTER T.T.: 12.0 - 20/G DRY ASPHALT
1.0
MUX
0.0
0.00
LONG. SLIP
100.00
FZ = 5544.3
VEL = 40.0
MULOCK = 0.48
MUPEAK = 0.88
RATIO = 1.84

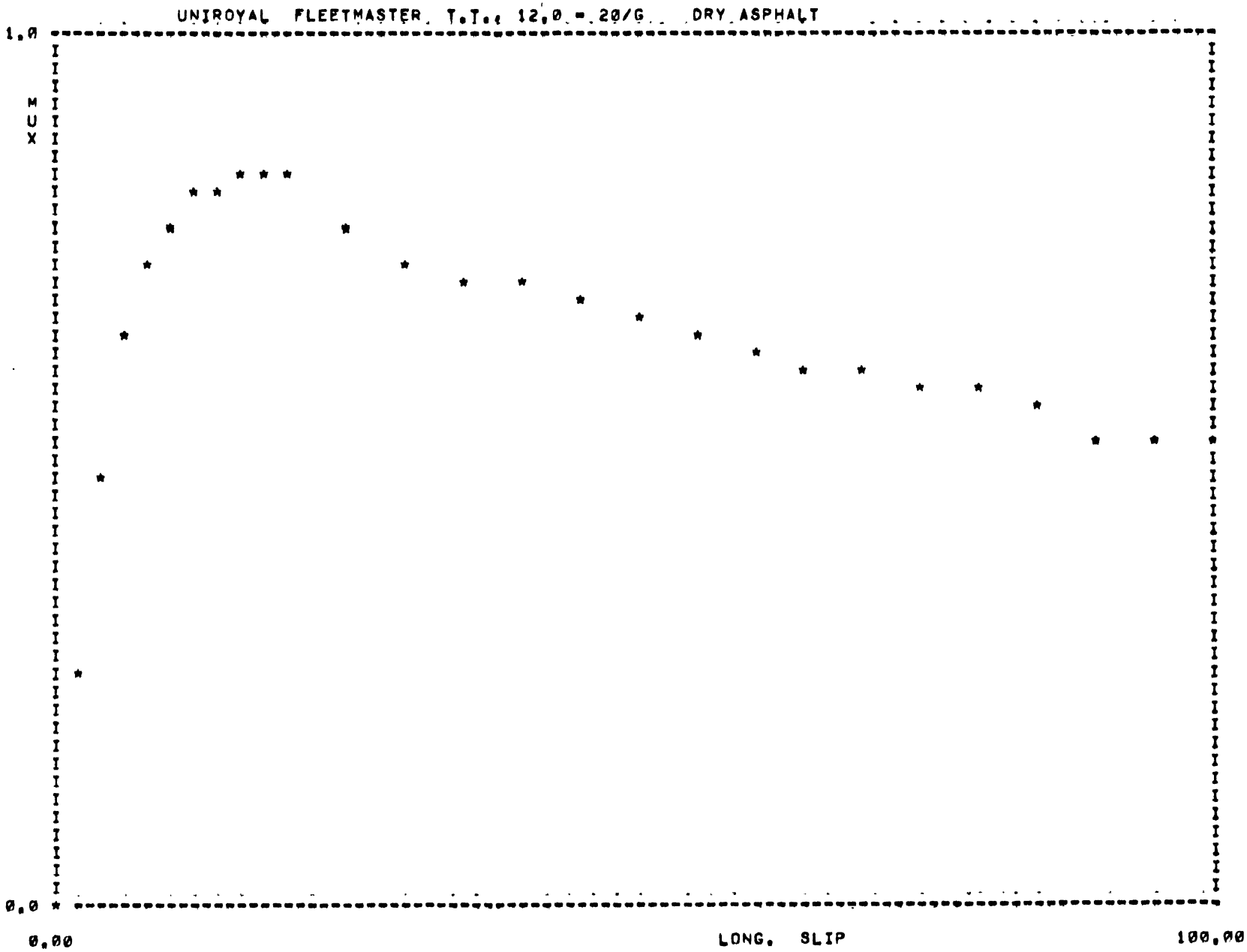

FZ = 3859.7 VEL = 60.0 MULOCK = 0.53 MUPEAK = 0.84 RATIO = 1.58

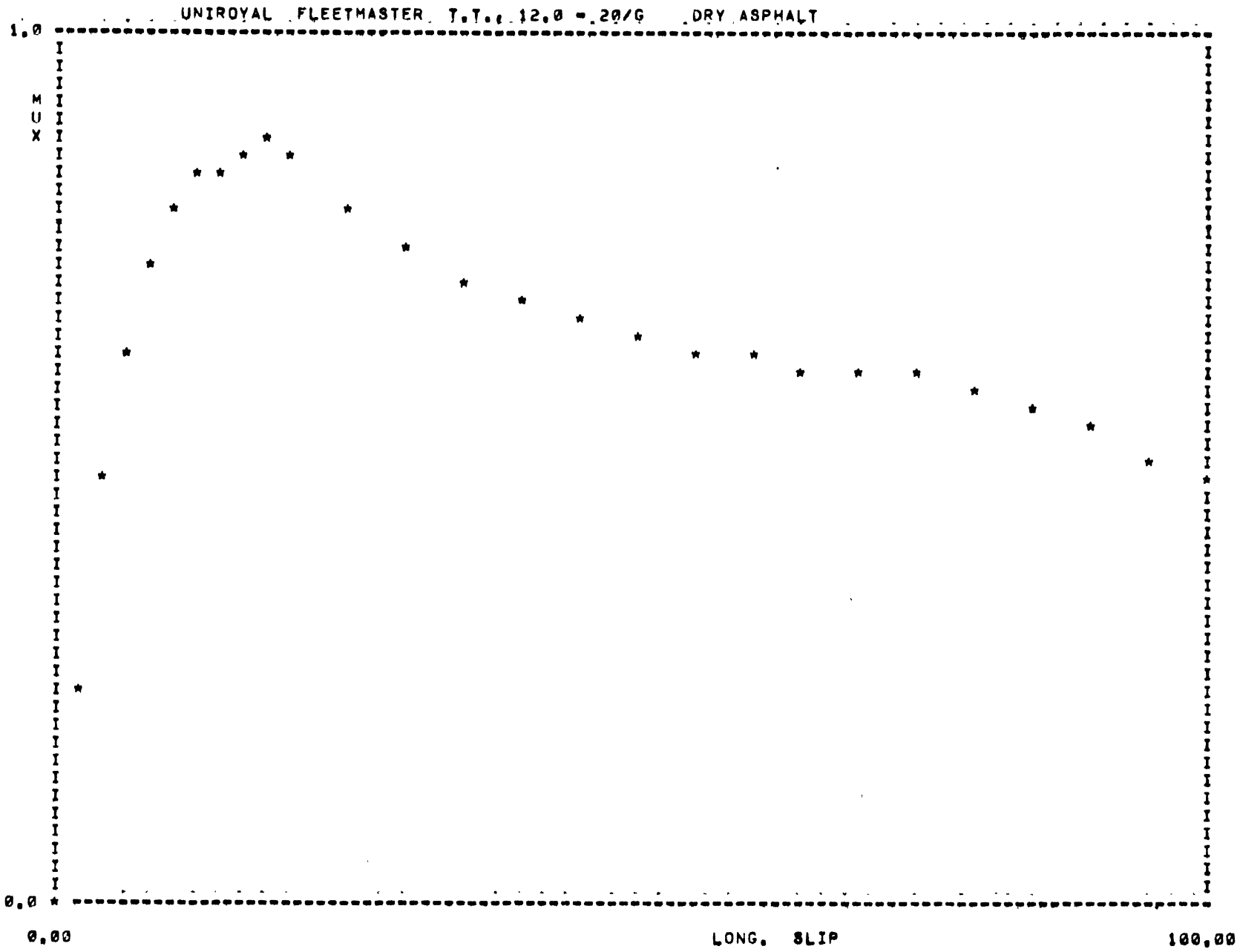

FZ = 5529.9 VEL = 60.0 MULOCK = .49 MUPEAK = .87 RATIO = 1.78

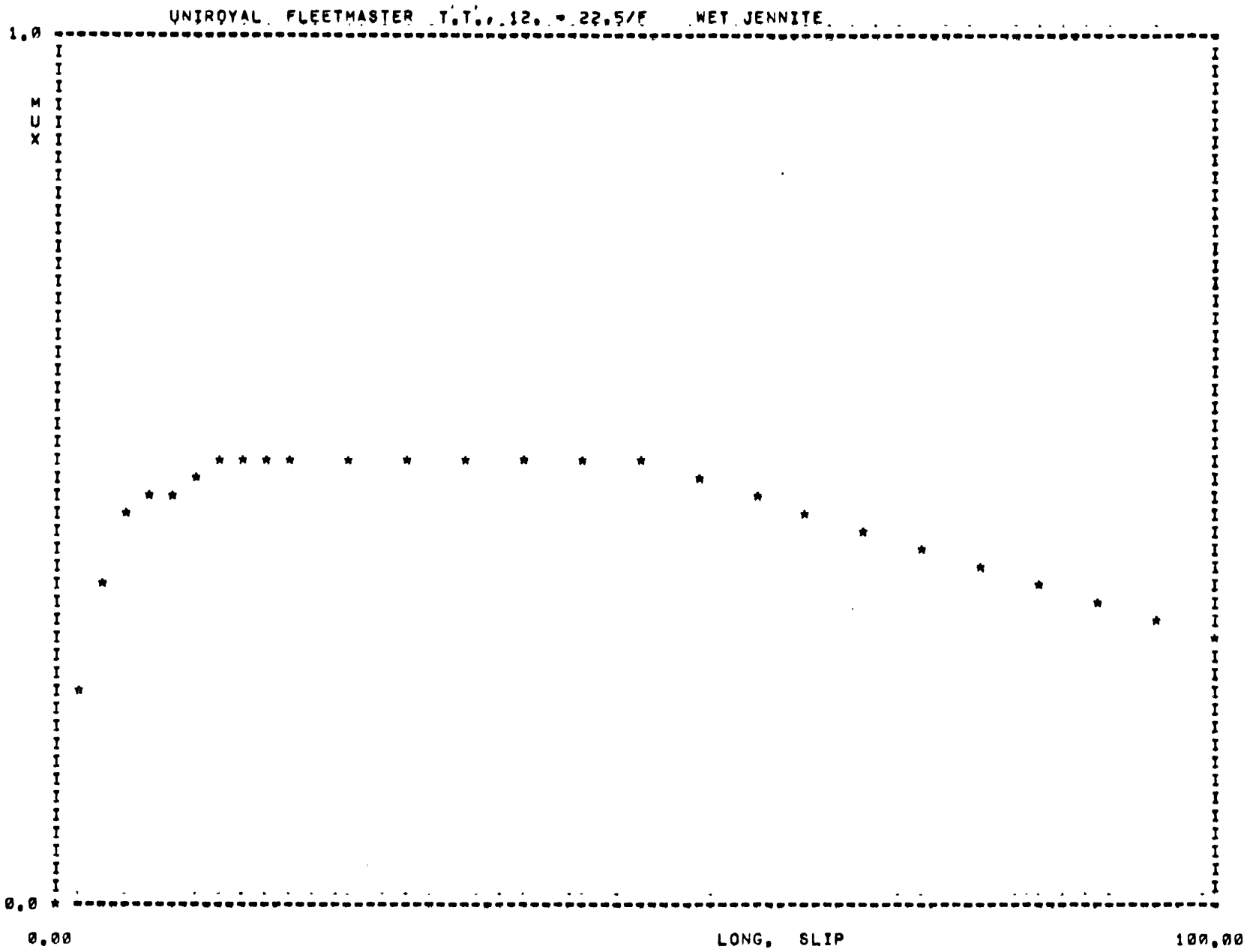

FZ = 3274.3 VEL = 20.0 MULOCK = 0.30 MUPEAK = 0.52 RATIO = 1.71

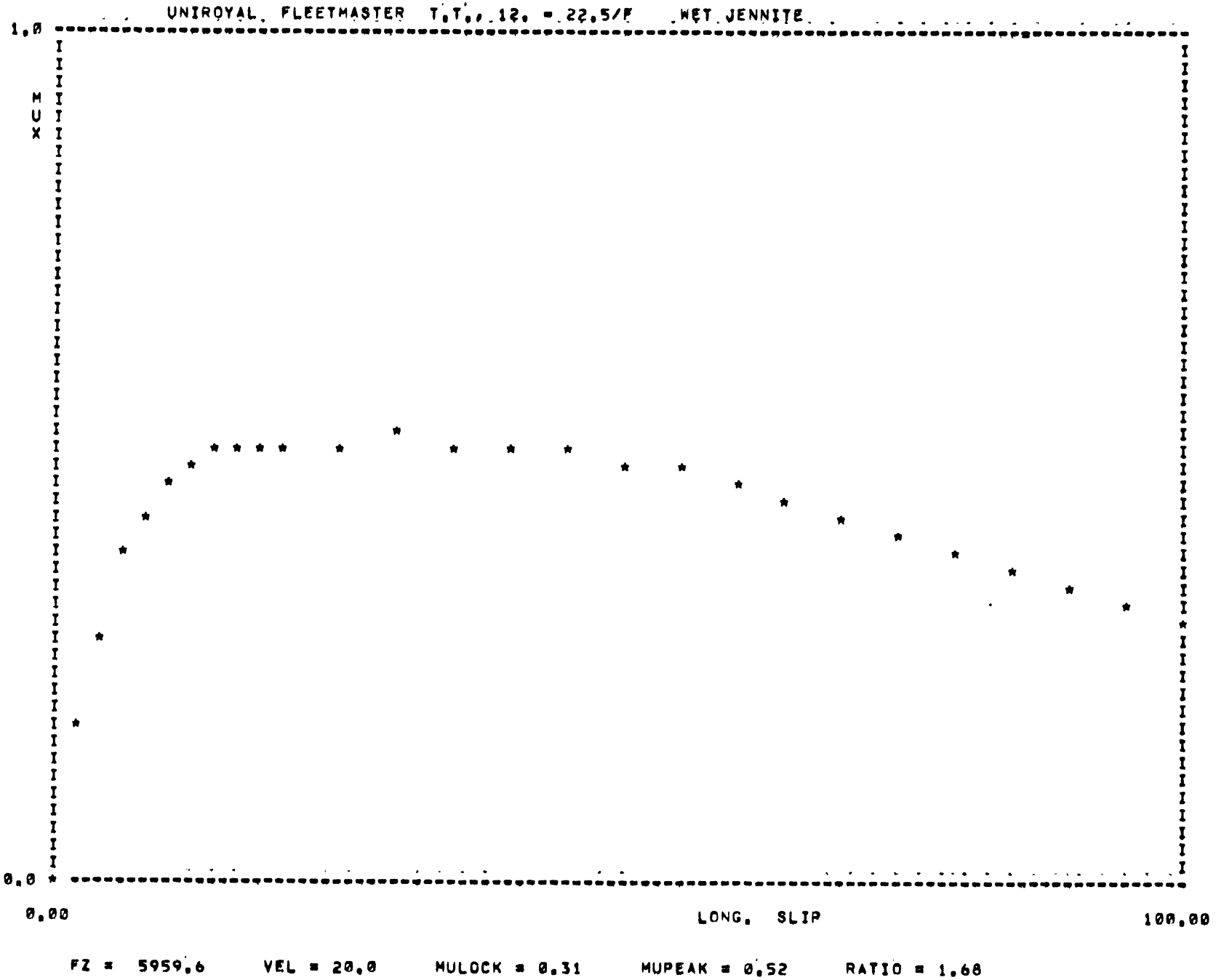

FZ = 5959.6 VEL = 20.0 MULOCK = 0.31 MUPEAK = 0.52 RATIO = 1.68

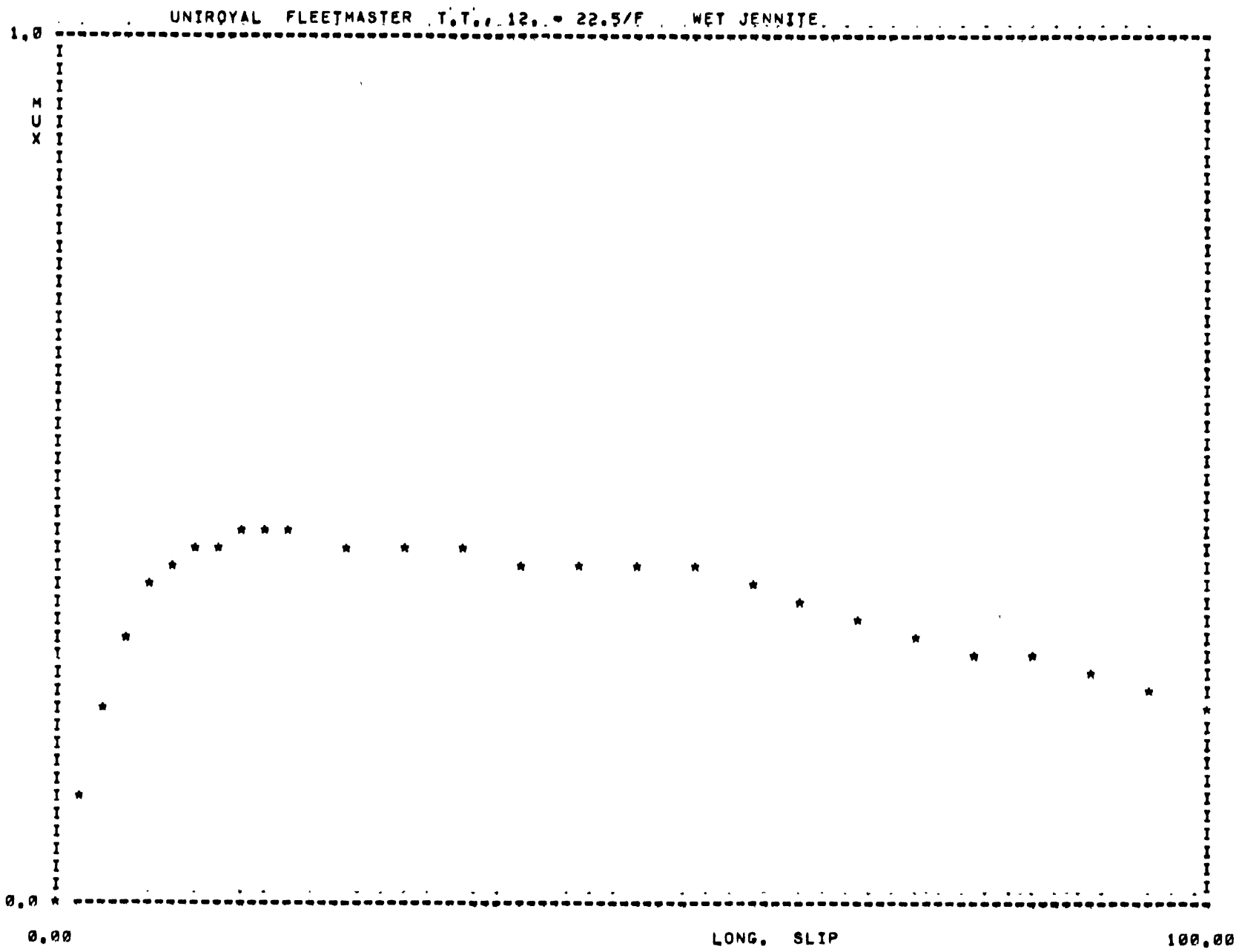

FZ = 9293.0 VEL = 20.0 MULOCK = 0.23 MUPEAK = 0.42 RATIO = 1.87

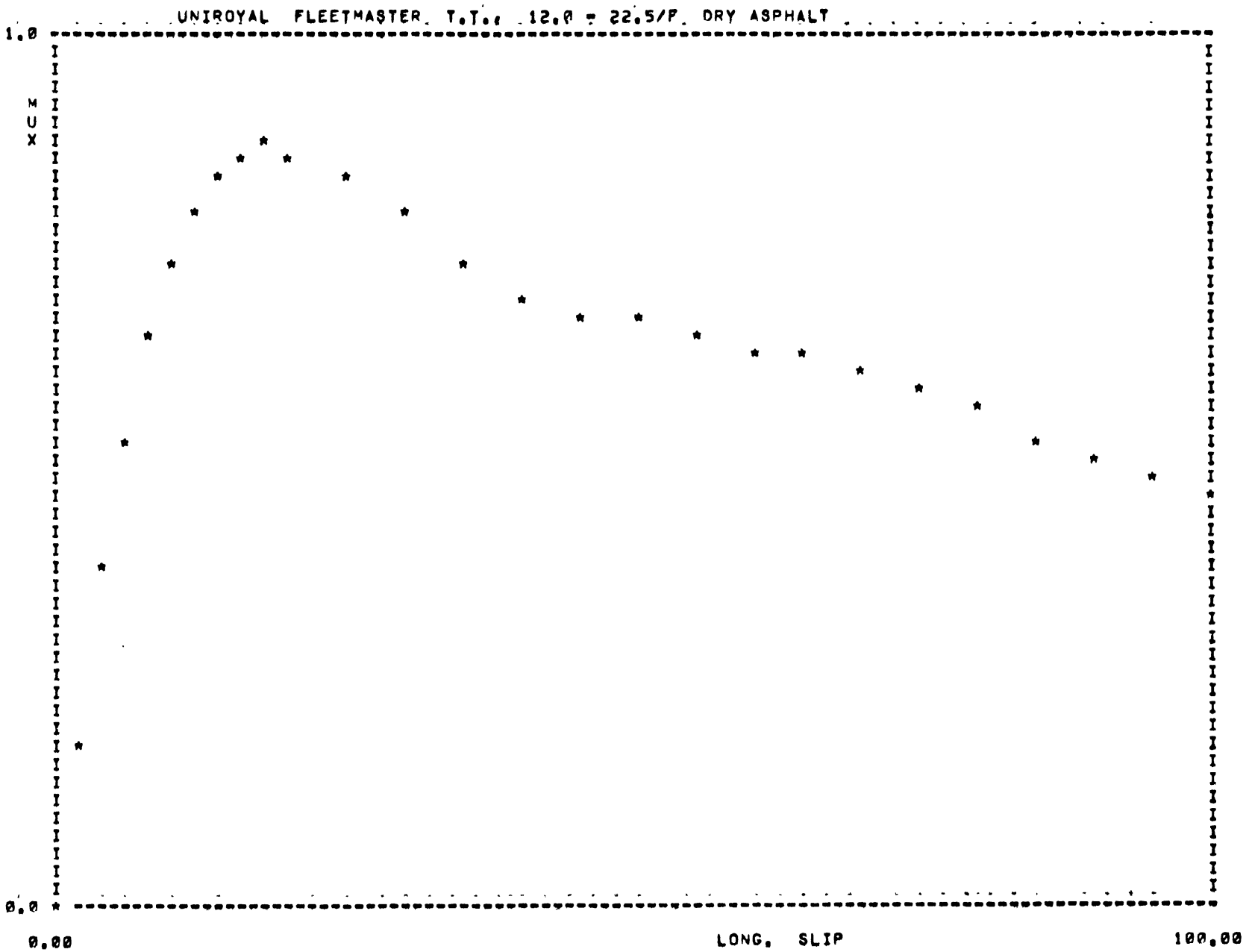

FZ = 6078.2 VEL = 40.0 MULOCK = 0.46 MUPEAK = 0.87 RATIO = 1.88

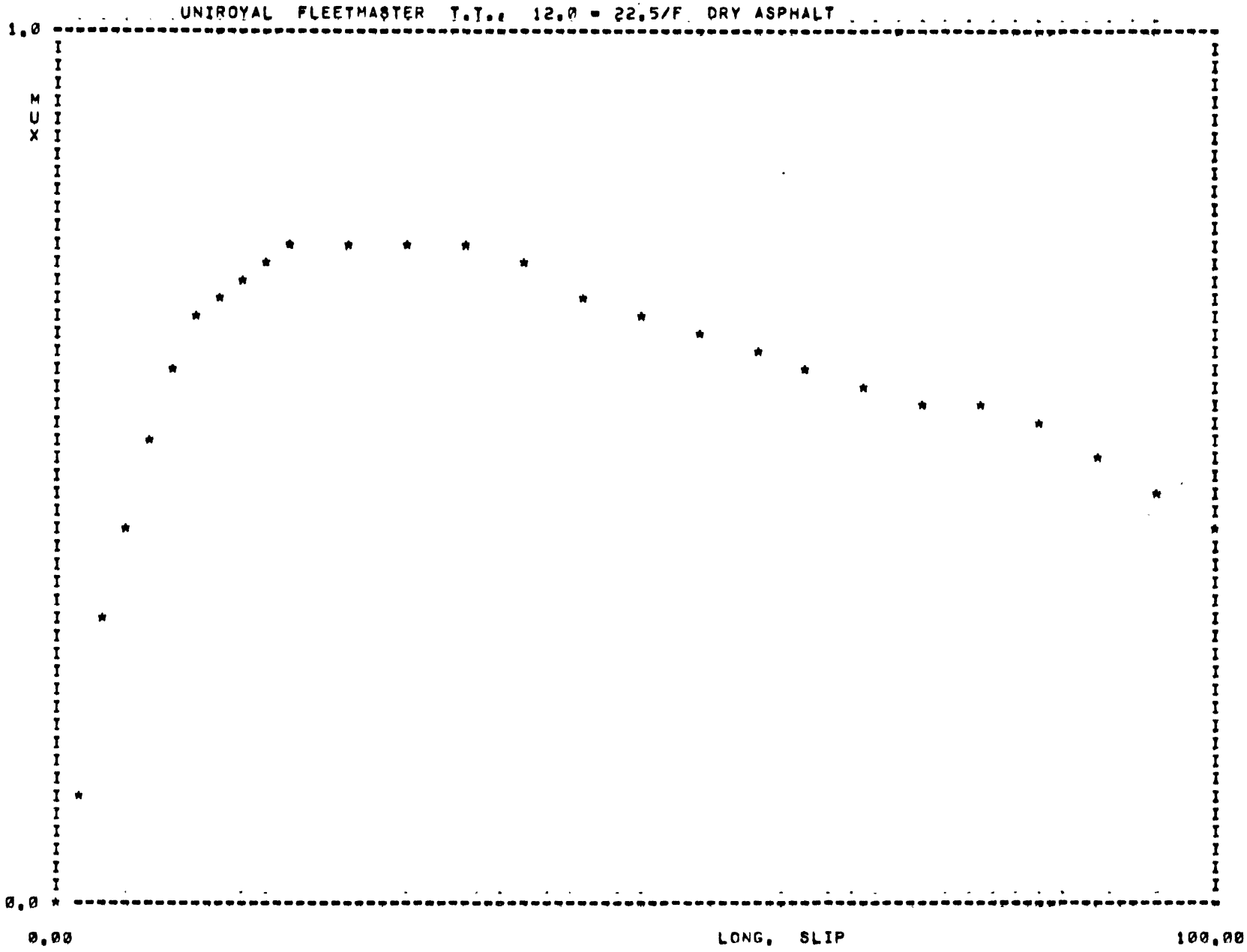

FZ = 7830.4 VEL = 40.0 MULOCK = 0.42 MUPEAK = 0.76 RATIO = 1.81

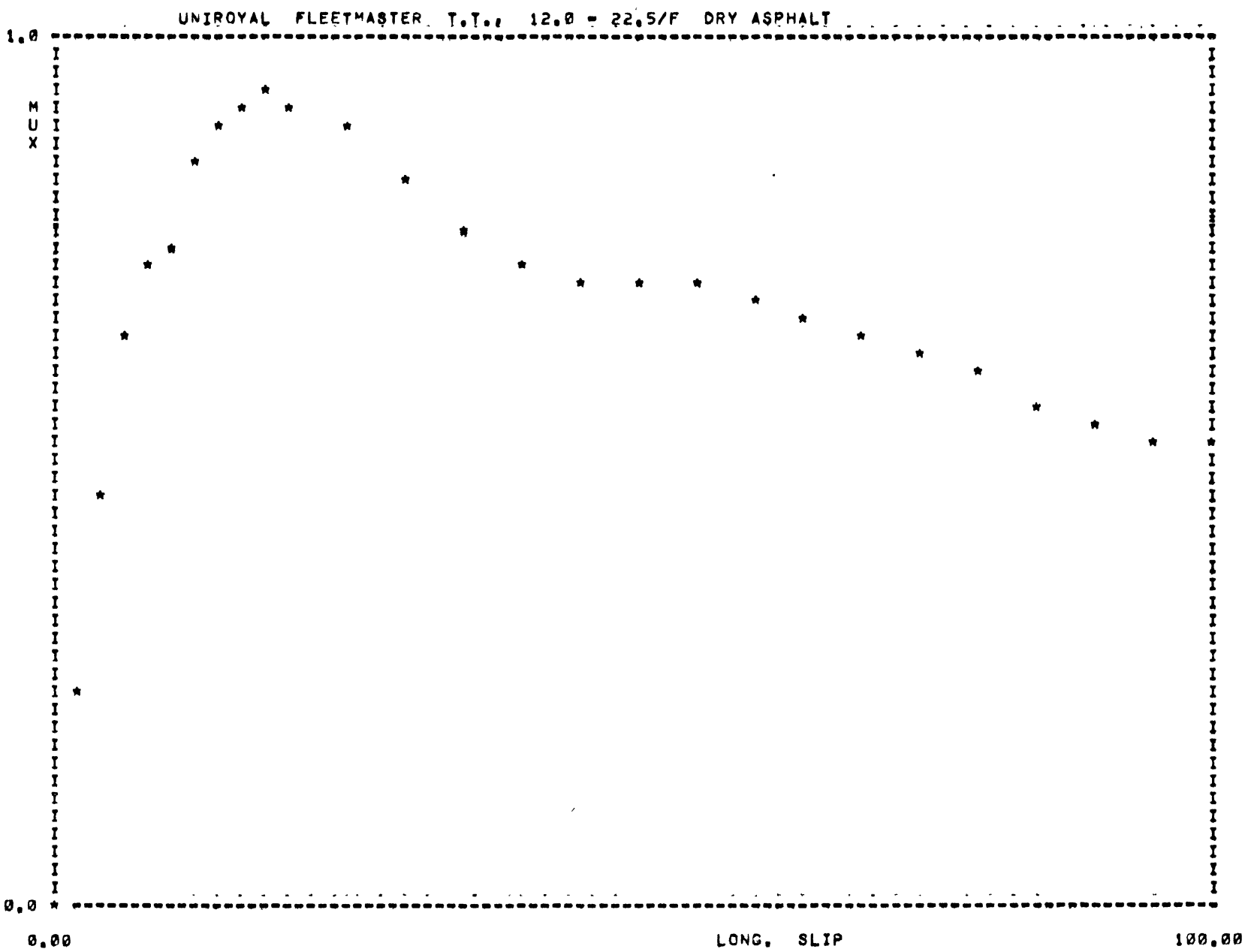

FZ = 3369.1 VEL = 60.0 MULOCK = 0.52 MUPEAK = 0.94 RATIO = 1.79

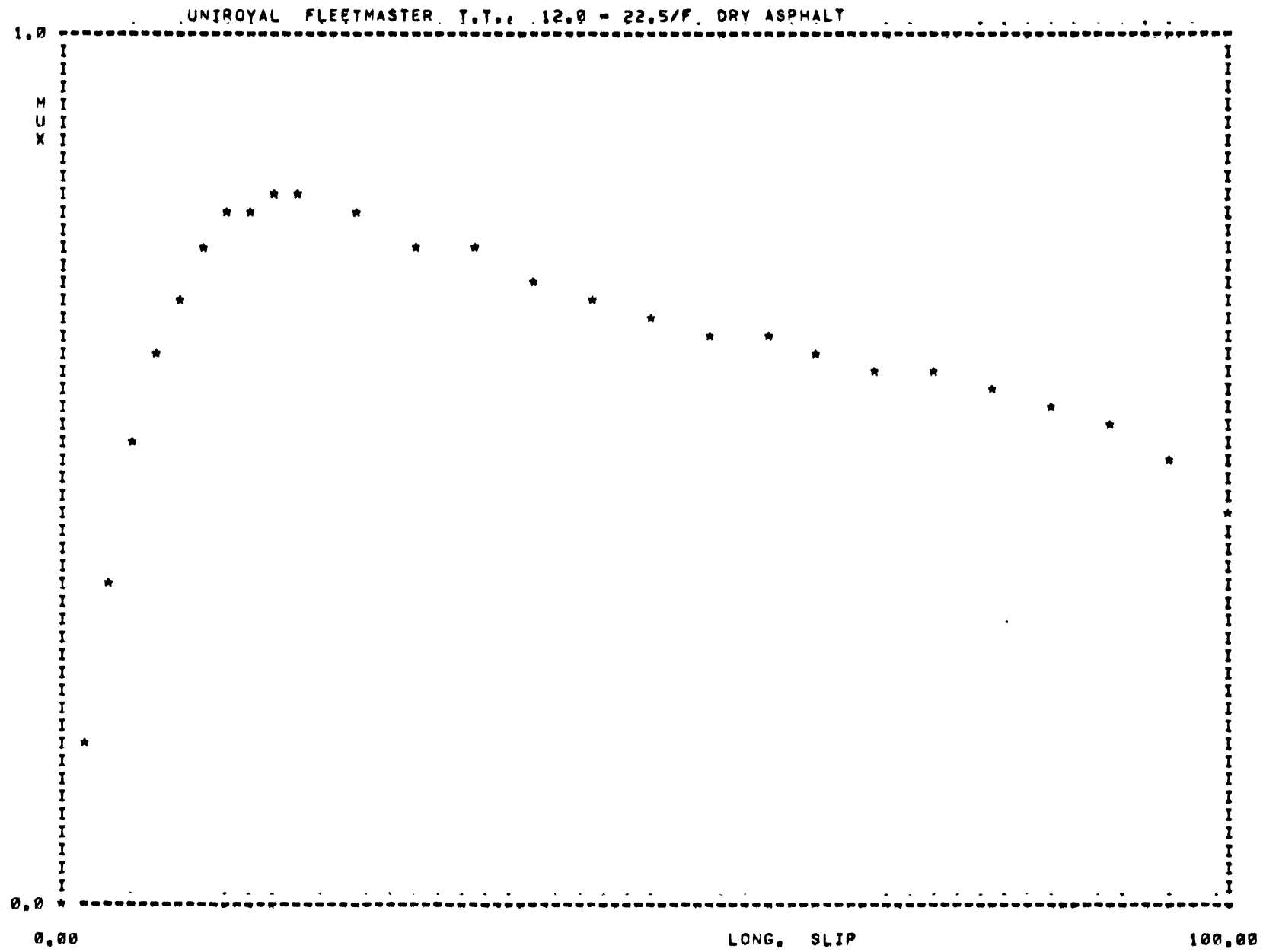

FZ = 6036.0 VEL = 60.0 MULOCK = 0.46 MUPEAK = 0.81 RATIO = 1.76

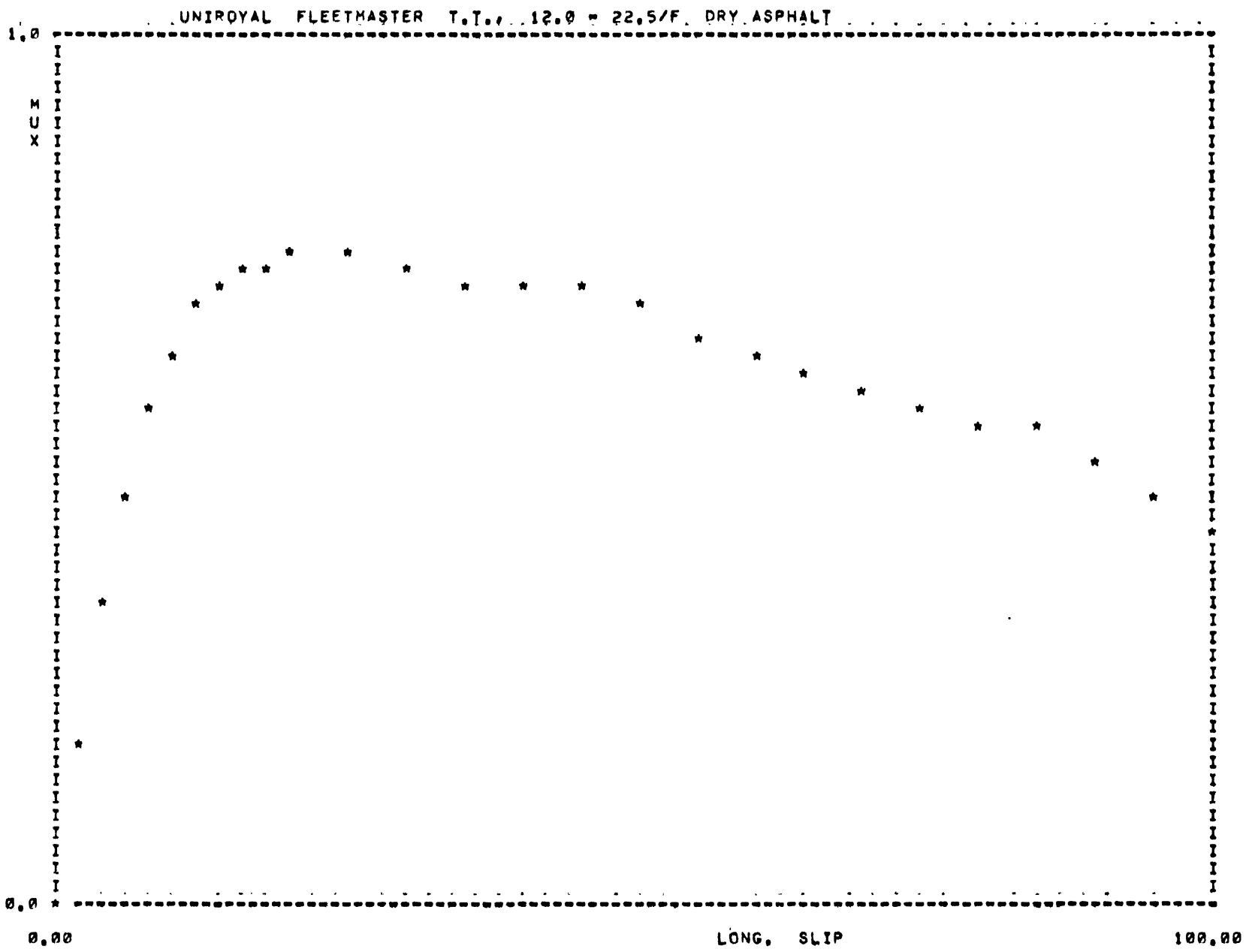

FZ = 7821.0 VEL = 60.0 MULOCK = 0.43 MUPEAK = 0.76 RATIO = 1.78

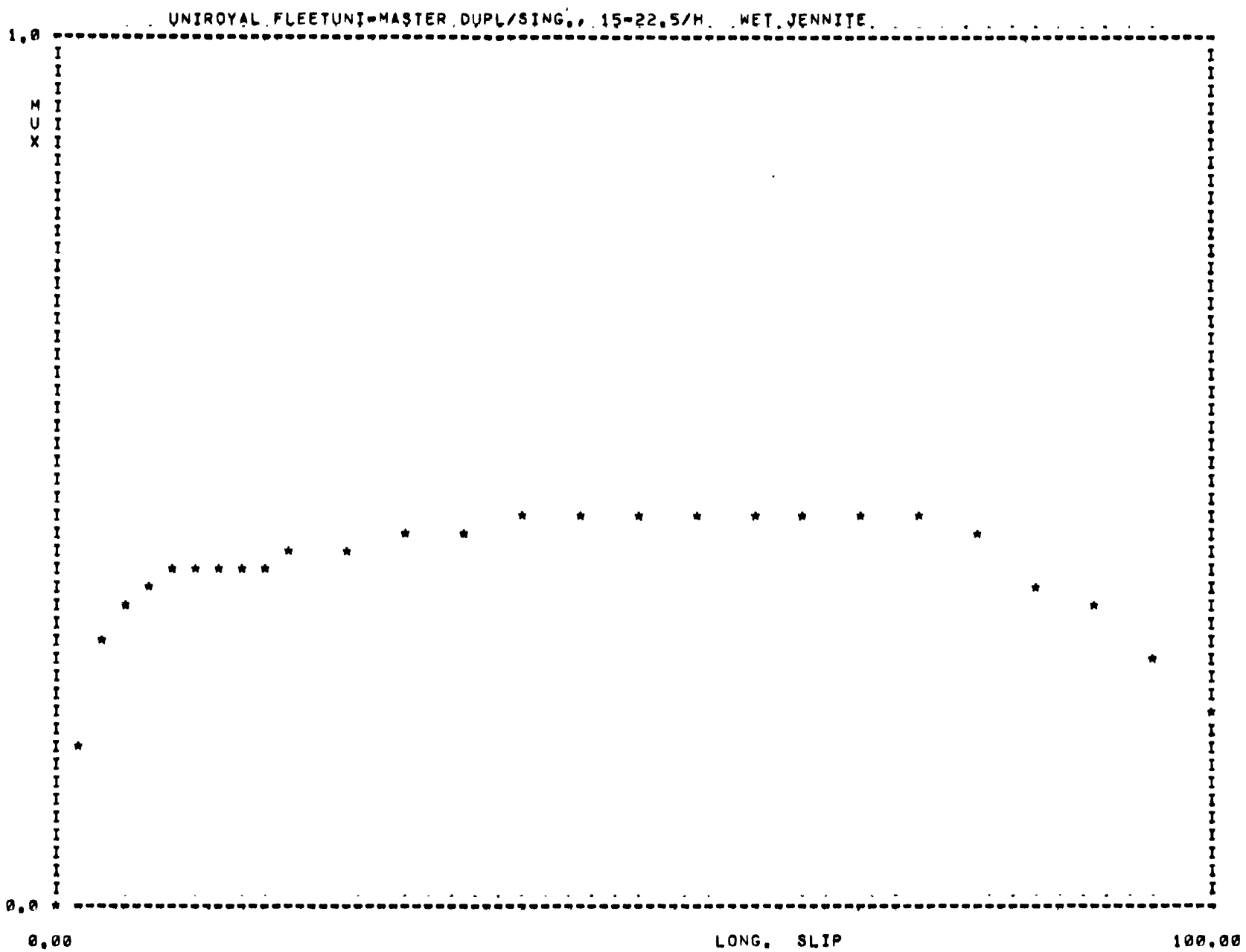

FZ = 4501.9 VEL = 20.0 MULOCK = 0.22 MUPEAK = 0.45 RATIO = 2.00

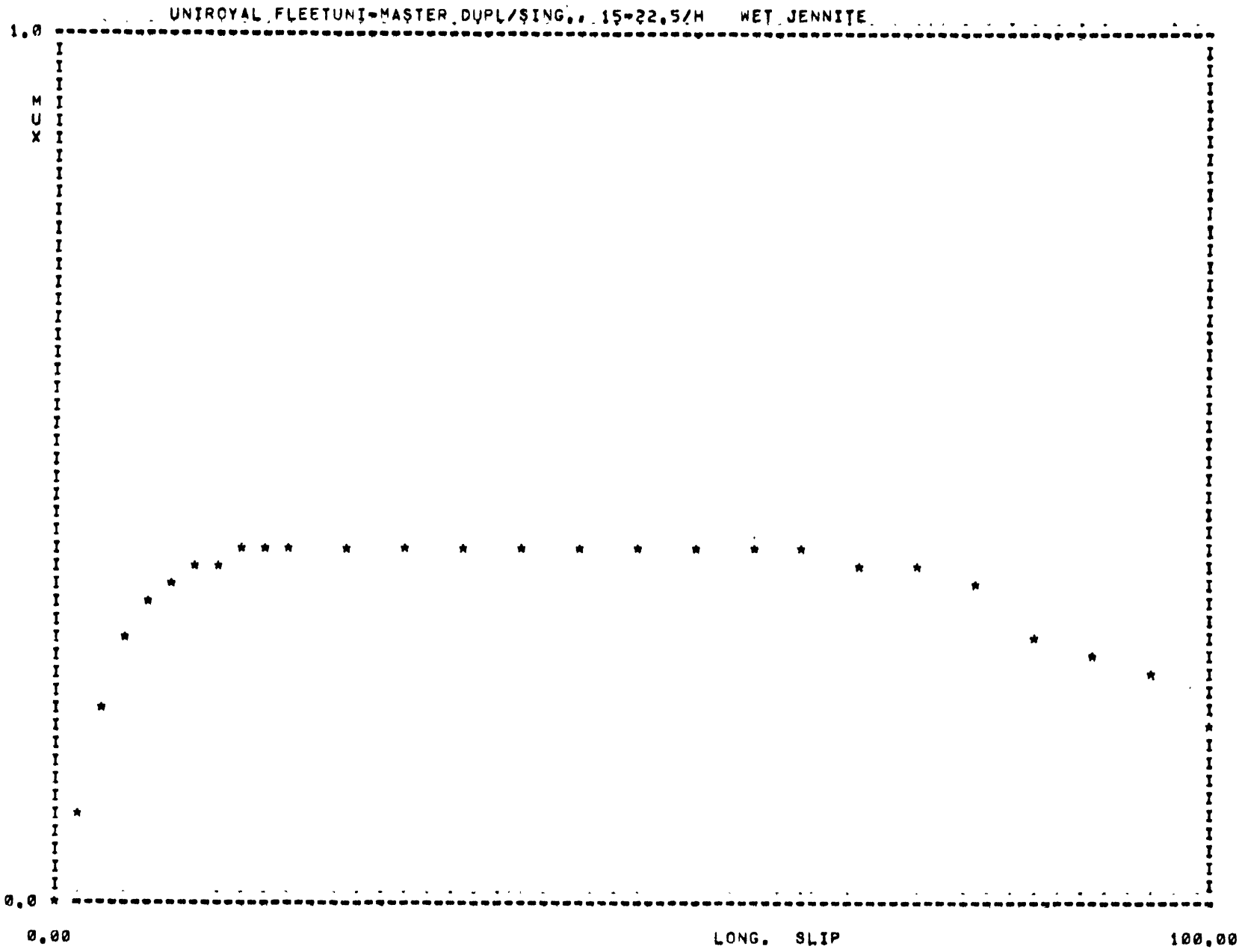

FZ = 8749.8 VEL = 20.0 MULOCK = 0.22 MUPEAK = 0.42 RATIO = 1.93

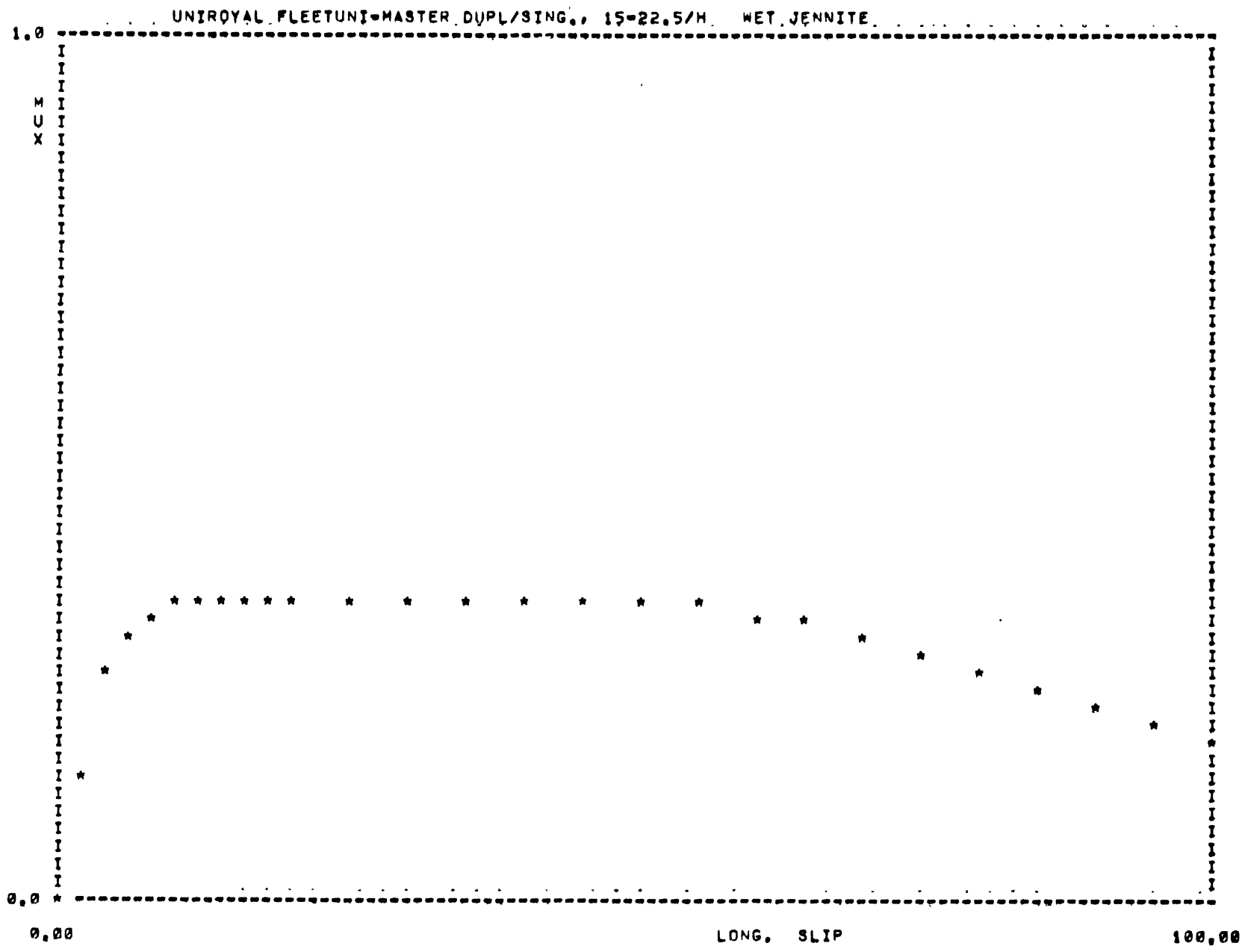

FZ = 13519.9 VEL = 20.0 MULOCK = 0.20 MUPEAK = 0.36 RATIO = 1.82

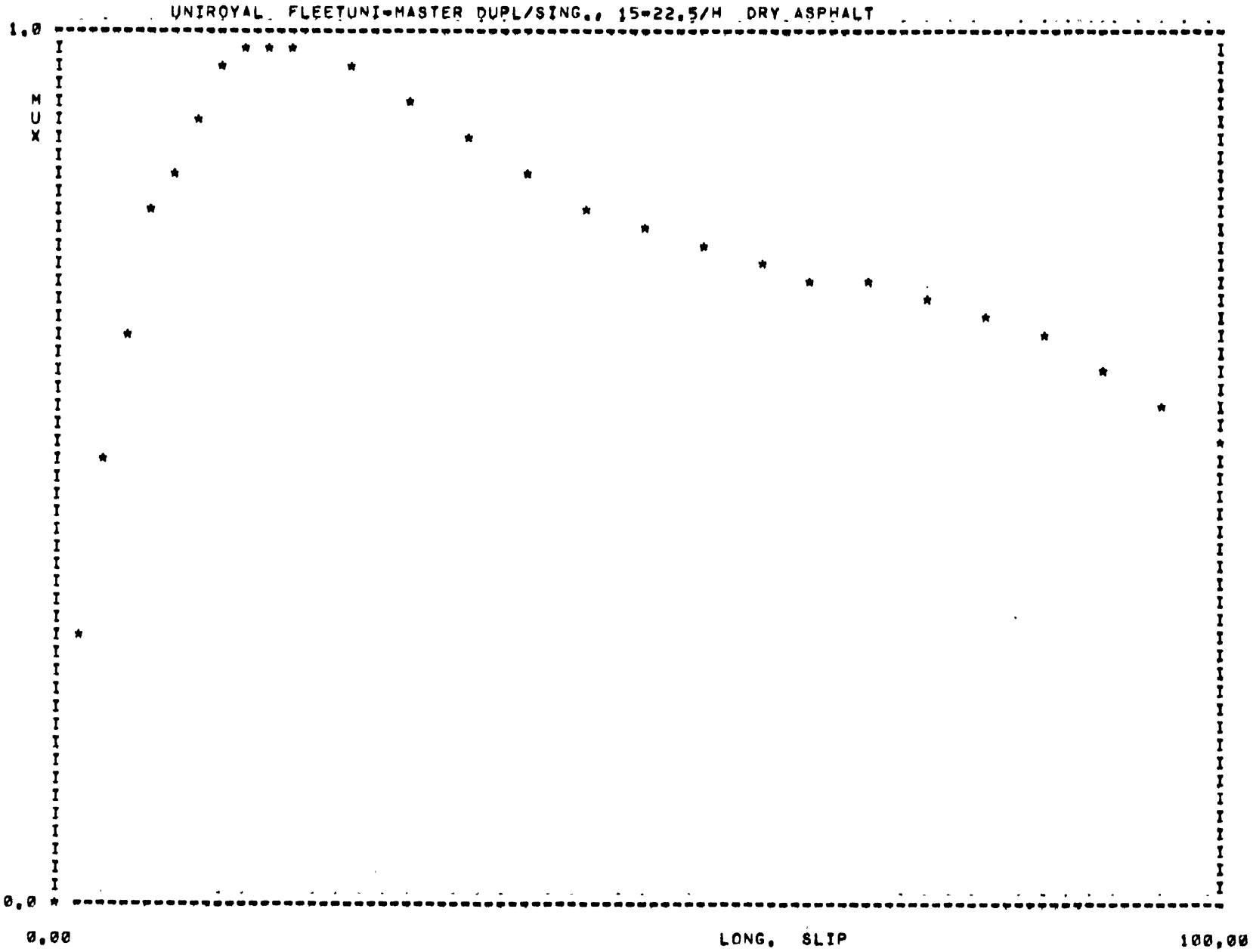

FZ = 4352,8 VEL = 40,0 MULOCK = 0,53 MUPEAK = 0,99 RATIO = 1,86

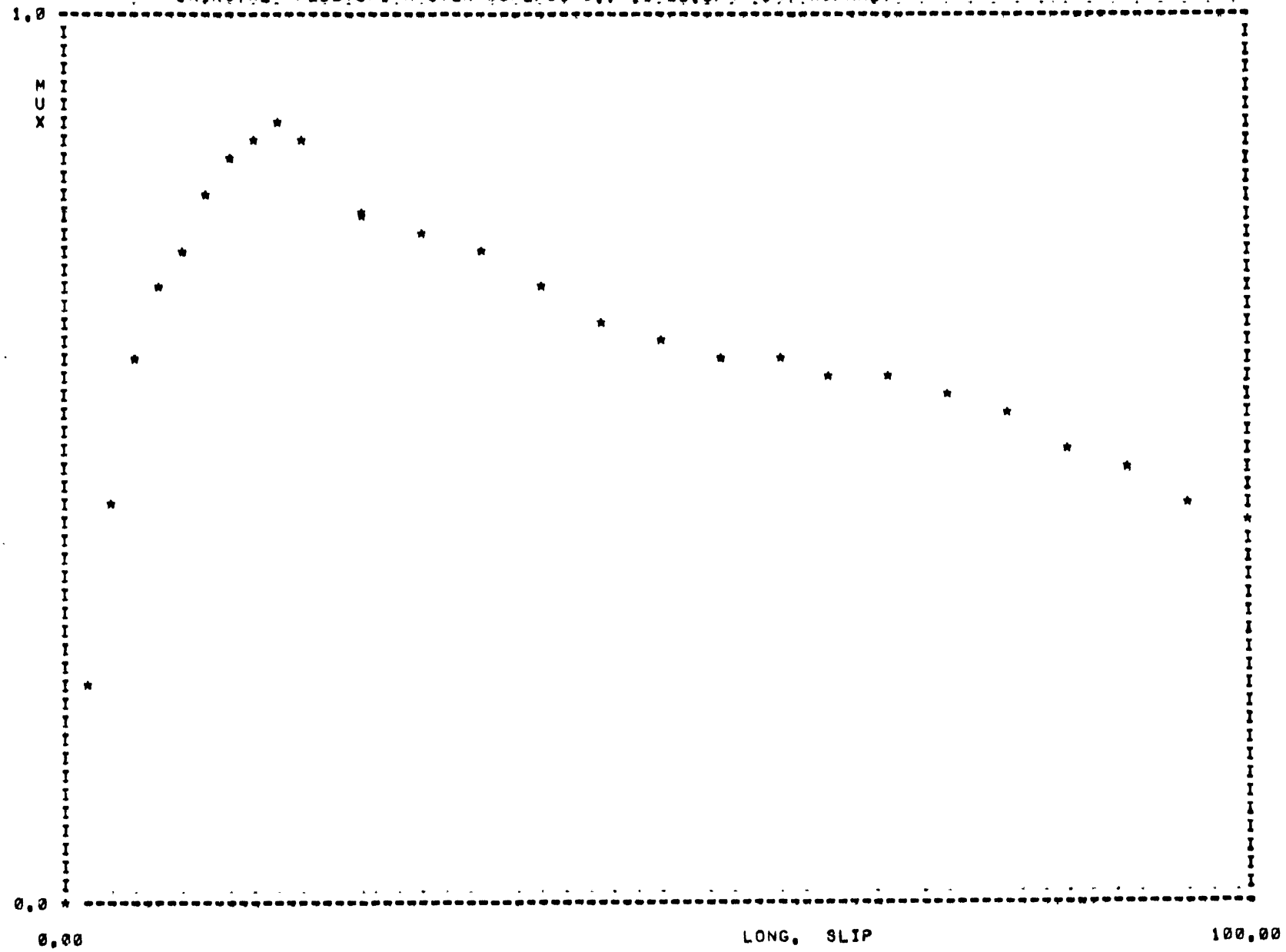

FZ = 6596.7 VEL = 40.0 MULOCK = 0.43 MUPEAK = 0.87 RATIO = 2.01

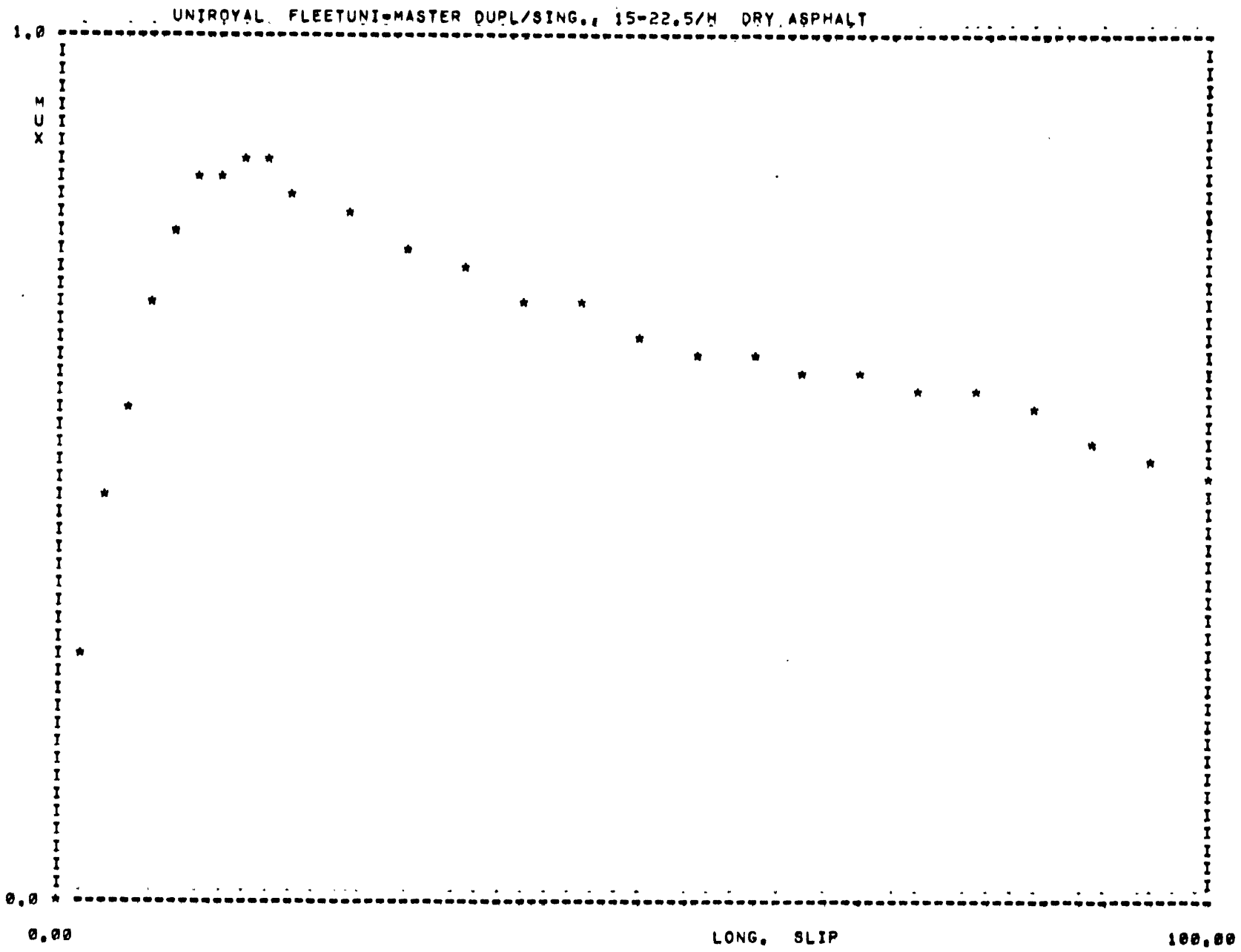

FZ = 4414.2 VEL = 60.0 MULOCK = 0.49 MUPEAK = 0.86 RATIO = 1.76

APPENDIX 2

MOBILE TRUCK TIRE DYNAMOMETER— LONGITUDINAL TRACTION PROPERTIES

BASIC CONFIGURATION

A mobile dynamometer has been constructed in the configuration of a semi-trailer device for use in measuring the longitudinal traction properties of truck tires. Shown in Figure 2.1, this trailer apparatus is of steel pipe and plate construction, with a nominal wheelbase of 20 feet. The test tire is located in the geometric center of the trailer, and is supported by a parallel arm suspension, shown in Figure 2.2. Since the parallel arms are pivoted about truly longitudinal centerlines, there is no kinematic interaction between longitudinal tire force, F_x, and vertical load, F_z.

The test tire is mounted on a spindle assembly which is in turn fastened to the outboard face of a multi-axis load cell. The load cell is a serial element between the test tire and the overall trailer structure. Tire loading is provided through a pressure-regulated air spring which is situated directly over the test wheel. This bellows-type spring permits easy load adjustment while providing a very low-rate coupling between the tire suspension and the trailer structure.

Braking torque is applied to the test wheel through a large hydraulic disc brake whose actuation pressure is servo-controlled.

The trailer rear axle is air-suspended to assist in attenuating ride vibrations as well as to provide, through closed loop leveling control, a means for establishing a zero-pitch-angle trim condition at each value of test tire loading.

The test trailer is towed by a highway tractor which is outfitted with hydraulic, pneumatic, electrical and data acquisition services in addition to a water delivery capability for pavement wetting.

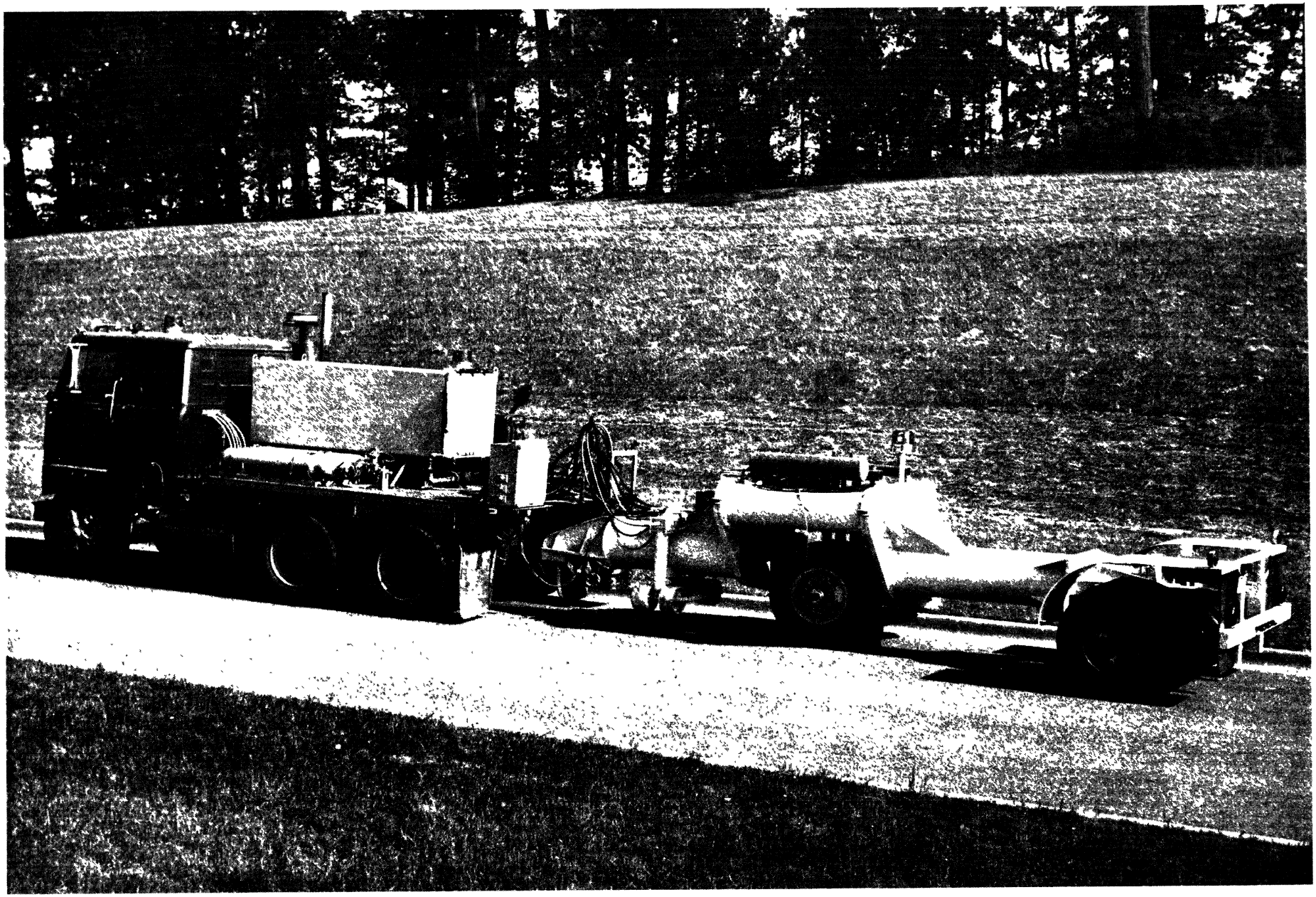

Figure 2.1

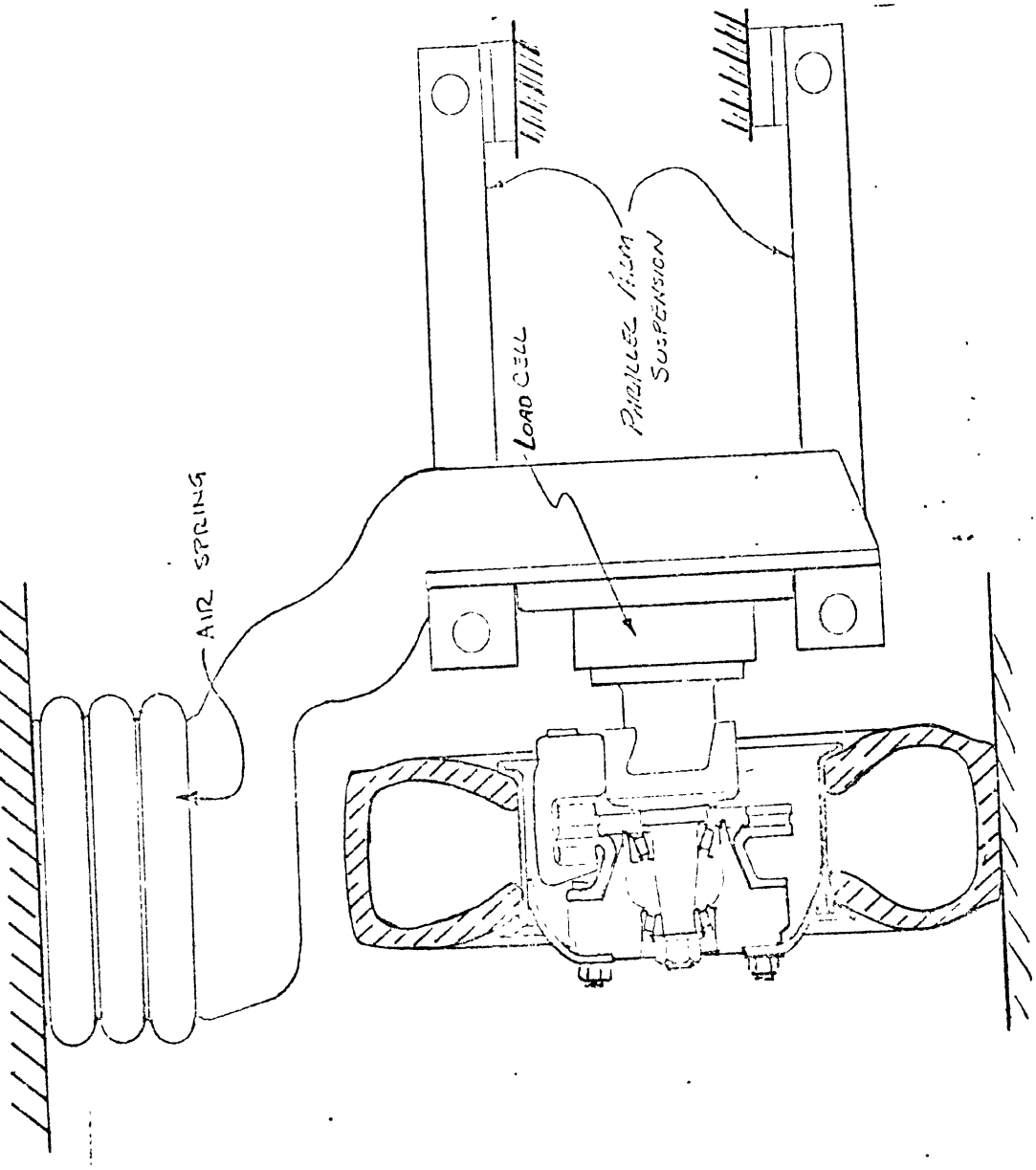

Figure 2.2 Test wheel suspension.

A tabulation of specifications for the test device follows:

Trailer Overall Length	23 feet
Trailer Gross Weight (with current ballast)	18,000 lbs
Maximum Test Tire Vertical Load (at current ballast conditions)	14,000 lbs
Maximum Test Tire F_z Rating (with added ballast)	20,000 lbs
Brake Torque Rating @ 60 mph	180,000 in-lbs
@ 30 mph	220,000 in-lbs
Load Cell Rating F_z	20,000 lbs
F_x	20,000 lbs
M_y	240,000 in-lbs
Dead Load Imposed by the Unsprung Mass on the Test Tire (including a 10:00 x 20/F tire)	1,850 lbs
Tire Size Range	All tires in the 20, 22, and 22.5" rim diameter sizes
Test Wheel Configuration	Disc wheel, 10 hole 11-1/4" diameter pattern

OPERATING PROCEDURE

For a given test condition consisting of a selected vertical load level, test velocity and road surface, the sequence of wheel slip cycling is preceded by a static set-up condition. With the test vehicle at rest, the tire support assembly is raised clear of the pavement and the vertical load data signal is adjusted to read "zero" load. This adjustment compensates for differences in "tare weight" which derive from the installation of different size tires and wheels.

The test tire assembly is lowered to the pavement and the air spring pressure regulator is adjusted to provide the desired value of vertical load for the test.

The vehicle is then accelerated to the desired test velocity on the selected surface. The wheel slip cycle is initiated by application of a ramp-fronted step command to the brake pressure servo-mechanism. The input command is sustained until a wheel lockup detection circuit triggers an automatic brake release. The entire lockup/release cycle is completed in 300 to 500 milliseconds, thus minimizing wear of the test tire. Repetitive slip cycles are conducted for gaining a statistically reliable data sample, and then the test system is adjusted to a new set of conditions for the next data sequence.

REFERENCES

1. Bernard, J. E., Winkler, C. B., and Fancher, P.S., A Computer Based Mathematical Method for Predicting the Directional Response of Trucks and Tractor-Trailers, Phase II Technical Report to NHTSA, Highway Safety Research Institute, Univ. of Michigan, Ann Arbor, June 1, 1973.

2. Goodenow, G.L., Kolhoff, T.R., and Smithson, F. D., "Tire-Road Friction Measuring System—A Second Generation," SAE Paper No. 680137, January 1968.

3. Davisson, J.A., "Design and Application of Commercial Type Tires," Fifteenth L. Ray Buckendale Lecture, SAE, SP-344, January 1969.

4. Clark, S.K., ed., Mechanics of Pneumatic Tires, NBS Monograph 122, November 1971: A United States Department of Commerce Publication: U.S. Government Printing Office, Washington, D.C. (853 pages).

5. Segel, L., "Tire Traction on Dry, Uncontaminated Surfaces," Proceedings of a Symposium on the Physics of Tire Traction, General Motors Research Laboratories, October 8-9, 1973, (in press).

6. Harned, J.L., Johnston, L.E., and Scharpf, G., "Measurement of Tire Brake Force Characteristics as Related to Wheel Slip (Antilock) Control System Design," SAE Paper No. 690214, January 1969.